Pharmacokinetic/pharmacodynamic models to optimize the treatment of infections caused by multidrug resistant gram-negative bacteria

Matthieu Jacobs

THÈSE

Pour l'obtention du grade de
DOCTEUR DE L'UNIVERSITÉ DE POITIERS
UFR de médecine et de pharmacie
Laboratoire pharmacologie des anti-infectieux (Poitiers)
(Diplôme National - Arrêté du 7 août 2006)

École doctorale : Biologie-santé - Bio-santé (Limoges)
Secteur de recherche : Pharmacie

Présentée par :
Matthieu Jacobs

Développement de modèles pharmacocinétiques et pharmacodynamiques pour l'optimisation du traitement des infections à bactéries à gram négatif multi-résistantes

Directeur(s) de Thèse :
William Couet, Nicolas Grégoire

Soutenue le 09 novembre 2015 devant le jury

Jury :

Président	**Katy Jeannot**	Maître de conférences, Université de Franche-Comté
Rapporteur	**Xavier Declèves**	Professeur des Universités, Université Paris Descartes
Rapporteur	**Alain Bousquet-Mélou**	Professeur, École nationale vétérinaire de Toulouse
Membre	**William Couet**	Professeur des Universités, Université de Poitiers
Membre	**Nicolas Grégoire**	Maître de conférences, Université de Poitiers
Membre	**Anne Geneteau**	Chef de projet pharmacocinétique, CEVA, Libourne

Pour citer cette thèse :
Matthieu Jacobs. *Développement de modèles pharmacocinétiques et pharmacodynamiques pour l'optimisation du traitement des infections à bactéries à gram négatif multi-résistantes* [En ligne]. Thèse Pharmacie. Poitiers : Université de Poitiers, 2015. Disponible sur Internet <http://theses.univ-poitiers.fr>

THESE

Pour l'obtention du Grade de

DOCTEUR DE L'UNIVERSITE DE POITIERS

(Faculté Médecine et Pharmacie)
(Diplôme National - Arrêté du 7 août 2006)

Ecole Doctorale : n°524 Bio-santé du PRES Limousin-Poitou-Charentes

Secteur de Recherche : Pharmacie

Présentée par :

Matthieu JACOBS

Développement de modèles pharmacocinétiques et pharmacodynamiques pour l'optimisation du traitement des infections à bactéries à Gram négatif multi-résistantes

Directeurs de Thèse :

Professeur William COUET
Docteur Nicolas GREGOIRE

Soutenue le 09 Novembre 2015

Devant la Commission d'Examen

JURY

Professeur Alain BOUSQUET MELOU	Rapporteur
Professeur William COUET	Examinateur
Professeur Xavier DECLEVES	Rapporteur
Madame Anne GENETEAU	Examinateur
Docteur Nicolas GREGOIRE	Examinateur
Docteur Katy JEANNOT	Examinateur

UNIVERSITE DE POITIERS

Faculté de Médecine et de Pharmacie

Année universitaire 2015-2016

PHARMACIE

Professeurs

- CARATO Pascal, Chimie Thérapeutique
- COUET William, Pharmacie Clinique
- FAUCONNEAU Bernard, Toxicologie
- GUILLARD Jérôme, Pharmaco chimie
- IMBERT Christine, Parasitologie
- MARCHAND Sandrine, Pharmacocinétique
- OLIVIER Jean Christophe, Galénique
- PAGE Guylène, Biologie Cellulaire
- RABOUAN Sylvie, Chimie Physique, Chimie Analytique
- SARROUILHE Denis, Physiologie
- SEGUIN François, Biophysique, Biomathématiques

Maîtres de Conférences

- BARRA Anne, Immunologie-Hématologie
- BARRIER Laurence, Biochimie
- BODET Charles, Bactériologie
- BON Delphine, Biophysique
- BRILLAULT Julien, Pharmacologie
- CHARVET Caroline, Physiologie
- DEBORDE Marie, Sciences Physico-Chimiques
- DEJEAN Catherine, Pharmacologie
- DELAGE Jacques, Biomathématiques, Biophysique
- DUPUIS Antoine, Pharmacie Clinique
- FAVOT Laure, Biologie Cellulaire et Moléculaire
- GIRARDOT Marion, pharmacognosie, botanique, biodiversité végétale
- GREGOIRE Nicolas, Pharmacologie
- GRIGNON Claire, PH
- HUSSAIN Didja, Pharmacie Galénique
- INGRAND Sabrina, Toxicologie
- MARIVINGT-MOUNIR Cécile Pharmaco chimie
- PAIN Stéphanie, Toxicologie
- RAGOT Stéphanie, Santé Publique
- RIOUX BILAN Agnès, Biochimie
- TEWES Frédéric, Chimie et Pharmaco chimie
- THEVENOT Sarah, Hygiène et Santé publique
- THOREAU Vincent, Biologie Cellulaire
- WAHL Anne, Pharmaco chimie, Produits naturels

PAST - Maître de Conférences Associé

- DELOFFRE Clément, Pharmacien
- HOUNKANLIN Lydwin, Pharmacien

Professeur 2nd degré

- DEBAIL Didier

Maître de Langue - Anglais

- JORDAN Steven

Poste d'ATER

- COSTA Damien

Poste de Moniteur

- VERITE Julie

Remerciements

Ce projet de thèse a été un projet de 3 ans, pendant lequel j'ai rencontré une merveilleuse équipe poitevine, qui m'a épaulée et m'a permis de me construire en tant que scientifique. Ce projet est avant tout un travail d'équipe mené avec des personnes formidables, qu'elles soient assurées de mon profond respect et de toute ma gratitude.

Professeur Alain Bousquet Mélou vous m'avez connu avant mes débuts en pharmacocinétique sur les bancs de l'école vétérinaire et vous avez été le premier à me faire découvrir cette discipline, je suis très honoré que vous ayez accepté de rapporter cette thèse.

Professeur Xavier Declèves, je vous remercie d'avoir accepté de rapporter ce travail et pour l'intérêt que vous y porterez, soyez assuré de toute ma reconnaissance.

Docteur Katy Jeannot, une partie de ce travail de thèse n'a été possible que grâce à vos travaux en microbiologie, je vous remercie de me faire l'honneur de participer à ce jury.

Madame Anne Geneteau, c'est un plaisir que vous ayez accepté de participer à ce jury, soyez assurée de toute ma reconnaissance.

Je remercie le **Professeur William Couet**, mon directeur de thèse, pour m'avoir accepté au sein de son unité. Pendant ces années, vous m'avez épaulé et conseillé, vous m'avez appris à prendre du recul face à ces équations et voir une étude dans sa globalité. Je vous remercie pour tous vos conseils, soyez assuré de mon profond respect.

Je remercie **Nicolas Grégoire**, mon co-directeur, pour sa patience, sa disponibilité, pour m'avoir conseillé et soutenu. J'ai appris énormément à tes côtés, sois assuré de mon profond respect.

Je remercie **Sandrine Marchand**, avec qui j'ai eu le plaisir de travailler sur les études in-vivo. Je te remercie pour ton aide, pour ta rigueur et tes conseils. Tu as toute ma gratitude.

Je remercie **Isabelle Lamarche** pour son aide précieuse. Ton calme, ta patience, ta disponibilité ont été indispensables lors de nos études. J'ai pris beaucoup de plaisir à travailler à tes cotés.

Je remercie toute l'équipe de l'U1070 pour leur aide, leurs conseils et pour la bonne ambiance : Patrice, Christophe, Jean-Christophe, Julien, Frédérique, Julian. Un merci spécial à Agnès et Murielle, pour leur amitié.

Je remercie tous mes amis doctorants de Poitiers : Alexia, Alexis, Sophie, Pamela, Guillaume, Anne-laure, Alex,… ainsi que mes amis d'Uppsala, Salim et Anne-Gaëlle pour toutes nos discussions scientifiques et pour les agréables moments que nous avons partagés.

Je remercie toute ma famille et en particulier mes parents, pour leur support et leur affection.

Contents

I. Introduction

For more than 70 years, antibacterial drugs have been regarded as the best human-made products to cure infections. Discovered in 1928 by Alexander Fleming, penicillin was the first antibacterial drug and a fabulous advance in medicine that saved millions of lives[1,2]. Due to their efficacy towards infections, antibiotics are largely consumed, in 2012, 3000 tons of antibacterial drugs were sold in EU for human medicine, and 8000 tons for veterinary medicine[3]. Unfortunately the use of antibiotics is also a major factor increasing the development of bacterial resistance. During his Nobel Prize speech in 1945[4], Alexander Fleming, warned that bacteria could become resistant to these remarkable drugs. Indeed the development of each new antibacterial drug has been followed by the detection of resistance to it. The development of resistance is a normal evolutionary process for microorganisms, but it is accelerated by the selective pressure exerted by the use of antibacterial drugs. Until 1980s the development of resistance was counteracted by discoveries of new classes of antibiotics active towards these resistant bacteria. However the last new classes of antibacterial drugs were discovered during the 1980s, and during the last 30 years bacterial resistance continued to develop without new barrier to slow this process down. The development of bacterial resistance has actually lead to bacteria resistant toward all known antibiotics, called pan resistant bacteria, that constitute a serious threat towards human health.

In 2014, the World Health Organization (WHO) published the first global report on antibiotic resistance with data from 114 countries[5]. Almost one year later, in February 2015, the European Centre for Disease Prevention and Control (ECDC), the European Food Safety Authority (EFSA) and the European Medicines Agency (EMA) published the first joint ECDC–EFSA-EMA report on consumption of antimicrobials and antimicrobial resistance in animals, food and humans[3]. The major point of these reports is that resistance of bacteria is a serious threat that is now observed in every region of the world and possesses the potential to affect anyone. Moreover these resistances concern common bacteria as *Escherichia coli*, *Klebsiella pneumoniae* and *Staphylococcus aureus*, usually encountered with health-care associated and community-acquired infections. The major cause of antimicrobial resistance in humans remains the inappropriate use of antibiotics. Therefore one of the major areas for management, control and prevention of antimicrobial resistance is the prudent use of antimicrobials[5].

This thesis focuses on the development of pharmacokinetics and pharmacodynamics models for antibiotics in order to improve the treatment of infections in critically ill patients. Pharmacometrics is a quantitative science using mathematical and statistical methods to characterize, understand, and predict drugs' pharmacokinetics (PK) and pharmacodynamics (PD). PK describes the relationship between dose and concentration with time, which takes into account drugs absorption, distribution and elimination. PD describes the relationship between concentration and effect, including therapeutic but also adverse effects. PK and PD models are linked together and resulting PK-PD models are powerful tools to describe and predict the time course of drug effect under various circumstances. These models are increasingly used to fit experimental and clinical data and some of these analyses are mandatory to the development of new drugs.

A. Bacterial resistance development

1. Mechanism of resistance

Antimicrobial resistance is the resistance of a microorganism to an antimicrobial drug that was originally effective for treatment of infections caused by it[5]. The mechanism of resistance, describing modifications occurring in sensitive bacteria to become resistant, depends mostly of the strain and of the antibiotics. At the moment numerous mechanisms have been described, that can be categorized into 4 patterns: inactivation of the antibiotic by bacterial enzyme, limitation of membrane passage by decrease of its permeability or by drug efflux pump, or modification of the drug target[6].

The first mechanism of resistance described was the inactivation of the drug before it can reach its site of action. It was encountered since 1945[7,8] with β-lactams, that were hydrolyzed by bacterial enzymes called β-lactamases. These antibiotics englobe penicillins, cephalosporins, cephamycins, carbapenems and monobactams, they are the antibiotics the most used in the world. In 2012, in UE, 2110 tons of β-lactams drugs were sold (e.g. 63 % of the antibiotics). Therefore resistance toward this class of antibiotics has a great impact on human health. In order to counteract this resistance, two strategies have been used: the development of new β-lactams with the ability to

escape β-lactamases or an association between a known β-lactam and a β-lactamase inhibitor, such as clavulanic acid, a naturally produced β-lactamase inhibitor discovered in 1976[9]. Unfortunately bacteria have endlessly produced new enzymes over time. Nowadays hundreds of β-lactamases have been discovered and classified using schemes based on function (the system of Bush-Jacoby-Medeiros[10,11]) or structure (Ambler classification[12]). One of the last enzyme discovered is a metallo-β-lactamases named 'New Delhi' which is coded by the NMD-1 gene carried on a plasmid, that provides resistance to all β-lactams[13] excepted to monobactam. This resistance presents a threat toward human health and its expansion is under surveillance by health agencies.

Another strategy employed by bacteria is to limit the passage of antibiotics through the membrane and so to limit access to their site of action. This can be obtained by modification of entry channels such as porins[14] (e.g. OmpF porin and quinolone resistance in *E. coli*[15-17] or OprD and carbapenem resistance in *P. aeruginosa*[18,19]) or by reduction of their number. Bacteria can also enhance the efflux of drug by pumping them out of the intracellular environment, via efflux systems such as MexEF-Oprn[20,21] or AcrAB–Tolc[22-24], that both contribute to multi-drug resistant in some bacterial strains. To overcome this resistance, it would be necessary to increase the dose, in order to achieve efficient concentration at the action site.

Last, bacteria can also modify the drug target (e.g. mutation in the ribosomal protein RpsL that confers resistance to streptomycin[25]). Just by itself a modification of the target can lead to low resistance but when cumulated with other mechanisms, high resistance can appear[26], that will render the drug inefficient. As an example fluoroquinolone resistance can be attributed to mutations within the drug's targets, DNA gyrase and topoisomerase IV[27,28].

2. Acquisition and transfer of resistance

Despite the variety of mechanism described, resistances can be intrinsic or acquired as a result of mutation in DNA or by horizontal transfer of genetic material (naked DNA, plasmids, bacteriophage …)[6,29].

A mutation is a spontaneous change in the DNA sequence that can change the natural expression of the gene coded by the sequence. A mutation on a gene coding for a protein can for example alter its structure and therefore provide resistance towards antibiotic targeting this protein. A mutation in the quinolone-resistance-determining-region coding for the DNA gyrase would provide a resistance toward quinolone, by modifying the structure of its action site[30,31]. A mutation can be partially characterized by the mutation rate of the bacteria which is an estimation of the rate per generation of mutation in the genome (or in specific area for a specific mutation). Derived from this definition, the frequency of mutation is the ratio of mutant in a given population at a given time[32]. The mutation rate depends on multiple factor such as the bacterial strain, the antibiotics used[33] or the environment of the bacteria[32,34].

Another way for bacteria to acquire resistance is by swapping genetic material with neighboring bacteria, this process is called horizontal gene transfer. Depending on the nature of the transfer, it is called transformation, transduction or conjugation. Transformation involves direct uptake and incorporation of short fragments of naked DNA[35]. Transduction involves transfer of DNA from one bacterium into another via bacteriophages. The size of the DNA fragment is limited by the phage head size[36,37]. Conjugation involves transfer of DNA mediated by conjugal plasmids or conjugal transposons, it requires cell to cell contact and can transfer long fragment of DNA[38]. Thus, the size of DNA fragment that can be transferred depends on the process involved and several genes providing resistance against various drugs or against one drug by different mechanisms is possible. For instance a mutation modifies only one gene already present in the bacteria and change its expression whereas extended-spectrum beta-lactamases (ESBLs) are plasmid-associated enzymes found in *Enterobacteriaceae* that provides resistance against multiple drugs[39].

Both mutation and horizontal gene transfer provoke a modification of the bacterial genome in order to provide a drug resistance. However, a resistance can also be native and the acquisition of this resistance will appear by the modulation of the expression of native genes, such as the over-expression (up regulation) of genes coding for the MexXY/OprM efflux pump that provide resistance against aminoglycosides and fluoroquinolones in *Pseudomonas*

aeruginosa[21,40], or the over-expression of pmrA gene that provide resistance against polymycins in *Pseudomonas aeruginosa*[41]. This kind of resistance is called adaptive resistance, since the resistance will be induced in the presence or drug and will reverse upon the removal of the antibiotics.

Mutation or horizontal gene transfer and adaptive resistance should not be opposed. A resistance native or obtained through mutation or horizontal transfer, reflects the mode of transmission of the resistance, whereas an adaptive resistance is a kind of resistance that mainly reflects the reversibility of the resistance. Thus resistances can be gathered in two types of antibiotic resistance, namely, heteroresistance and adaptive resistance[14,42-45]. A heteroresistance is considered stable and irreversible in a given bacteria. This resistance leads to a resistant subpopulation of bacteria which can be mixed with a sensitive subpopulation. The resistant subpopulation is usually in minority and would need higher drug concentration to be killed. An adaptive resistance describes a process evolving over time that is induced by the presence of antibiotic and that reverses upon its removal. The reversibility of a resistance in a whole population will be discussed in the next chapter (I.A.3 Fitness cost).

Moreover an adaptive resistance can be acquired by horizontal gene transfer, such as the transmission of plasmid with gene coding for efflux pump[46,47]. A mutation can also occur on gene coding for an adaptive resistance and therefore modify its comportment (e.g. Mutation in the PmrB in *Pseudomonas aeruginosa* and colistin resistance[48]). In this case the mutation may split the population into 2 sub-populations, mutants and not mutants, and each one can produce an adaptive resistance. Therefore heteroresistance and adaptive resistances may be concomitant.

3. Fitness cost

The presence of an antibiotic resistance gene clearly benefits to bacteria when the corresponding antibiotic is present. However the acquisition of antibiotic resistance may also be associated with a physiological cost for the bacteria, called fitness cost[49-51]. This cost could be due to the energetic burden caused by the synthesis of new proteins, the over expression of genes or to the production of impaired proteins necessary to the bacteria

physiology. It is usually measured by a diminution of the growth rate[52-54], but it can also induce other deleterious effect as an impaired mobility[55].

A major impact of fitness cost would be the possible reversibility of the resistance in a population when a reduction of the pressure of selection occurs. This means that without pressure of selection (e.g. without antibiotic), a sensitive population would better fit in the new environment than a resistant population. Therefore the sensitive population would grow faster and would result in a drop in the frequency of resistant bacteria measured in isolates[56]. However this reversibility is variable, in particular because the fitness cost, which varies with the bacteria and the type of resistance. It may be high[57] or very low and even inexistent[58]. But bacteria can also adapt to the fitness cost with compensatory mutation occurring to prevent the fitness cost without loss of resistance[56,59,60]. Although compensatory mutations are limited[61], the reversibility of resistance due to fitness cost remains difficult to estimate.

B. PK/PD methods used in optimizing dosing

There are both experimental and clinical evidence to support that dosing schedule may influence resistance development and that dosing regimen may be optimized by proper use of PK/PD[62-64]. In this chapter, some PD and PK/PD methods and parameters will be presented. Those include minimum inhibitory concentration, PK/PD indices and description of the full time course of concentration and effect using PK/PD modeling.

1. Minimum inhibitory concentration (MIC)

The MIC is defined as the lowest static concentration (constant concentration with time) of antibiotics that inhibits the visible growth of bacteria after overnight incubation. The method consists in the preparation of a range of antibiotic concentrations, usually two-fold serial concentration dilutions, followed by the addition of an inoculum corresponding to approximately $5x10^5$ colony-forming units (CFU)/mL. The tubes are then incubated depending on the strain for 18 to 24 hours. Then the MIC is defined as the lowest concentration of antibiotic at which there is no turbidity (no visible growth) of the microorganism, which usually happens at approximately 10^7 CFU/mL[65].

During several decades MIC was predominantly used to predict antibiotic efficacy and dosage regimen were adjusted to obtain minimal plasma concentrations equal or higher than MIC. It is still consider as a 'gold standard' by microbiologists to determine bacterial susceptibility to antimicrobials[65]. Despite its popularity MIC presents several disadvantages as a PD parameter. It is a threshold value estimated by visual inspection observation of a two-fold serial concentration dilution which is poorly accurate. Furthermore MIC is determined at only one time point and therefore it neither provides information on the time-course of bacterial killing[66-68] nor on the emergence of resistance[69,70]. Another limitation is that MIC is determined at a single and relatively low initial bacterial inoculum (i.e. usually in the absence of resistant populations)[65], and do not provide information on a potential inoculum effect (e.g. the possible change of MIC with high inoculum[71]).

However the MIC remains a parameter easy to estimate and provides a quick comparison of the sensitivity of a particular strain toward various antibiotics. It can also be used in association with the mutant prevention concentration (MPC)[72], the minimal concentration that allows no mutant recovery when more than 10^{10}cells are applied to drug-containing agar[73]. The MIC_{99} and the MPC can be used to define a mutant selection window, corresponding to a range of concentrations that would kill drug sensitive bacteria but not the resistant one and therefore potentially induce selection pressure[64].

To overcome some of the MICs limitations, antimicrobial agents PD can be better studied by observing changes in CFU over time in the presence of a range of drug concentrations[70,74-77].

2. *In-vitro* time-kill studies

a) The different settings

Time-kill studies are performed *in-vitro* to assess the change of CFU with time after an initial bacterial inoculum has been exposed to various antibiotic concentrations. These experiments are easier to perform than *in-vivo* experiments, and allow a greater flexibility in the study design. Depending on the aim of the study, the design can be drove to assess the effect of one or several antibiotics in combination[78,79], to evaluate the influence of the

inoculum size on the drug effect[74,80], or the effect of changing broth composition to assess the mechanism of resistance of a bacteria[81] …. . A wide variety of experimental setups have been described and thanks to a controlled environment, results are not affected by as many factors of variability as during *in-vivo* experiments (immune system or drug disposition, local infection…). However extrapolation of *in-vitro* results to the *in-vivo* setting should be done with caution.

Noticeably *in-vitro* infection experiments [82] may use static[70,74-77] or changing antibiotic concentrations to simulate the dynamic time-course of concentrations observed in patients [69,83-85]. It is also possible to mix these approaches.[86-88] These experimental settings provide information on the time-course of antibiotic effects and the development of resistance and are well suited to develop PK/PD models that will be presented later [89]. The latter mathematical models can characterize bacterial killing and resistance [67] and optimize antibiotic dosage regimens.

Static concentration time-kill studies [82] are efficient and cost-effective and allow studying a large range of antibiotic concentrations. Yet they present several potential drawbacks. Antibiotics such as β-lactam antibiotics are not very stable and may be degraded with time, which needs to be considered and possibly corrected for, seriously complicating the approach. Another potential problem comes from the fact that growth medium nutrients may get depleted or/and toxic bacterial metabolites may accumulate over time, which may have an effect on bacterial growth or death. Therefore performing static concentration time-kill studies over more than 24 h may require to change the growth medium regularly (e.g. every 24 h), increasing the amount of work.

Dynamic *in-vitro* infection settings such as the one-compartment and hollow-fiber systems can mimic human PK [67], by changing drug concentrations thanks to the introduction of fresh broth medium using various pumps. The control of these flow rates permits to simulate different half-lives of drugs and also allows the elimination of toxic bacterial metabolites. Therefore, these dynamic experiments are often run over several days or even weeks [90], [91] and typically use multiple dosing [92]. However the simplest systems use filters leading to clotting problems which depending on the bacteria may be almost impossible to solve. The advantage of hollow-fiber systems is that they do not present this limitation. However their disadvantage is their elevated cost. Therefore

these dynamic *in-vitro* settings may complement and validate results of initial experiments conducted with static concentration time-kill conditions before translation to animal studies and ultimately to patients.

b) Quantification of bacterial count

Time-kill studies are based on the quantification of bacterial counts over time. For bacterial quantification, various dilutions are prepared for each sample and spread onto agar plates either manually or automatically with a spiral platter. After 18 to 24 h of incubation at a given temperature (usually 37°C), the number of colony is counted manually or with an automated colony counter[93,94]. An image analysis of a plate photography may also be done. The lower limit of quantification is usually in the range of 10–400 CFU/ml[70,75,95]. However the antibiotic present in the broth may be plated on agar along with bacteria, especially after bacteria have been exposed to high concentrations, , inhibits bacteria growth and therefore bias the bacteria count. This phenomenon is known as the carryover effect[96]. To minimize this effect the sample may be centrifuged and then reconstituted with sterile saline to the original volume. The characterization of heteroresistance, also called population analysis profile (PAP), can be performed by counting irreversible resistant subpopulations of bacteria, onto agar plates supplemented with the corresponding antibiotic at different concentrations [74,97].

Bacterial count on agar plates is the gold standard method to determine the bacterial load. Alternative methods of quantification exist, such as the real time PCR[98] or flow cytometry[99,100], but they require specific equipment. These methods require an extraction of the bacteria from the environment (broth for *in-vitro* studies and tissues for *in-vivo* studies) and the sample may be altered during this analytic process. The bioluminescence technique is a non-destructive, real-time reporter of bacterial metabolism that can be used to monitor the effect of antimicrobials and to quantify the bacteria[101,102]. This technique uses microorganisms expressing the lux operon which emit light, as a result of the activity of bacterial luciferase in metabolically active bacteria[103,104]. The advantages of this imaging technique is that it can be used for *in-vitro*[102,105,106] and in-vivo[107-111] studies, without killing the animal at

each time of measure. However an imaging device is needed and the insertion of the lux operon may modify the sensibility of the bacteria to the antibiotic. Yet these bioluminescent strains may be used for academic research.

3. PK/PD indices

In the 1940s and 1950s, Eagle et al.[112-114] investigated the dose-activity relationship between bactericidal antibiotics and bacteria, and identified different patterns of bactericidal activity. The first pattern was observed with penicillin that showed no improvement of bactericidal activity despite increasing the dosage above a certain level. This pattern corresponds to time-dependent antibiotics such as in β-lactams and macrolides. The saturation of the killing rate occurs at relatively low concentrations, usually four or five times the MIC. The second pattern was observed with aminoglycoside, for which an increase of the antibiotic concentration led to a more rapid killing of the bacteria. This corresponds to concentration-dependent antibiotics, including aminoglycosides and fluoroquinolones. The investigations made by Eagle et al. were the first demonstration that MIC is not enough to describe bacterial activity and that the pharmacokinetics of the antibiotics need to be taken into account to have a better understanding of the antibiotics activity and to define precise targets. Vogelman et al[115] and Craig[66] investigated the PK/PD relationship of antibiotics and defined three PK/PD indices based on a measure of the drug exposure and the MIC of the bacteria. The terminology of these PK/PD indices have been standardized[116] into fAUC/MIC, fC_{max}/MIC and fT>MIC. The fAUC/MIC is the area under the unbound concentration–time curve over 24h divided by the MIC; fC_{max}/MIC is the unbound peak concentration divided by the MIC and $fT_{>MIC}$ is the cumulative percentage of time over 24h when the unbound drug concentration is above the MIC.

The determination of the best PK/PD index describing the effect of an antibiotic on a bacteria is obtained by plotting bacterial counts (e.g. log10 CFU/mL) measured at one specified time (e.g. 24h) versus the value of each the three PK/PD indices. The classification of the antibiotic as “time dependent” or “concentration dependent”

depends on the index that better fits the pharmacodynamic endpoint when assuming the following sigmoidal EMAX model:

$$E = E_0 - \frac{PD_{max} * X^{\gamma}}{EX_{50}^{\gamma} + X^{\gamma}}$$ **Equation 1**

Where E is the summary PD endpoint (e.g. log10 CFU/mL), E_0 is the effect representing the value of the PD endpoint without drug treatment, X is one of the PK/PD indices, PD_{max} is the maximum effect obtained when increasing exposure results in no further killing, EX_{50} is the magnitude of X that is needed to achieve 50% of PD_{max} and γ is the sigmoïdicity factor.

Numerous studies have been conducted mostly in mice in order to identify the best PK/PD indices for antibiotics on pathogens using different conditions of experimentation. These studies showed that the activity of β-lactams was dependent on fT>MIC[115,117,118], that of aminoglycosides and fluoroquinolones dependent on either fCmax/MIC or fAUC/MIC [115,119,120] and that of glycopeptides and macrolides was considered as dependent on fT>MIC[66] although more recent studies suggest that they rather depend on fAUC/MIC[121] .

At the moment PK-PD indices are considered as the gold standard to evaluate the PK-PD of antibiotics and their evaluation is recommended by the regulatory agencies (EMA, FDA)[122] for new antibiotics. Once the PK/PD index of an antibiotic for a bacteria is determined, a target is defined in order to achieve the desired bactericidal effect (e.g.: fCmax/MIC > 6 or (fT >MIC)>80%). Then simulations of the antibiotic concentrations versus time profiles can be performed, using previously estimated PK parameters, in order to select a dosing regimen that permits to attain the defined target. These simulations can also take into account the variability in PK and in PD (MIC distribution) through Monte-Carlo methods.

4. PK/PD modelling

The PK/PD indices are summary endpoints based on the MIC, which do not provide any information on the time course of antimicrobial activity. Therefore a lot of information is lost in the process of generating these endpoints,

such as the regrowth of bacteria that can be observed after an initial decay although the antibiotic concentration is kept constant, and suggesting a changing effect with time. These complexities can be analyzed by a modeling approach that allows description of the full time course of antimicrobial activity.

The simplest PK/PD model was originally proposed by Zhi et al[123]. It is composed of a compartment representing a single bacterial population (S) with and exponential growth characterized by a growth rate constant (k_{growth}) and a natural death rate constant (k_{death}), as presented in Equation 2:

$$\frac{dS}{dt} = \left[k_{growth} - k_{death}\right] \cdot S \qquad \textbf{Equation 2}$$

Where S is the bacteria concentration.

However there are usually insufficient data to separately estimate the growth and the natural death rate constants, therefore the apparent growth rate constant ($k_g = k_{growth} - k_{death}$) is commonly reported in PK/PD studies[86,120]. In the absence of antibiotics bacteria grow until a stationary bacterial level (Popmax) is reached. This self-limiting growth can be modeled by a logistic function[89,124], as presented in Equation 3.

$$\frac{dS}{dt} = \left[k_g \cdot \left(1 - \frac{S}{Popmax}\right) \right] \cdot S \qquad \textbf{Equation 3}$$

The antibacterial effect is generally modeled by a sigmoïdal Emax model, that could either inhibit the bacterial growth[125,126] (Equation 4) or increase the bacterial killing[127,128], as presented in Equation 5.

$$\frac{dS}{dt} = \left[k_g \cdot \left(1 - \frac{Imax \cdot C}{IC_{50} + C}\right) \cdot \left(1 - \frac{S}{Popmax}\right) \right] \cdot S \qquad \textbf{Equation 4}$$

where Imax is the maximal rate constant of growth inhibition and IC50 the antibiotic concentration yielding 50% of kmax.

$$\frac{dS}{dt} = \left[k_g \cdot \left(1 - \frac{S}{Popmax}\right) - \frac{kmax \cdot C}{KC_{50} + C} \right] \cdot S \qquad \textbf{Equation 5}$$

where kmax is the maximal rate constant of bacterial killing and KC50 the antibiotic concentration yielding 50% of kmax.

The emergence of resistance can be described by two different approaches. The most frequent approach is to assume that the total bacterial population is composed of several distinct subpopulations which differ in drug susceptibility[83,129,130]. The most part of the bacterial population is considered to be sensitive. A bacterial regrowth would be observed when the drug concentration is sufficient to kill the sensitive bacteria but not the resistant ones. An initial decay, attributed to the killing of the sensitive subpopulation, would be observed until the growing resistant population becomes predominant and induces a regrowth. The resistant subpopulation can be considered as present in the starting inoculum, when high inoculum is used[83] (Equations 6 and 7).

$$\frac{dS}{dt} = \left[k_g \cdot \left(1 - \frac{S+R}{Popmax}\right) - \frac{kmax \cdot C}{KC_{50} + C} \right] \cdot S$$ With Initial S = Inoc*(1-PropR) **Equation 6**

$$\frac{dR}{dt} = \left[k_{gR} \cdot \left(1 - \frac{S+R}{Popmax}\right) - \frac{kmaxR \cdot C}{KC_{50} + C} \right] \cdot R$$ With Initial R = Inoc * PropR **Equation 7**

Where K_{gR} is the apparent growth rate constant of the resistant population; kmaxR, the maximal rate constant of bacterial killing in the resistant population; Inoc, the size of the inoculums and PropR, the proportion of resistant in the inoculum.

An alternative approach consists in considering a pure inoculum with only one bacterial population and to describe the mutation of these bacteria with a first order mutation rate[83].

$$\frac{dS}{dt} = \left[k_g \cdot \left(1 - \frac{S+R}{Popmax}\right) - \frac{kmax \cdot C}{KC_{50} + C} \right] \cdot S - MutF.S$$ With Initial S = Inoc **Equation 8**

$$\frac{dR}{dt} = \left[k_{gR} \cdot \left(1 - \frac{S+R}{Popmax}\right) - \frac{kmaxR \cdot C}{KC_{50} + C} \right] \cdot R + MutF.S$$ With Initial R = 0 **Equation 9**

Where MutF is the mutation rate of the sensitive bacteria. Some models also used a first rate constant describing the transfer back from R to S. However most of these models estimated this constant negligible compared to mutF and set its value to zero[75,83].

Mostly both approaches describe the bacterial resistance as an irreversible phenomenon. Resistant subpopulation is modelled as being less sensitive toward the antibiotic than the sensitive (wild) subpopulation. The resistance of the bacteria can be modelled through a lower kmax[131] , a greater KC_{50}[125] or both[83].

An adaptive resistance model has been proposed previously by Tam et al.[90] and also by Nielsen et al[132]. In this case, all bacteria are initially considered sensitive. Decay is observed, when bacteria are put in presence of antibiotics. Concomitantly a gradual development of resistance occurs over time in function of the antibiotic concentration. The resistance gradually decreases the efficiency of the antibiotics towards bacteria until it becomes inferior to the natural growth rate and consequently a regrowth is observed. When treatment is interrupted the resistance phenomenon can be reversed. Nielsen et al.[132,133] described this adaptive process with two compartments, one describing the hypothetical amount associated to the absence of adaptation, AROff, initially fixed to 1 and one describing the amount associated to the adaptation, Aron, initially fixed to 0. Upon colistin exposure transfers occurred between these two amounts, which affects the fraction of amounts in the two compartments. The transfers between AROff and ARon for adaptive resistance are described in Equations 11 and 12. K_{on} and k_{off} describe the rate of development and reversal of adaptive resistance, respectively.

$$k_{on} = k_{onslope} * C^{\gamma} \qquad \textbf{Equation 10}$$

Where $K_{onslope}$ is the resistance rate constant in the presence of colistin.

$$\frac{dAR_{off}}{dt} = k_{off} * AR_{on} - k_{on} * AR_{off} \qquad \text{With initial } AR_{off} = 1 \qquad \textbf{Equation 11}$$

$$\frac{dAR_{on}}{dt} = k_{on} * AR_{off} - k_{off} * AR_{on} \qquad \text{With initial } AR_{off} = 0 \qquad \textbf{Equation 12}$$

In case of adaptive resistance the antibiotic effect is reduced by a function of the proportion of resistance development (Aron) powered by a parameter β (Equation 13).

$$\frac{dS}{dt} = k_g * \left(1 - \frac{S}{Popmax}\right) * S - \frac{\text{kmax} \cdot \text{C}}{\text{KC}_{50} + \text{C}} * (1 - AR_{on}{}^{\beta}) * S \qquad \textbf{Equation 13}$$

The antimicrobial effect can also be modelled in a more mechanistic way, as performed by Bulitta et al[74], in a model that describes the competitive binding between colistin, Mg^{2+} and Ca^{2+} to the outer bacterial membrane. Another example is the modeling of the inoculum effect, defined as the reduced antibacterial drug effect observed against high bacterial population[134]. Nielsen et al.[75,132] described the inoculum effect with a model that assumed that growing bacteria can become resting (non-growing) as a function of the total density, whereas Bulitta et al.[74,131] used a model describing cell-to-cell communication associated with quorum sensing.

C. Colistin the last line of defense

Colistin, also known as polymycin E, is a cationic antimicrobial peptide, produced by some strains of bacteria, e.g. *Bacillius polymyxa*. It is composed of at least 30 different compounds, mainly colistin A and colistin B[135,136] and it is administered as colistin methanesulfonate (colistimethate), its inactive prodrug. Having entered clinical use in 1959, colistin has been on the market for more than fifty years, but due to concern about nephrotoxicity and neurotoxicity[137,138], it was replaced by antibiotics safer to use in the 1970s. However in the last decade colistin has regained interest toward the medicine community for two reasons. Firstly bacterial resistance towards commonly used antibiotics have largely increased in all regions of the world during the last years in common bacteria. However due to its replacement in the 1970s, colistin did not exercised a pressure of selection during the last 30 years and still exhibits rapid and concentration dependent bacterial activity against Gram negative bacteria notably *Pseudomonas aeruginosa*. Secondly there is a limited number of alternatives due to the dry antimicrobial drug development pipeline leading to limited options against multidrug resistant bacteria. Nowadays colistin is used in the treatment against multidrug-resistant Gram-negative bacteria (MDR-GNB), including *Acinetobacter baumannii*,

Pseudomonas aeruginosa and *Klebsiella pneumonia* [135,137,139]. However having entered clinical use in 1959, CMS/colistin was not developed with the same procedures that are now mandated by international drug regulatory agencies. As a result PK and PD information required to underpin prescribing recommendations in the product information is lacking. Colistin is prescribed in special populations such as critically ill patients whom specific illness can alter the pharmacokinetics of the drug and therefore its efficiency. Colistin and CMS can been removed from plasma in patients undergoing hemodialysis. CMS can also be aerosolized in patients with cystic fibrosis that suffer of pulmonary infection.

1. PK of colistin

The reliability and the accuracy of PK study depend on the quality of the data collected and especially on the analytical methods used to measure drug concentrations. CMS is unstable in plasma and common matrices and can spontaneously convert into colistin[140]. Therefore analytical assays should give both precise and specific measures of colistin, *i.e.* distinguish colistin from its prodrug, CMS. Indeed CMS and colistin are undistinguishable by microbiological assay[141] that was originally used[142] . The recent development of chromatographic procedures such as HPLC with fluorimetric detection[143] or liquid chromatography–tandem mass spectrometry (LC-MS/MS)[144,145] has permitted more accurate PK studies. However confusions were made due to the multiple ways the CMS doses were reported in publications. In Europe and Asia, doses are expressed in number of internal units (UI) or/and in number of milliGrams of the chemical CMS (i.e. CMS sulfate). In the remaining global regions (USA, Australia …) doses are expressed in number of milliGrams of colistin base activity (CBA), based on microbiological standardization[146,147]. One milliGram of CBA is not equivalent to one milliGram of CMS sulfate, thus doses expressed in milliGrams can be misunderstood depending on the region of interest. Recommendations to authors have been made during the First International Conference on Polymyxins (Prato, Italy): to cease reporting doses in terms of milliGrams of CMS and to provide equivalence of the dose in the others units, such as one million of international units (MIU), are equivalent to 30 mg of colistin-based activity (CBA) or 80 mg of CMS sulfate[147].

a) PK in animals

The first accurate assessments of colistin and CMS PK were obtained in rats after intravenous administration of colistin in 2003 [148], and after intravenous administration of CMS in 2004[149]. The protein binding of the colistin was determined by equilibrium dialysis and the unbound fraction of colistin estimated at 43-45%. A difference of binding between colistin A and B was noted with respectively a free fraction at 36% and 52%. The colistin elimination half-life in rats was 74.6 ± 13.2 min with less than 1 % of colistin being excreted unchanged in urine after colistin administration. However after CMS administration relatively large amounts of colistin were recovered in urine. Therefore the authors concluded that most of the colistin measured in urine was the result of post-excretion CMS hydrolysis. It was estimated that only 6.8% of the CMS dose was converted systemically into colistin. Finally CMS elimination half-life was estimated at 23.6 ± 3.9 min that was significantly shorter than that of colistin. These results were confirmed by other groups[150], with some discrepancies about the exact fraction of CMS converted into colistin, estimated at 15.5 % by Marchand et al[150], confirming however that only a limited fraction of the CMS dose is actually converted into colistin. Marchand et al[151] have also investigated the influence of the route of administration in rats, and estimated that after nebulization of CMS , two thirds of the CMS dose were directly absorbed in the systemic circulation, and one third was converted into colistin pre-systemically.

b) PK in critically ill patients

The first pharmacokinetic study performed in patients using HPLC to measure colistin concentrations was performed in 2003 by Li et al[152] followed by Markou in 2008[153]. These two studies were performed in critically ill patients, however one study simply described CMS and colistin PK at steady state and the other measured only colistin. A more complete PK study of colistin and CMS in critically ill patient was performed in 2009 by Plachouras et al[154]. In this study, colistin and CMS concentrations were measured in 18 patients after administration of CMS at 3 MUI every 8h. The model used to describe the concentrations was composed of 2 compartments for CMS and 1 compartment for colistin. The key findings of this study were a colistin half-life longer than that of CMS (14.4 h and 2.3 h respectively), a colistin plasma peak concentration achieved several hours (7h on average) post CMS administration, and a slow increase of colistin concentration after CMS administration. Therefore to attain a

threshold concentration at 2 mg/L, the authors have suggested the use of a 9 MUI loading dose (equivalent to 720 mg of CMS sulfate or 270 mg of CBA) . These results were confirmed in 2011 by Garonzik at al.[155] in a PK study conducted in 105 critically ill patients. In addition to the large number of patients included, Garonzik was able to identify some covariates explaining the inter-individual variability of some PK parameters such as the creatinine clearance on the clearances of CMS and colistin or the body weight on the volume of distribution of CMS. Although this study was conducted at steady-state and did not include concentrations measurements after the first CMS administration, the authors suggested a dosage regimen with a loading dose based on the weight and a maintaining dose based on the creatinine clearance. In 2011, Couet et al.[156] performed the first PK study in healthy volunteers, with measures of colistin and CMS concentrations, in plasma and urine. The fraction of CMS excreted unchanged in urine was estimated for the first time in human, i.e. 70 %. Moreover in this study the authors described a relatively early colistin peak since time to peak was close to 2h post CMS administration. This observation was also made in 2014 by the same group in a study included 73 critically ill patients[139]. In this study, the authors estimated that the apparent volume of distribution of colistin was approximately 7-folds lower than previously published by Plachouras et al[154], resulting in a shorter estimation of the colistin half-life (3.2 h vs 14.4h). This short half-life suggests that colistin steady state should be reached in few hours, which from a PK standpoint do not support the use of a loading dose (LD). However the use of a LD could be justified from a pharmacodynamics point of view since it should lead to high peak concentrations of colistin and therefore improve its efficiency, which constitutes the rational for such front-loading strategies[157].

2. PD of colistin

a) Mechanism of action

Colistin, as a member of the polymycin family, is active against Gram negative bacteria. It presents a bactericidal effect with rapid killing rate[138,158]. Polymycins interact with the Lipopolysaccharides (LPS) of the outer membrane of the Gram negative bacteria[74,138,159] and displace Mg^{2+} and Ca^{2+} ions cross-bridging between adjacent negatively charged LPS[74,158,159]. It results in an increased permeability of the outer membrane and allows uptake of a variety of

molecules including the drug itself, as described by Hancock, in a self-promoting uptake model[160]. The polymycins also interact with the phospholipid bilayer of the cytoplasmic membrane[160-162] forming channels. The modification of the cytoplasmic membrane permeability leads to leakage of cytoplasmic molecules and to bacteria death.

b) PD parameters values

As for other polymyxins, colistin exhibits a concentration dependent antibacterial effect[138]. It exhibits a median MIC at 0.5 µg/mL for *Acinetobacter baumannii* and *Klebsiella pneumonia (with a MIC_{90} at 1 µg/mL)* strains and presents a median MIC at 1 µg/mL for *Pseudomonas aeruginosa* strains (with a *MIC90 at 2µg/mL)*[163]. The effect of colistin on *Pseudomonas aeruginosa* has been correlated to fAUC/MIC in both *in-vitro*[95] and in-vivo studies[164]. The target breakpoint has been estimated *in-vitro* between 22.6 and 30.4 depending on the strain [95]. *In-vivo*, fAUC/MIC targets required to achieve a 2-log kill were estimated between 27.6 and 36.1, in a thigh infection model, while the corresponding values were 36.9 to 45.9 in a lung infection model[164]. For example, a fAUC/MIC of 27.6 is equivalent to an average total concentration at steady state of 4.6 µg/mL, considering a MIC of 2 µg/mL and a free fraction of 50 %.

Although these estimations can help to determine effective dosage regimens, they do not provide any information about the emergence of resistance over time. Some PK/PD modeling studies have been performed in order to describe the full time course of the colistin efficacy. Bulitta et al[74], have built a model that describes the competitive binding between colistin, Mg^{2+} and Ca^{2+} to the outer membrane of *Pseudomonas aeruginosa.* In their mechanistic model they also described the resistance to colistin with the presence of three subpopulations in the inoculum. By contrast Mohamed et al.[133] described the development of resistance as an adaptive process that is developing over time and that can reverse. This later model was used to perform PK/PD simulations leading to recommend the use of a fixed loading dose followed by an 8 or 12 hourly maintenance dose.

3. Resistance to colistin

In 1966, Brown et al. demonstrated that low concentrations of Mg^{2+} decrease the activity of polymycin on *Pseumonas Aeruginosa*[81], therefore they described the first resistance to polymycin mediated by the growth condition of the bacteria. Seven years later, Gilleland et al. reported the first polymyxin adaptive resistance phenotype on *Pseudomonas aeruginosa*[165]. They described the acquisition of resistance to polymycins in bacteria growing in non-Mg^{2+}-limited medium containing polymycins. The resistance was correlated with architectural change in the outer membrane that decreases its permeability and therefore protects the cytoplasmic membrane toward polymyxins and antimicrobial peptides. They also described the loss of the resistance when the resistant bacteria grew in a medium without polymycins, and described the reversible phenotype of the resistance.

Since then, many studies have focused on the mechanism of the adaptive resistance. Two systems have been identified to play a major role in the resistance to polymycin: the PhoP/PhoQ system[166] or the PmrA/PmrB system[41,167-170]. Both systems are able to stimulate the transcription of PmrA-activated genes, conducting to a modification of the LPS by addition of 4-amino-4-deoxy-L-arabinose (L-Ara4N) on the lipid A [167] . This modification decreases the negative charge of LPS (initial site of action of colistin) and causes polymycin resistance. Resistance to colistin and to polymycin have been identified and characterized in several Gram negative pathogens such as: *Escherichia coli* [171,172], *Salmonella enterica*[173], *Pseudomonas aeruginosa* and *Acinetobacter baumannii.*

II. Aims

The general aim of this thesis was to describe the pharmacokinetic (PK) and the pharmacodynamics (PD) of colistin using a PK/PD modeling approach in order to provide better a understanding of PK and PD process to guide optimization of dosing regimens in some specific populations and different routes of administration.

The specific aims were:

- to describe the pharmacokinetics of colistin after CMS aerosol delivery for treating pulmonary infections in critically ill patients
- to assess colistin pharmacokinetics (PK) in intensive care unit patients requiring intermittent HD (ICU-HD)
- to compare the ability of static and dynamic *in-vitro* infection models to identify the "true " PK/PD model and to estimate model parameters accurately and precisely, using simulations
- To develop a semi-mechanistic PD model to characterize the reversible and/or non-reversible resistance of *Pseudomonas aeruginosa* occurring in the presence of colistin, using bioluminescence imaging.

III. Studies

This thesis is based on the following papers:

- Matthieu Boisson, Matthieu Jacobs, Nicolas Grégoire, Patrice Gobin, Sandrine Marchand, William Couet, Olivier Mimoz. 2014. **Comparison of Intrapulmonary and Systemic Pharmacokinetics of Colistin Methanesulfonate (CMS) and Colistin after Aerosol Delivery and Intravenous Administration of CMS in Critically Ill Patients.** Antimicrob Agents Chemother **58:**7331-7339.
- M. Jacobs, N. Grégoire, B. Mégarbane, P. Gobin, D. Balayn, S Marchand, O. Mimoz , W. Couet. **Population pharmacokinetics of colistin methanesulphonate (CMS) and colistin in critically ill patients with acute renal failure requiring intermittent haemodialysis**. (In review in AAC)

- M. Jacobs, N. Grégoire, W. Couet, J. B. Bulitta. **Distinguishing Antimicrobial Models with Different Resistance Mechanisms via Population Pharmacodynamic Modeling**. (In review in PLOS computational biology)

- Jacobs M., Grégoire N., Chauzy A., Jeannot K., Nielsen E.I., Marchand S., Friberg L.E., Plésiat P., Couet W. **Pharmacokinetic – Pharmacodynamics modelling of the quickly occurring and partially reversible adaptive resistance of *Pseudomonas aeruginosa* to colistin using a bioluminescent strain** *in-vitro. (In manuscript)*

A. Colistin and aerosol delivery

Comparison of Intrapulmonary and Systemic Pharmacokinetics of Colistin Methanesulfonate (CMS) and Colistin after Aerosol Delivery and Intravenous Administration of CMS in Critically Ill Patients

Matthieu Boisson,[a,b] Matthieu Jacobs,[b,c] Nicolas Grégoire,[b,c] Patrice Gobin,[a,b] Sandrine Marchand,[a,b,c] William Couet,[a,b,c] Olivier Mimoz[a,b,c]

CHU Poitiers, Poitiers, France[a]; INSERM U1070, Poitiers, France[b]; Université de Poitiers, Poitiers, France[c]

Abstract

Colistin is an old antibiotic that has recently gained a considerable renewal of interest for the treatment of pulmonary infections due to multidrug-resistant Gram-negative bacteria. Nebulization seems to be a promising form of administration, but colistin is administered as an inactive prodrug, colistin methanesulfonate (CMS); however, differences between the intrapulmonary concentrations of the active moiety as a function of the route of administration in critically ill patients have not been precisely documented. In this study, CMS and colistin concentrations were measured on two separate occasions within the plasma and epithelial lining fluid (ELF) of critically ill patients (n= 12) who had received 2 million international units (MIU) of CMS by aerosol delivery and then intravenous administration. The pharmacokinetic analysis was conducted using a population approach and completed by pharmacokinetic-pharmacodynamic (PK-PD) modeling and simulations. The ELF colistin concentrations varied considerably (9.53 to 1,137 mg/liter), but they were much higher than those in plasma (0.15 to 0.73 mg/liter) after aerosol delivery but not after intravenous administration of CMS. Following CMS aerosol delivery, typically, 9% of the CMS dose reached the ELF, and only 1.4% was presystemically converted into colistin. PK-PD analysis concluded that there was much higher antimicrobial efficacy after CMS aerosol delivery than after intravenous administration. These new data seem to support the use of aerosol delivery of CMS for the treatment of pulmonary infections in critical care patients.

Introduction

Aerosol delivery of antibiotics for the treatment of pulmonary infections has recently gained considerable attention, and approval has been obtained for this administration route worldwide for several compounds, including tobramycin (1, 2), aztreonam (3), and colistin (4, 5). Dry-powder formulas have been optimized, and at the same time, a new generation of pocket nebulizers was developed to favor aerosol delivery of antibiotics in ambulatory patients, such as a cystic fibrosis patient, in order to improve their quality

of life. However, aerosol delivery of antibiotics for the treatment of nosocomial pulmonary infections is also quite popular. And yet, there is no general consensus regarding the administration method, and in practice, it is quite difficult to provide clinical evidence demonstrating the superiority of the aerosol delivery of antibiotics over that of other routes of administration in critically ill patients. Therefore, a comparison of antibiotic concentrations at the site of infection after intravenous administration and aerosol delivery, followed by predictions of the resulting antimicrobial activity using modern pharmacokinetic-pharmacodynamic (PK-PD) modeling approaches, may provide valuable information. Numerous physicochemical parameters, including particle size, aerodynamic diameter, density, and charge, which are in part determined by the type of aerosol generator, determine how much of the drug may reach the alveolar space after aerosol delivery. However, patient physiopathology, such as impaired expiratory airflow or atelectasis, may also have a major impact on antibiotic distribution within the lung after aerosol delivery. Overall, only a limited fraction of the inhaled dose is likely to reach the target, and antibiotic characteristics, such as solubility, permeability, and affinity for efflux transport system present at the blood alveolar barrier, will also determine the intrapulmonary concentration-versus-time profile. Eventually, PK-PD characteristics that vary by antibiotic must also be considered for the optimization of aerosol treatment. Even with this relative complexity, promising results have been obtained with colistin after nebulization in rats by several groups, including Marchand et al. (6) and Yapa et al. (7), and the objective of this study was to describe the pharmacokinetics of colistin after CMS aerosol delivery for treating pulmonary infections in critically ill patients.

MATERIALS AND METHODS

Study population. The study was performed in 12 adult patients hospitalized in the intensive care unit (ICU) of the University Hospital of Poitiers, France, who developed ventilator-associated pneumonia during their stay between October 2011 and August 2012. Patients were eligible if they were between 18 and 85 years of age, were intubated, and had a pneumonia caused by Gram-negative bacteria sensitive to colistin. Patients were not eligible if they had received colistin within 7 days prior to the study, had creatinine clearance of <30 ml/min, or had a personal or family history of myasthenia. At the study onset, the following data were collected: age, sex, weight, diagnosis on admission, serum urea, serum creatinine, simplified acute physiology score (SAPS II), and sequential organ failure assessment (SOFA) score. Creatinine clearance was calculated according to the Cockroft-Gault formula (8). The study protocol was approved by the local ethics committee (CPP Ouest III, approval no. 2009009578-28). In all patients, informed consent was obtained from their nearest relatives prior to the initiation of the study. A total of 6 women and 6 men were enrolled. Their demographic, clinical, and biological data are shown in Table 1.

TABLE 1 Patient demographic and clinical characteristics

Patients	Age (years)	Gender	Weight (Kg)	Diagnosis at admission	SOFA score[α]	SAPS II score[α]	Creatinine clearance[β] (mL/min)
1	44	F	53	Respiratory decompensation	2	19	156
2	66	F	88	Tracheo-œsophageal fistula	3	47	125
3	18	M	59	Craniocerebral trauma	10	40	170
4	59	M	65	Cardiopulmonary arrest	4	33	120
5	72	F	65	Pneumonia	9	43	85
6	68	F	77	Peritonitis	11	42	66
7	64	M	115	Peritonitis	1	38	104
8	36	M	90	Multiple trauma	2	17	250
9	43	F	70	Multiple trauma	11	47	133
10	74	M	88	Cardiopulmonary arrest	9	67	88
11	74	F	86	Tracheo-œsophageal fistula	3	36	111
12	33	M	92	Thoracic injury	3	22	205
Mean ± SD	**54 ± 19**		**79 ±17**		**6 ± 4**	**38 ±14**	**134 ± 53**

[α]At study onset

[β]According to Cockroft and Gault formula

CMS administration. The patients were treated with CMS (Colimycine; Sanofi-Aventis, Paris, France). Treatment was initiated with a 2-million international unit (MIU) dose of CMS, corresponding to 160 mg of CMS sulfate or 60 mg of colistin-based activity (CBA) (9), dissolved in 10 ml of saline and nebulized over 30 min via a vibrating mesh nebulizer (Aeroneb Pro; Aerogen, Galway, France). Thus, 8 h later, the same dose of CMS was dissolved in 50 ml of saline and infused intravenously (i.v.) over 60 min. Intravenous administrations were

then repeated every 8 h until the end of treatment or therapeutic deescalation. The CMS solutions were prepared extemporaneously.

Sampling procedures. (i) Blood samples. Blood samples were collected immediately before and at 0.33, 0.66, 1, 1.5, 2, 2.5, 3, 4, 5, 6, 7, and 8 h after the beginning of aerosol delivery and after starting the first intravenous infusion via a distinct line. Two extra blood samples were collected at steady state at the same time as the bronchoalveolar lavage (BAL) fluid. The blood samples were immediately centrifuged (3,000 X *g* for 10 min) at 4°C, and the plasma was stored at −80°C until analysis.

(ii) BAL fluid samples. Mini-bronchoalveolar lavage (mini-BAL) was performed as previously described (10). Mini-BAL was performed with a 16-French (Fr) double sterile catheter (BAL, KimVent; Kimberly-Clark, Roswell, GA) inserted through the endotracheal tube. Two 20-ml aliquots of saline solution were instilled and then immediately aspirated with a syringe; these two BAL fluid samples were pooled and rapidly centrifuged (at 3,000 X *g* for 10 min), and the supernatants were stored at −80°C until analysis. For patients 1 to 6, mini-BAL was performed at 1 h and 3 h after initiating the aerosol delivery and then at steady state, 2 to 3 days later, and 1 h and 3 h after starting the n^{th} intravenous infusion ($7 < n < 12$). For patients 7 to 12, mini-BAL was performed at 5 h and 8 h after initiating aerosol delivery and then at steady state, 2 to 3 days later, and 5 h and 8 h after starting the n^{th} intravenous infusion ($7 < n < 12$). Urine samples were collected in 6 patients over 8 h at various times.

Colistin and CMS assay in plasma, urine, and BAL fluid. The samples were rapidly centrifuged, as previously described. Plasma was separated and kept frozen before analysis, as previously described (11–13). A previously described liquid chromatography-tandem mass spectrometry (LC-MS/MS) assay was used for CMS and colistin concentration measurements in plasma and urine (12) and BAL fluid (6) samples. The limit of quantification of the assay was 0.04 μg/ml.

Urea analysis in plasma and BAL fluid. The urea concentrations were determined in BAL fluid by LC-MS/MS, and the analysis was adapted from a previously described method (14). Eight-point calibration standards were made in 0.9% NaCl between 100 and 1.25 $\mu g \cdot ml^{-1}$. The limit of quantification (LOQ) for urea determination in BAL fluid was estimated at 1.25 $\mu g \cdot ml^{-1}$. The intra- and interday variabilities were characterized at these four concentrations, with precision and accuracy of <15% for 75, 25, and 2.5 $\mu g \cdot ml^{-1}$ concentrations and <20% for the LOQ. The urea concentrations in plasma were measured by photometric detection using an automatic analyzer (Modular automatic analyzer; Roche, France).

Determination of CMS and colistin concentrations in epithelial lining fluid. The actual ELF concentrations of CMS or colistin (C_{ELF}) were obtained from measured BAL fluid concentrations after correction for dilution (6), according to the equation $C_{ELF} = C_{BAL}$ ($Urea_{plasma}/Urea_{BAL}$), where C_{BAL} corresponds to the CMS or colistin concentration measured in BAL fluid, and $Urea_{BAL}$ and $Urea_{plasma}$ correspond to the concentrations of urea determined in BAL fluid and plasma, respectively.

Population PK modeling. The pharmacokinetic (PK) analysis was performed using the CMS and colistin ELF, urine, and plasma total concentrations (Fig. 1). Differences in the molecular masses between CMS (1,632 g/mol) and colistin (1,167 g/mol) were considered for calculation of the biotransformation rate, and it was assumed that only CMS was excreted in urine (11, 15). All data were analyzed simultaneously using a nonlinear mixed-effects model, with S-ADAPT (version 1.52), using the Monte Carlo parametric expectation maximization (MC-PEM) estimation algorithm with the S-ADAPT-TRAN translator (version 1.01) (16). The structural PK model is presented in Fig. 2. The ELF compartments were added to the plasma compartments to characterize CMS and colistin intrapulmonary distributions. The ELF volumes of distribution (V_{ELF}) were supposed to be the same for CMS and colistin. The fraction of the CMS dose delivered by aerosol delivery that reached ELF either directly or after being converted into colistin was defined as F_{aero}, and the presystemic clearance for CMS conversion into colistin was referred to as CL_{ps_CMS}. The first-order intercompartmental transfer clearances between ELF and plasma compartments were considered for CMS (clearance of CMS from lung to plasma and plasma to lung [CL_{IN_CMS} and CL_{OUT_CMS}], respectively) and colistin (clearance of colistin from lung to plasma and plasma to lung [CL_{IN_COL} and CL_{OUT_COL}], respectively). The typical PK parameters of the population were estimated, as well as the interindividual variability (IIV) (assuming a log-normal distribution), the interoccasion variability (IOV), and the residual variability. The residual variability was modeled as proportional for both CMS and colistin in ELF and plasma and combined (additive plus proportional) for the CMS urine concentration (Table 2). The effects of various covariates on the model parameters were not tested in this ancillary study, since this was done in an accompanying study (N. Grégoire, O. Mimoz, B. Mégarbane, E. Comets,D. Chatelier, S. Lasocki, R. Gauzit, D. Balayn, P. Gobin, S. Marchand, W. Couet [17]) with 73 critical care patients, but they were taken into account accordingly. The final model was assessed by an inspection of the observed versus predicted concentrations, residual variability, precision of parameter estimates, visual predictive check (VPC), and normalized prediction distribution errors (NPDE) (data not shown).

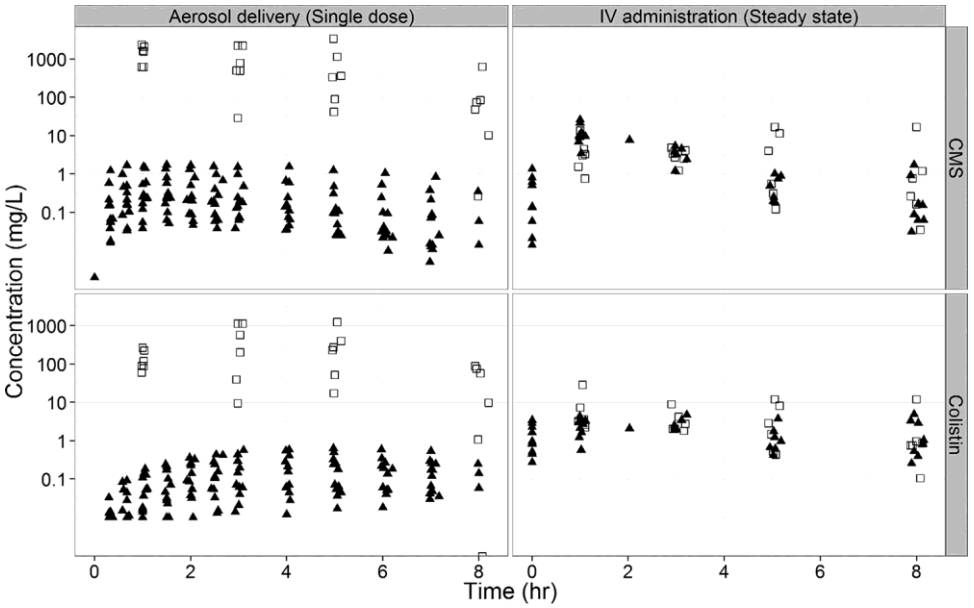

FIG 1 CMS (top panels) and colistin (bottom panels) concentrations in ELF (open squares) and plasma (filled triangles) following a single dose via aerosol ori.v. administration at steady state.

Time-kill curve experiments. An inoculum of 5 X 10^6 CFU/ml of *Pseudomonas aeruginosa* strain PAO1 (CIP 104116; Institut Pasteur, Paris, France), a wild-type strain, was prepared by a suspension of the bacteria from an 18-h logarithmic-growth-phase culture in Mueller-Hinton broth (Fluka BioChemika; Sigma-Aldrich, France). The experiments were performed in 10-ml glass tubes. Colistin was added to obtain concentrations of 0.25, 0.5, 1, 2, and 4 μg/ml (corresponding to 0.5 to 8X the MIC). The tubes were incubated at 37°C for 30 h. The bacteria were counted at 0, 2, 6, 8, 24, and 30 h. The number of CFU was counted after incubation at 37°C for 18 to 24 h. The limit of quantification (LOQ) was 100 CFU/ml. Four replicates were performed for each concentration. At least one growth control, without added colistin, was included in each experiment. Four replicates were performed for each concentration.

Pharmacodynamic modeling. Time-kill curves were analyzed using nonlinear mixed-effects modeling in the S-ADAPT software via the importance sampling algorithm (p method = 4 in S-ADAPT) (18). Model- ing was facilitated by the S-ADAPT-TRAN tool and utilized estimation settings that were previously qualified for a robust estimation of mechanism-based models (16, 19). Viable counts were fitted on a $\log_{10}$ scale, and viable counts below the limit of quantification were handled by using the Beal M3 method as implemented in S-ADAPT (20). The PD model was derived from Jumbe et al. (21), Gumbo et al. (22), and Campion et al. (23). This model included a preexisting susceptible (S) and a preexisting resistant (R) population. Both populations

did not interconvert and were assumed to have the same maximal killing rate constant (k_{max}) and the same growth rate constant (k_g). These populations differed, however, in their drug concentration yielding 50% of the k_{max} (KC_{50}), and the KC_{50} of the resistant population (KC_{50R}) was greater than that of the susceptible population (KC_{50S}).The typical PD parameters of the population were estimated, as well as the interindividual variability (IIV) (assuming a log-normal distribution) and the residual variability. The residual variability was modeled as additive on a log scale. The final model was assessed by an inspection of the observed versus predicted bacterial counts, residual variability, precision of the parameter estimates, and visual predictive check (VPC) (data not shown).

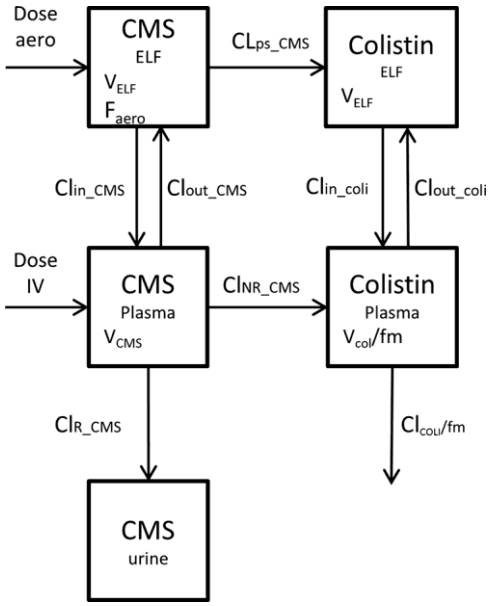

FIG 2 Structural pharmacokinetic model. V_{ELF}, volume of distribution in lung compartment; F_{aero}, fraction of the aerosol dose that reaches systemic circulation; CL_{OUT_CMS}, clearance of CMS from central to lung compartments; CL_{IN_CMS}, clearance of CMS from lung to central compartments; CL_{ps_CMS}, clearance of CMS presystemic conversion in colistin; CL_{OUT_COLI}, clearance of colistin from central to lung compartments; CL_{IN_COLI}, clearance of colistin from lung to central compartments; V_{CMS}, volume of distribution of CMS; CL_{R_CMS}, renal clearance of CMS; CL_{NR_CMS}, nonrenal clearance of CMS; V_{COL}, volume of distribution of colistin; CL_{COL}, total clearance of colistin; f_m, fraction of the CMS dose not excreted unchanged that is converted into colistin.

TABLE 2 Residual error for CMS and colistin

Residual error	Proportional %CV (RSE%)[a]	Additive (μg/ml)
CMS plasma	34 (20)	
Colistin plasma	30 (9)	
CMS ELF	77 (60)	
Colistin ELF	59 (26)	
CMS urine	59 (83)	170 (40)

[a] CV, coefficient of variation; RSE, relative standard error.

TABLE 3 Estimated population pharmacokinetic parameters of CMS and colistin for the final model based on the data from the 12 patients of the current study

Drug by sample type	Description	Parameter	Units	Typical value (RSE%)	IIV %CV[a] (RSE%)	IOV %CV[b] (RSE%)
Lung						
CMS	Fraction of the dose that reaches the ELF	F_{aero}		0.09 (26)	91 (43)	
	Clearance of CMS from lung to plasma	CL_{IN_CMS}	μl/min	15.1 (31)	57 (52)	
	Clearance of CMS from plasma to lung	CL_{OUT_CMS}	μl/min	6.0 (90)	128 (67)	
	Presystemic clearance of CMS to colistin	CL_{ps_CMS}	μl/min	2.6 (37)	108 (50)	
CMS and colistin	Epithelial lining fluid vol	V_{ELF}	ml	1.2 (0.24)		
Colistin	Clearance of colistin from lung to plasma	CL_{IN_COL}	μl/min	9.8 (31)	75 (73)	
	Clearance of colistin from plasma to lung	CL_{OUT_COL}	μl/min	12.7 (58)	107 (81)	
Plasma						
CMS	Vol of distribution of CMS	V_{CMS}	Liters	15.3 (12)	38 (47)	
	Renal clearance of CMS	CL_{R_CMS}	ml/min	64.6 (6.8)	93 (55)	61 (40)
	Nonrenal clearance of CMS	CL_{NR_CMS}	ml/min	46.3 (0.06)		
Colistin	Apparent vol of distribution of colistin	V_{COL}/f_m	Liters	13.7 (15)	44 (58)	
	Apparent total clearance of colistin	CL_{COL}/f_m	ml/min	53.1 (8.4)	38 (74)	42 (46)

[a] IIV %CV, interindividual variability (expressed as a coefficient of variation).
[b] IOV %CV, interoccasion variability (expressed as a coefficient of variation).

Prediction of bacterial killing. Predictions of colistin effect versus time were performed with Berkeley Madonna (version 8.3.18; University of California) over a 24-h time period by comparing two dosing regimens: 2 MIU of CMS administered by aerosol delivery over 30 min at time zero, followed by two consecutive 2-MIU doses administered i.v. over 30 min starting at times 8 h and 16 h; and 2-MIU doses of CMS administered i.v. over 60 min starting at times zero, 8 h, and 16 h. For each dosage regimen, 1,000 Monte Carlo predictions were performed: 1,000 PK and PD parameter values were generated randomly according to their distributions and used to generate 1,000 profiles of colistin concentrations in the ELF

(data not shown) and 1,000 profiles of bacterial counts in the ELF. The pharmacodynamics of colistin was considered the same in ELF and *in-vitro*. Each prediction began with a starting inoculum of 10^6 CFU/ml.

RESULTS

The CMS and colistin concentrations were much higher (approximately 100- to 1,000-fold) in the ELF than those in plasma following the initial CMS aerosol delivery (Fig. 1). The CMS and colistin concentrations were similar in the ELF and plasma after multiple i.v. administrations at steady state (Fig. 1). Overall, the range of colistin concentrations was higher within the ELF (9.53 to 1,137 mg/liter) and lower in plasma (0.15 to 0.73 mg/liter) after aerosol delivery than with intravenous administration of CMS (1.48 to 28.9 mg/liter in ELF and 0.15 to 4.7 in plasma).

PK modeling allowed proper characterization of the effect of route of administration on intrapulmonary CMS and colistin disposition. The interindividual variability (IIV) included for intrapulmonary parameters ($CL_{IN\ AND\ OUT}$ for CMS and colistinand CL_{ps_CMS}) were large (57 to 128%) (Table 3).The visual predictive check (VPC) showed that the model fitted the data without major bias (Fig. 3). The observed concentrations were evenly scattered around the typical profile, and about 10% of the observed data were outside the 90% predicted confidence intervals. The CMS concentrations in ELF were slightly overpredicted at 1 h, and the colistin concentrations in plasma were slightly underpredicted at 1 h.

The parameter estimates are presented in Table 3. Following CMS aerosol delivery, 9% of the dose typically reached the ELF, with only 1.4% absorbed as colistin due to presystemic biotransformation. The distributional clearances in and out for CMS and colistin were within the same order of magnitude and 2- to 5-fold higher than those of CMS-to-colistin presystemic conversion.

Kill curve experiments showed an initial decay of CFU with time, followed by regrowth at all concentrations tested (0.25 to 4 μg/ml) (Fig. 4), which was also depicted by the CFU-versus-time curves simulated by the PD model with two subpopulations of bacteria (susceptible and resistant), suggesting also that the faster initial decay at higher colistin concentrations was accompanied by earlier regrowth (Fig. 4), as previously observed (17). Noticeably, the 50% effective concentration (EC_{50}) for the so-called resistant bacteria (EC_{50R}, 25.3 mg/liter) was much (37-fold) greater than that of the susceptible one (EC_{50S}, 0.69 mg/liter). The full parameter estimates are presented in Table 4.

Selected PK and PD models with parameter estimates were used and integrated for PK-PD simulations. Accordingly, it would take approximately 12 h from 95% predictions to achieve a total kill of wild-type *P. aeruginosa* following an aerosol delivery, whereas the i.v. doses did not achieve this objective. Moreover, the percentage of bacterial counts below the lower LOQ (LLOQ) (100 CFU/ml) at 24 h was much higher after aerosol delivery, at 98.5%, than that after i.v. administration, at 11%. Aerosol delivery was more effective than i.v.

administration on lung bacteria, according to the bacterial count predictions. Noticeably, the predicted effect following an initial 9-MIU i.v. CMS loading dose was not much different from that obtained after an initial 2- or 3-MIU i.v. dose (data not shown).

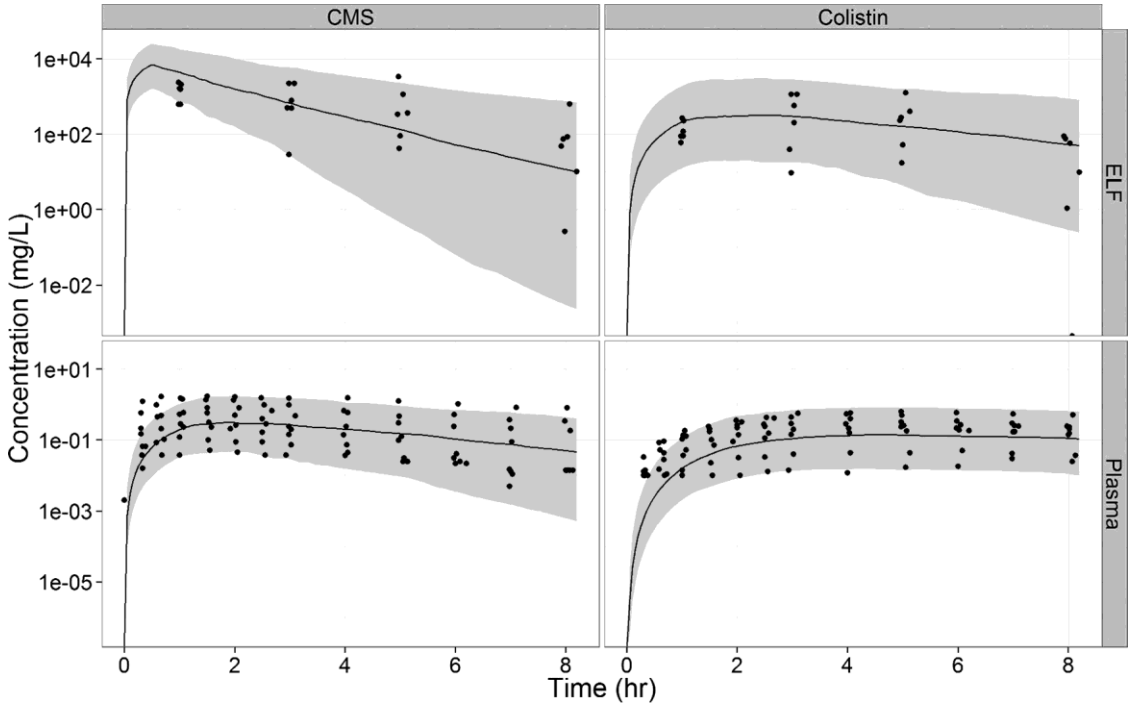

FIG 3 Observed colistin and CMS concentrations in ELF and plasma with model predictions (as medians [solid lines] and 90% prediction intervals [gray shaded areas]) using parameter estimates.

DISCUSSION

Only a few studies have been conducted to investigate colistin concentrations within ELF using chromatographic assays, and in these, patients were treated by CMS either i.v. or by aerosol delivery but not by both routes, which limits comparisons. Following i.v. administration of 2 MIU of CMS, Imberti et al.(24) could not measure colistin in BAL fluid. In contrast, Athanassa et al. (25) measured relatively higher (on the order of 10 times) colistin concentrations in the ELF than those in serum after aerosol delivery with 1 MIU of CMS, but the ELF colistin concentrations were 20 μg/ml at the most and therefore much lower than the concentrations that we report here, even considering the 2-fold difference in the dose of nebulized CMS (25). However, those authors also reported serum colistin concentrations with a peak ranging between 1 and 2 μg/ml in most patients after aerosol delivery of 1 MIU of CMS, which is by far higher than what could be anticipated from any other study using the same type of nebulizer.

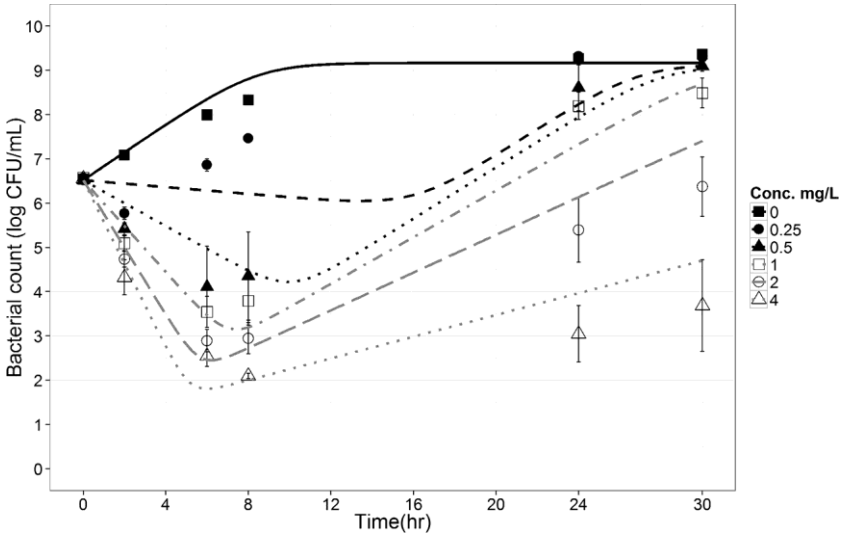

FIG 4 Time-kill curves for *P. aeruginosa* exposed to colistin at concentrations (Conc.) ranging from 0 to 4 mg/liter for a starting inoculum of 5 X 10^6 CFU/ml. The results (dots and error bars) are the means and standard deviations of the results from four replicates. Included are the model predicted curves (lines) with mean parameter estimates.

TABLE 4 Pharmacodynamic parameter estimates with typical values, interindividual variability, and relative standard error of the PK-PD model, as estimated using data from static experiments

Parameter	Abbreviation	Units	Typical value (RSE%)[a]	IIV %CV[b] (RSE%)
Maximum killing rate constant	E_{max}[c]	h^{-1}	3.3 (13.22)	26.7 (54)
Apparent growth rate constant	k_g	h^{-1}	0.76 (5.5)	18 (57)
Antibiotic concn yielding 50% of E_{max} in susceptible population	EC_{50S}	mg/liter	0.69 (35)	44 (62)
Antibiotic concn yielding 50% of E_{max} in resistant population	EC_{50R}	mg/liter	25.3 (25)	48 (51)
Maximum concn of bacteria reached in *in vitro* system	Pop_{max}	Log_{10} CFU/ml	9.17 (0.93)	24 (58)
Initial inoculum	Inoc	Log_{10} CFU/ml	6.38 (0.71)	
Mutation frequency	Log_{10}Mutf		−5.5 (4.57)	
Additive residual error			0.34 (7)	

[a] RSE%, relative standard error (expressed as a percentage).
[b] IIV %CV, interindividual variability (expressed as a coefficient of variation).
[c] E_{max}, maximum possible effect of the drug.

In the present study, the intrapulmonary distribution of colistin was assessed after CMS aerosol delivery and then after i.v. administration. For ethical reasons and according to the proper use of colistin, the treatment order could not be randomized, since it would not have been possible to interrupt CMS i.v. administration in order to switch to aerosol delivery in the middle of treatment. However, because preclinical data showed much higher ELF colistin concentrations after CMS aerosol delivery than after i.v. administration in rats (14), it was decided that the 1st CMS dose should be nebulized, and subsequent doses would be administered intravenously. Plasma samples were collected after these two initial doses for PK

analysis in order to limit a potential effect of intraindividual variability on colistin disposition with time, which would not be unlikely in critically ill patients. However, colistin ELF concentrations after CMS aerosol delivery were expected to be much higher than those after i.v. administration. Consequently, the ELF concentrations of colistin measured after the 1st i.v. administration of CMS might have been artificially overestimated due to the presence of compound remaining from the previous CMS aerosol delivery. The simultaneous data analysis with a population approach used in this study would have been able to manage this issue. However, the analytical uncertainty on ELF concentration assessment due in part to the correction by a dilution factor estimated from urea measurements would have been a complicating factor. It was therefore decided to administer CMS i.v. for several days before measuring the colistin ELF concentrations and concomitant plasma levels at steady state.

It is often considered that colistin pharmacokinetics with i.v. administration of CMS in critically ill patients may vary significantly with the brand of CMS used, which has also been documented in a controlled experiment in rats (26). Accordingly, the plasma data obtained in the present study after giving CMS i.v. are in full agreement with those obtained by our group using the same brand of CMS in the same types of patients (17) but only partially consistent with those ofother previously published articles (28, 29).

The major finding of this study was that both CMS and colistin ELF concentrations are much higher (in the order of 100- to 1,000-fold on average) after CMS aerosol delivery than after i.v. administration, which is fully consistent with observations in rats (7, 14). The only major difference with the rat experiments was that after aerosol delivery in patients, most of the CMS was lost with expired airflow, since on average, only 9% of the CMS dose eventually reached the systemic circulation, compared with approximately 69% in rats (7, 14), using the Penn-Century system for deep intrapulmonary delivery. This limited systemic absorption in patients suggests limited systemic toxicity after CMS aerosol delivery. The fraction of the CMS dose converted presystemically into colistin in patients (1.4%) was lower than that in rats (6, 7). However, the kinetics of formation and the absorption of colistin after CMS aerosol delivery are difficult to characterize. Furthermore, it should be remembered that reported CMS concentrations correspond only to apparent values, since unchanged CMS and partially converted derivatives cannot be differentiated using even the most modern analytical assays (12, 26), which precludes a precise interpretation of CMS experimental data. Recently, Yapa et al. (7) used a relatively complex multicompartmental model to characterize colistin absorption after aerosol delivery in rats. Gontijo et al (14) previously used a relatively simpler model but with a nonlinear component. In comparison, a simple model was used in the present study, in particular due to the lack of early data points in the ELF. Also, for this reason, hypotheses were required to reduce the model parameter number, and it was decided to keep the same ELF volume for CMS and colistin. Using a traditional compartmental approach, ELF volume has no physiological meaning, and values up to 30 liters have been estimated (30). Yet, it may be noticed that the 1.2-ml value obtained in the present study and that is common to both CMS and colistin is close to the actual physiological ELF volume in humans (31, 32).

This low ELF volume is mostly responsible for the relatively high CMS and colistin concentrations measured within the ELF, although most of the CMS aerosolized dose (about 90%) was lost with expired airflow. By comparing the ELF concentrations of colistin in patients, obtained after aerosol delivery of 2 MIU of CMS, with the MICs of most susceptible bacteria, one may also consider that 2 MIU of CMS may be a higher dose than is necessary. In fact, CMS concentrations are several orders of magnitude greater (approximately 4- to 20-fold on average) than colistin concentrations within the ELF, and although it is negatively charged and therefore less toxic, allowing its administration as a prodrug of colistin, CMS is also a tension-active compound, with a potential local toxicity at such extremely high concentrations. A better efficacy-to-toxicity ratio might therefore be obtained with lower doses.

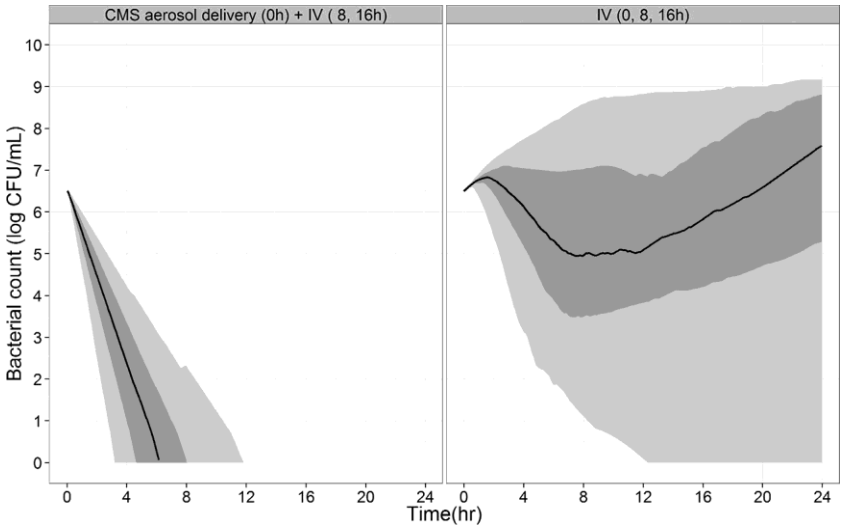

FIG 5 Predicted bacterial count over time after CMS aerosol delivery (2 MIU followed by 2 MIU i.v. at 8 h and 16 h) or i.v. administration (2 MIU every 8 h). The median (solid line), 25th to 75th percentile (dark grey area), and 5th to 95th percentile (light grey area) of the predicted counts are illustrated.

Since these data clearly demonstrate a major effect of the CMS route of administration on colistin concentrations, with much higher ELF concentrations obtained after CMS aerosol delivery using a vibrating mesh nebulizer in critically ill patients than those after intravenous administration, a PK-PD modeling approach was used to assess the effect of route of administration on the antimicrobial effect of colistin within the lung. Antibiotic PK-PD relies most often on the PK-PD index differentiating between concentration and time-dependent antibiotics, with targets determined from the plasma concentrations. It is usually admitted that for colistin, the relevant index is the area under the concentration-time curve for plasma (AUC_{plasma})/MIC ratio, with a breakpoint determined at 27/35 from unbound plasma concentrations (33, 34). Whether antibiotic plasma concentrations reflect tissue concentrations at the

infectious site is an important question that has frequently been addressed (35–37). Based on these new pharmacokinetic data, colistin plasma concentrations do not reflect intrapulmonary concentrations and therefore cannot be used to compare antimicrobial activity in the lungs after aerosol and intravenous administrations of CMS. An alternative would be to use ELF instead of plasma concentrations to compare the effect of the route of administration on antimicrobial efficacy in the lungs. However, it would then be necessary to define a new AUC_{ELF}/MIC target. Furthermore, this PK-PD index may predict colistin antimicrobial efficacy at steady state, but it is of limited value for assessing the initial CFU decay after CMS treatment initiation, especially since bacterial susceptibility and therefore MIC might rapidly change with time during the initial hours following exposure to the antibiotic, as demonstrated by the regrowth phenomenon observed in the time-kill curves (Fig. 4). It was therefore decided to use a PK-PD modeling approach to predict colistin antimicrobial activity, as was previously done by Mohamed et al. (38). We used a simple model with two subpopulations, S and R, to describe the regrowth. Although this model has no mechanistic meaning, it is the most robust and should be selected in the absence of precise information on the regrowth mechanism (27). This PK-PD model was capable of predicting a clear superiority of CMS aerosol delivery over intravenous administration in terms of antimicrobial activity, consistent with the EC_{50R} value estimated at 25.3 µg/ml when ELF concentrations vary between 40 and 1,136 µg/ml after aerosol delivery and 0.5 and 26 µg/ml after intravenous administration of CMS. Because of the relatively high EC_{50R} value, the so-called resistant bacteria would be almost totally resistant in a range of ELF concentrations (<10 µg/ml) obtained in clinical practice after CMS i.v. administrations. Noticeably, the estimated EC_{50R} value was about 6-fold higher than the highest colistin concentrations used for the kill curve experiments, which may not be ideal. However, the relative standard error (RSE%) values were relatively low, attesting to correct estimations. Furthermore, we have recently observed relatively large differences between EC_{50S} and EC_{50R} using a similar experimental setting (17). According to these data, only aerosol delivery provided sufficiently high and microbiologically efficient colistin concentrations. Therefore, a major effect of the route of administration on the antimicrobial effect was predicted using this *P. aeruginosa* PAO1 strain. However, this effect would have been less spectacular using another strain with a lower EC_{50R} value. Yet, in clinical practice, a single aerosol delivery with 2 MIU of CMS is unlikely to clear all bacteria in an irreversible manner, as suggested by these simulations (Fig. 5). An explanation might be that colistin does not distribute evenly within the lung and has difficulties reaching some specific areas, such as hypo-oxygenated tissue, where bacteria could develop. The measured ELF concentrations might then dramatically overestimate actual colistin concentrations at the infection site. *In-vivo* experiments should now be conducted to complete these findings. However, these new data seem to support the use of CMS aerosol delivery on top of i.v. administration for the treatment of pulmonary infections in critical care patients.

ACKNOWLEDGMENTS

M. Jacobs is supported by a doctoral fellowship from the University of Poitiers and the "Conseil Régional de Poitou-Charentes."

REFERENCES

1. **Drobnic ME, Suñé P, Montoro JB, Ferrer A, Orriols R.** 2005. Inhaled tobramycin in non-cystic fibrosis patients with bronchiectasis and chronic bronchial infection with *Pseudomonas aeruginosa*. Ann. Pharmacother. **39:**39 – 44. http://dx.doi.org/10.1345/aph.1E099.
2. **Ramsey BW, Pepe MS, Quan JM, Otto KL, Montgomery AB, Williams- Warren J, Vasiljev-K M, Borowitz D, Bowman CM, Marshall BC, Marshall S, Smith AL.** 1999. Intermittent administration of inhaled to- bramycin in patients with cystic fibrosis. Cystic Fibrosis Inhaled Tobra- mycin Study Group. N. Engl. J. Med. **340:**23–30.
3. **McCoy KS, Quittner AL, Oermann CM, Gibson RL, Retsch-Bogart GZ, Montgomery AB.** 2008. Inhaled aztreonam lysine for chronic airway *Pseudomonas aeruginosa* in cystic fibrosis. Am. J. Respir. Crit. Care Med. **178:**921–928. http://dx.doi.org/10.1164/rccm.200712-1804OC.
4. **Conole D, Keating GM.** 2014. Colistimethate sodium dry powder for inhalation: a review of its use in the treatment of chronic *Pseudomonas aeruginosa* infection in patients with cystic fibrosis. Drugs **74:**377–387. http://dx.doi.org/10.1007/s40265-014-0181-0.
5. **Lu Q, Girardi C, Zhang M, Bouhemad B, Louchahi K, Petitjean O, Wallet F, Becquemin MH, Le Naour G, Marquette CH, Rouby JJ.** 2010. Nebulized and intravenous colistin in experimental pneumonia caused by *Pseudomonas aeruginosa*. Intensive Care Med. **36:**1147–1155. http://dx.doi.org/10.1007/s00134-010-1879-4.
6. **Marchand S, Gobin P, Brillault J, Baptista S, Adier C, Olivier JC, Mimoz O, Couet W.** 2010. Aerosol therapy with colistin methanesulfon- ate: a biopharmaceutical issue illustrated in rats. Antimicrob. Agents Chemother. **54:**3702–3707. http://dx.doi.org/10.1128/AAC.00411-10.
7. **Yapa SWS, Li J, Porter CJ, Nation RL, Patel K, McIntosh MP.** 2013. Population pharmacokinetics of colistin methanesulfonate in rats: achieving sustained lung concentrations of colistin for targeting respiratory infections. Antimicrob. Agents Chemother. **57:**5087–5095. http://dx.doi.org/10.1128/AAC.01127-13.
8. **Cockcroft DW, Gault MH.** 1976. Prediction of creatinine clearance from serum creatinine. Nephron **16:**31– 41. http://dx.doi.org/10.1159/000180580.
9. **Nation RL, Li J, Cars O, Couet W, Dudley MN, Kaye KS, Mouton JW, Paterson DL, Tam VH, Theuretzbacher U, Tsuji BT, Turnidge JD.** 2013. Consistent global approach on reporting of colistin doses to promote safe and effective use. Clin. Infect. Dis. **58:**139 –141. http://dx.doi.org/10.1093/cid/cit680.
10. **Boselli E, Breilh D, Duflo F, Saux MC, Debon R, Chassard D, Al- laouchiche B.** 2003. Steady-state plasma and intrapulmonary concentrations of cefepime administered in continuous infusion in critically ill patients with severe nosocomial pneumonia. Crit. Care Med. **31:**2102–2106. http://dx.doi.org/10.1097/01.CCM.0000069734.38738.C8.
11. **Couet W, Grégoire N, Gobin P, Saulnier PJ, Frasca D, Marchand S, Mimoz O.** 2011. Pharmacokinetics of colistin and colistimethate sodium after a single 80-mg intravenous dose of CMS in young healthy volunteers. Clin. Pharmacol. Ther. **89:**875– 879. http://dx.doi.org/10.1038/clpt.2011.48.

12. **Gobin P, Lemaître F, Marchand S, Couet W, Olivier JC.** 2010. Assay of colistin and colistin methanesulfonate in plasma and urine by liquid chromatography-tandem mass spectrometry (LC-MS/MS). Antimicrob. Agents Chemother. **54:**1941–1948. http://dx.doi.org/10.1128/AAC.01367-09.
13. **Marchand S, Frat JP, Petitpas F, Lemaître F, Gobin P, Robert R, Mimoz O, Couet W.** 2010. Removal of colistin during intermittent haemodialysis in two critically ill patients. J. Antimicrob. Chemother. **65:**1836 – 1837. http://dx.doi.org/10.1093/jac/dkq185.
14. **Gontijo AV, Grégoire N, Lamarche I, Gobin P, Couet W, Marchand S.** 2014. Biopharmaceutical characterization of nebulized antimicrobial agents in rats: 2. Colistin. Antimicrob. Agents Chemother. **58:**3950 –3956. http://dx.doi.org/10.1128/AAC.02819-14.
15. **Li J, Milne RW, Nation RL, Turnidge JD, Smeaton TC, Coulthard K.** 2003. Use of high-performance liquid chromatography to study the pharmacokinetics of colistin sulfate in rats following intravenous administration. Antimicrob. Agents Chemother. **47:**1766 –1770. http://dx.doi.org/10 .1128/AAC.47.5.1766-1770.2003.
16. **Bulitta JB, Bingölbali A, Shin BS, Landersdorfer CB.** 2011. Development of a new pre- and post-processing tool (SADAPT-TRAN) for nonlinearmixed-effects modeling in S-ADAPT. AAPS J. **13:**201–211. http://dx.doi .org/10.1208/s12248-011-9257-x.
17. **Grégoire N, Mimoz O, Mégarbane B, Comets E, Chatelier D, Lasocki S, Gauzit R, Balayn D, Gobin P, Marchand S, Couet W.** 2014. New colistin population pharmacokinetic data in critically ill patients suggesting an alternative loading dose rationale. Antimicrob. Agents Chemother. **58:** 7324 –7330. http://dx.doi.org/10.1128/AAC.03508-14.
18. **Bauer RJ, Guzy S, Ng C.** 2007. A survey of population analysis methods and software for complex pharmacokinetic and pharmacodynamic models with examples. AAPS J. **9:**E60 –E83. http://dx.doi.org/10.1208/aapsj0901007.
19. **Bulitta JB, Landersdorfer CB.** 2011. Performance and robustness of the Monte Carlo importance sampling algorithm using parallelized S-ADAPT for basic and complex mechanistic models. AAPS J. **13:**212–226. http://dx.doi.org/10.1208/s12248-011-9258-9.
20. **Beal SL.** 2001. Ways to fit a PK model with some data below the quantification limit. J. Pharmacokinet. Pharmacodyn. **28:**481–504. http://dx.doi.org/10.1023/A:1012299115260.
21. **Jumbe N, Louie A, Leary R, Liu W, Deziel MR, Tam VH, Bachhawat R, Freeman C, Kahn JB, Bush K, Dudley MN, Miller MH, Drusano GL.** 2003. Application of a mathematical model to prevent *in-vivo* amplification of antibiotic-resistant bacterial populations during therapy. J. Clin. Invest. **112:**275–285. http://dx.doi.org/10.1172/JCI200316814.
22. **Gumbo T, Louie A, Deziel MR, Parsons LM, Salfinger M, Drusano GL.** 2004. Selection of a moxifloxacin dose that suppresses drug resistance in *Mycobacterium tuberculosis*, by use of an *in-vitro* pharmacodynamic infection model and mathematical modeling. J. Infect. Dis. **190:**1642–1651.

http://dx.doi.org/10.1086/424849.

23. **Campion JJ, McNamara PJ, Evans ME.** 2005. Pharmacodynamic modeling of ciprofloxacin resistance in *Staphylococcus aureus*. Antimicrob. Agents Chemother. **49:**209 –219. http://dx.doi.org/10.1128/AAC.49.1.209-219.2005.

24. **Imberti R, Cusato M, Villani P, Carnevale L, Iotti GA, Langer M, Regazzi M.** 2010. Steady-state pharmacokinetics and BAL concentration of colistin in critically Ill patients after IV colistin methanesulfonate administration. Chest **138:**1333–1339. http://dx.doi.org/10.1378/chest.10-0463.

25. **Athanassa ZE, Markantonis SL, Fousteri MZ, Myrianthefs PM, Boutzouka EG, Tsakris A, Baltopoulos GJ.** 2012. Pharmacokinetics of inhaled colisti- methate sodium (CMS) in mechanically ventilated critically ill patients. Intensive Care Med. **38:**1779 –1786. http://dx.doi.org/10.1007/s00134-012-2628-7.

26. **He H, Li JC, Nation RL, Jacob J, Chen G, Lee HJ, Tsuji BT, Thompson PE, Roberts K, Velkov T, Li J.** 2013. Pharmacokinetics of four different brands of colistimethate and formed colistin in rats. J. Antimicrob. Chemother. **68:**2311–2317. http://dx.doi.org/10.1093/jac/dkt207.

27. **Jacobs M, Grégoire N, Couet W, Bulitta JB.** 2013. Characterization of semi-mechanistic pharmacokinetic-pharmacodynamic models of antibacterial activity via Monte Carlo simulations, poster 933. 23rd Eur. Congr. Clin. Microbiol. Infect. Dis., 27 to 30 April 2013, Berlin, Germany.

28. **Garonzik SM, Li J, Thamlikitkul V, Paterson DL, Shoham S, Jacob J, Silveira FP, Forrest A, Nation RL.** 2011. Population pharmacokinetics of colistin methanesulfonate and formed colistin in critically ill patients from a multicenter study provide dosing suggestions for various categories of patients. Antimicrob. Agents Chemother. **55:**3284 –3294. http://dx.doi.org/10.1128/AAC.01733-10.

29. **Plachouras D, Karvanen M, Friberg LE, Papadomichelakis E, Antonia- dou A, Tsangaris I, Karaiskos I, Poulakou G, Kontopidou F, Armagani- dis A, Cars O, Giamarellou H.** 2009. Population pharmacokinetic analysis of colistin methanesulfonate and colistin after intravenous administration in critically ill patients with infections caused by Gram- negative bacteria. Antimicrob. Agents Chemother. **53:**3430 –3436. http://dx.doi.org/10.1128/AAC.01361-08.

30. **Lodise TP, Sorgel F, Melnick D, Mason B, Kinzig M, Drusano GL.** 2011. Penetration of meropenem into epithelial lining fluid of patients with ventilator-associated pneumonia. Antimicrob. Agents Chemother. **55:** 1606 –1610. http://dx.doi.org/10.1128/AAC.01330-10.

31. **Fernandes CA, Vanbever R.** 2009. Preclinical models for pulmonary drug delivery. Expert Opin. Drug Deliv. **6:**1231–1245. http://dx.doi.org/10.1517/17425240903241788.

32. **Rennard SI, Basset G, Lecossier D, O'Donnell KM, Pinkston P, Martin PG, Crystal RG.** 1986. Estimation of volume of epithelial lining fluid recovered by lavage using urea as marker of dilution. J. Appl. Physiol. (1985) **60:**532–538.

33. **Bergen PJ, Bulitta JB, Forrest A, Tsuji BT, Li J, Nation RL.** 2010. Pharmacokinetic/pharmacodynamic investigation of colistin against

Pseudomonas aeruginosa using an *in-vitro* model. Antimicrob. Agents Che- mother. **54:**3783–3789. http://dx.doi.org/10.1128/AAC.00903-09.

34. **Dudhani RV, Turnidge JD, Coulthard K, Milne RW, Rayner CR, Li J, Nation RL.** 2010. Elucidation of pharmacokinetic/pharmacodynamic de- terminant of colistin activity against *Pseudomonas aeruginosa* in murine thigh and lung infection models. Antimicrob. Agents Chemother. **54:** 1117–1124. http://dx.doi.org/10.1128/AAC.01114-09.
35. **Dahyot C, Marchand S, Bodin M, Debeane B, Mimoz O, Couet W.** 2008. Application of basic pharmacokinetic concepts to analysis of microdialysis data: illustration with imipenem muscle distribution. Clin. Pharmacokinet. **47:**181–189. http://dx.doi.org/10.2165/00003088-200847030-00004.
36. **Liu P, Rand KH, Obermann B, Derendorf H.** 2005. Pharmacokinetic- pharmacodynamic modelling of antibacterial activity of cefpodoxime and cefixime in *in-vitro* kinetic models. Int. J. Antimicrob. Agents **25:**120 –129. http://dx.doi.org/10.1016/j.ijantimicag.2004.09.012.
37. **Marchand S, Dahyot C, Lamarche I, Mimoz O, Couet W.** 2005. Micro- dialysis study of imipenem distribution in skeletal muscle and lung extracellular fluids of noninfected rats. Antimicrob. Agents Chemother. **49:** 2356–2361. http://dx.doi.org/10.1128/AAC.49.6.2356-2361.2005.
38. **Mohamed AF, Karaiskos I, Plachouras D, Karvanen M, Pontikis K, Jansson B, Papadomichelakis E, Antoniadou A, Giamarellou H, Armaganidis A, Cars O, Friberg LE.** 2012. Application of a loading dose of colistin methanesulfonate in critically ill patients: population pharmacokinetics, protein binding, and prediction of bacterial kill. Antimicrob. Agents Chemother. **56:**4241– 4249. http://dx.doi.org/10 .1128/AAC.06426-11.

B. Colistin and Hemodialysis

Population pharmacokinetics of colistin methanesulphonate (CMS) and colistin in critically ill patients with acute renal failure requiring intermittent haemodialysis

M. Jacobs[1], N. Grégoire[1], B. Mégarbane[2], P. Gobin[1], D. Balayn[1], S Marchand[1], O. Mimoz[1] , W. Couet[1].

1 INSERM U1070, Université de Poitiers et CHU Poitiers, Poitiers, France.

2 Hôpital Lariboisière, Paris, France.

Keywords: Colistin, pharmacokinetics, Haemodialysis

Synopsis

Objectives: To characterize the pharmacokinetics (PK) of colistin and its prodrug colistin methanesulphonate (CMS) in patients receiving intermittent haemodialysis, and to suggest dosing regimen recommendations.

Patients and methods: Eight intensive care unit patients receiving intermittent HD for acute renal failure (ICU-HD) and treated by CMS (Colimycine®) intravenously. Blood samples were collected between two consecutive HD sessions. CMS and colistin concentrations were measured by a specific chromatographic assay and analysed using a PK population approach. Monte-Carlo simulations were then conducted to predict the probability of target attainment (PTA) under various scenarios.

Results: CMS non renal clearance was increased in ICU-HD patients to compensate for the absence of renal clearance. By comparison with ICU patients with preserved renal function, colistin exposure was increased by 3-fold in ICU-HD patients, probably because a greater fraction of the CMS can be converted into colistin. To maintain colistin plasma concentrations high enough (> 3 mg/L) to reach high PTA values, at least for minimum inhibitory concentrations (MIC) lower than 0.5 mg/L, dosing regimen of CMS should be 1.5 MIU twice daily for a non-HD day, HD should be conducted at the end of a dosing interval and a supplemental dose of 1.5 MIU should be administered along with the scheduled dose just after the HD session (i.e. total of 4.5 MIU for HD day) .

Conclusions: This study has confirmed and complemented previously published data and suggests an a priori clear and easy to follow dosing strategy for CMS in ICU-HD patients with acute renal failure.

Introduction

Over the last years, colistin (polymyxin E) was increasingly used as a last option for the treatment of infections caused by multi-drug resistant Gram-negative bacteria as *Pseudomonas aeruginosa, Acinetobacter baumannii* and *Klebsiella pneumonia*(1, 2).

Colistin is administered as a prodrug, the colistin methanesulphonate (CMS), which is mostly excreted unchanged in urine (70%) and partly converted in colistin (30% at the most), whereas renal excretion of colistin is negligible (3). Then in patients with renal failure a greater fraction of the CMS dose may be converted into colistin(4) and therefore everything else being equal, colistin plasma concentrations at steady-state should increase.

It has recently been shown that in critical care patients colistin plasma concentrations at steady-state are mostly governed by renal function and that creatinine clearance can be used for dosing regimen adaptation(4). Dosing recommendations were also made for patients under intermittent haemodialysis (HD) (4-7). However because colistin pharmacokinetics (PK) may vary with the CMS brand (4, 8, 9),the aim of this study was to assess colistin pharmacokinetics (PK) in intensive care unit patients requiring intermittent HD (ICU-HD) and treated with the same brand as previously used to investigate colistin PK in healthy volunteers(3) and ICU patients with preserved or moderately altered renal function[7].

Materials and methods

Study population

This population PK study was conducted in two sites: University Hospital of Poitiers, France and Hôpital Lariboisière, Paris, France. The study protocol was approved by the local ethics committee (CPP Ouest III, approval n°09.02.01) and French national authorities (ANSM n°2009-009578-28). Informed consent was obtained from all patients or their relatives. Patients were eligible for enrolment in the study if they were aged between 18 and 85 years, receiving CMS as part of their treatment, according to dosage regimens freely chosen by physicians, and under intermittent HD for acute renal failure. Patients were not eligible if they had received colistin for 7 days prior to study. At study onset, the following data were collected: age, sex, weight, diagnosis on admission, serum urea, serum creatinine and Simplified Acute Physiology Score (SAPS II). A total of 2 women and 6 men were enrolled. Their demographic, clinical and biological data are summarized in Table 1.

Table 1: Demographic and clinical characteristics of ICU-HD patients

ID	Gender	Age (yr)	Weight (kg)	Serum Creatinine (µmol/L)	Urine flow (mL/h)	SAPS II score	Loading Dose (MIU)	Maintenance dose (MIU /q8h)	Receiving aerosol
1	M	71	83	172	0	60	2	0.5	yes
2	M	62	100	470	0	49	2	2	no
3	M	36	58	304	0	39	1	1	no
4	M	39	88	375	0	63	0.5	0.5	no
5	F	82	80	329	0	70	0.4	0.4	yes
6	M	73	80	223	25	55	9	0.5	yes
7	F	63	52	296	37.5	75	0.8	0.5	yes
8	M	66	75	315	0	42	2	2	no
median		65	80	310	-	58	1.5	0.5	

Haemodialysis

Intermittent hemodialysis sessions (Gambro, AK 200) were performed during 4 hours before CMS dosing, with blood flow setting at 300 mL/min and dialysis effluent at 500 mL/min, using a 1.6 m^2 B3 polymethylmethacrylate membrane (Toray industries, Tokyo, Japan)

CMS Administration

CMS (Colimycine, Sanofi, Paris, France) was administered intravenously every 8h. The median first dose was1.5 MIU (range from 0.4 to 9 MIU) and the median maintenance dose was 0.5 MIU q8h (0.4 to 2MIU q8h) (1 MIU is equivalent to 80 mg of CMS sodium)(10).CMS was dissolved in 50 mL of saline solution and administered over 60 min. The solutions were prepared just before administration. Some patients (n=5) received also CMS as aerosol (dose range from 1 to 2 MIU twice a day), after dissolution in 10 mL of saline and nebulization over 30 min with a vibrating-mesh nebulizer (Aeroneb Pro, Aerogen, Galway, France).

Samples collection

Venous blood samples (n=90) were collected between haemodialysis sessions. Blood samples were collected immediately before and at 0.5, 1, 2, 3, 8 h after the beginning of the first infusion and at various times following consecutive administrations. Samples were immediately centrifuged (3 000 g, 10 min) at 4°C and plasma was stored at -20°C until analysis.

Determination of CMS and colistin concentrations in plasma

CMS and colistin concentrations were measured as previously described (3, 5, 9, 11) with a validated liquid chromatography-tandem mass spectrometry (LC-MS/MS) assay with a limit of quantification at 0.04 mg/L.

Population PK modelling

CMS and colistin plasma concentrations were analysed simultaneously using a non-linear mixed-effect model, with Monolix (Lixoft, version 4.3.2). A previously reported PK model (9, 12) was fitted to the data. CMS pharmacokinetics was described using a one-compartment model. CMS renal clearance (CL_{RCMS}) was fixed at 0, whereas clearance, equal to non-renal clearance (CL_{NRCMS}) and volume of distribution (V_{CMS}) were estimated. A one-compartment model was also used for colistin pharmacokinetics but only apparent volume of distribution (V_{col}/f_m) and apparent total clearance (CL_{col}/f_m) could be estimated, where f_m corresponds to the unknown fraction of CMS non-renally cleared that was eventually converted into colistin(4). The clearances of CMS and colistin due to haemodialysis sessions were set to values previously determined experimentally with the same brand of CMS and the same haemodialysis apparatus, i.e. 90 mL/min and 137 mL/min respectively(5). The contribution of aerosol co-treatment on plasma CMS and colistin concentrations, was taken into consideration by fixing as independent estimates the relevant pharmacokinetic parameters values previously estimated(12). The typical PK parameters of the population were estimated as well as the inter-individual variability (IIV) (assuming a log-normal distribution). The residual variability was modelled as combined (additive and proportional) for CMS and colistin plasma concentrations. Differences of objective function values (OFV) were used to discriminate between different models, with a reduction of at least 10.83 (corresponding to a p-value <0.001 for 1 degree of freedom) required to choose the more complex model. Covariate model building was performed in a stepwise fashion with forward inclusion ($p<0.05$) and backward deletion ($p<0.01$). The covariates evaluated included body weight, age, creatinine clearance, serum urea concentration and temperature. Model performance was assessed by visual inspection of diagnostic plots, normalized prediction distribution errors (NPDE), the evaluation of the residual error and the precision of parameter estimates.

Simulations

Two types of simulations were conducted.

First CMS and colistin concentrations were simulated after a single 3MIU dose of CMS in the following 3 types of patients over a 48h period without HD session:

- a typical patient ICU-HD patient, using PK parameters values estimated in the present study.
- a typical ICU patient with preserved renal function (ICU-85 patient) using PK parameters values previously estimated by us for creatinine clearance (CL_{CR}) equal to 85 mL/min (and therefore CL_{RCMS}=68.5 mL/min)(9).
- a virtual ICU patient (ICU-00 patient) with the same PK parameters values as in the previous group (9), except for CL_{CR} and therefore CMS renal clearance fixed at zero (CL_{CR}= CL_{RCMS} =0 mL/min).

Then a 1,000-patient Monte Carlo simulation, was carried out using Berkeley Madonna (version 8.3.18; University of California) to evaluate the probability of target attainment (PTA) in a typical ICU-HD patient with an intermittent HD session every 2 Days, between 8:00 am and 12:00 am, and twice daily administrations of 1.5 MIU of CMS at 8:00 am and 8:00 pm on Days without HD session. And on days with HD session, simulations were conducted considering that the CMS morning dose was administered just after HD, that is at 12:00 am instead of 8:00 am, and could be either 1.5 or 3.0 MIU. Previous estimates of HD clearance were used ($CL_{HD,CMS}$ = 90 mL/min and $CL_{HD,COL}$= 137 mL/min)(5). PK-PD target was defined as a free $AUC_{0\text{-}24h}$/MIC greater than 48, assuming 50% protein binding(13, 14). PTA were evaluated for each dosing regimen across a range of MICs from 0.125 to 2 mg/L, 24h periods of time including or not HD sessions.

Results

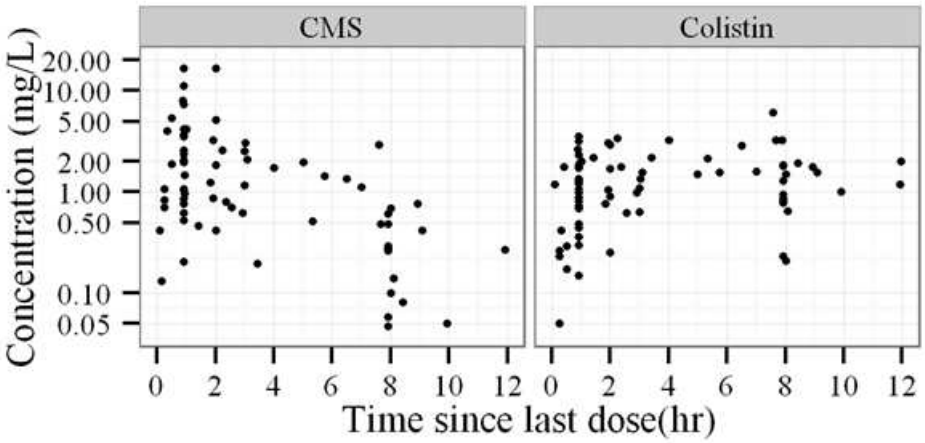

Figure 1: Plasma concentrations of CMS (left) and colistin (right) measured in ICU-HD patients. Times are relative to the last dose.

Measured plasma concentrations of CMS and colistin are shown on Figure 1. Goodness of data fit plots was satisfactory with unbiased individual fits (not shown), NPDE values were lower than 2 and no obvious bias was observed versus time (Figure 2). No covariate was included in the model, due to non-significant decrease of the objective function values. The residual variability (Table 2) was low for colistin plasma concentrations (15% proportional and 0.13 mg/L additive) and moderate for CMS plasma concentrations (48% proportional and 0.11 mg/L additive).

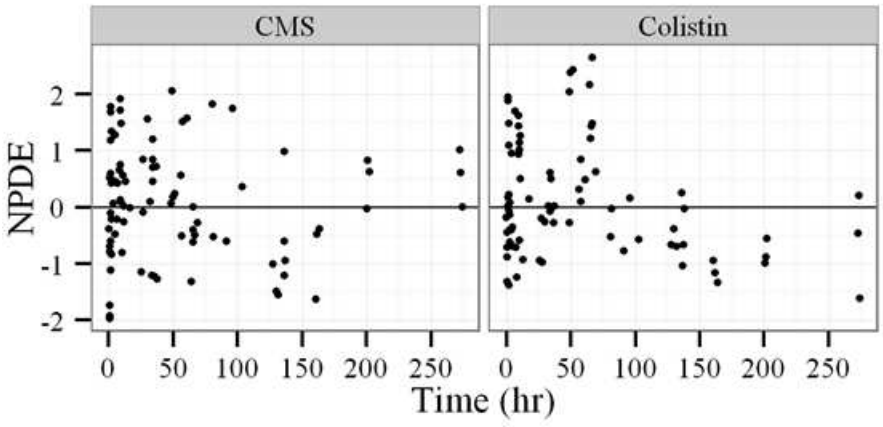

Figure 2: Normalized Prediction Distribution Errors (NPDE) as a function of time for CMS (left) and colistin (right) plasma concentrations. Times are relative to the first dose.

Estimated PK parameters values in ICU-HD patients are presented in Table 2 by comparison with those obtained in ICU-85 patients(9). Typical CL_{NRCMS} in these ICU-HD patients, was estimated at 113 mL/min, and typical CMS volume of distribution at 21 L, with a resulting elimination half-life equal to 2.1 h. Typical colistin apparent clearance (CL_{col}/f_m) was estimated at 37.7 mL/min and typical apparent volume of distribution (V_{col}/f_m) at 28 L, with a corresponding colistin half-life equal to 9.8 h. The precision on parameter estimates (expressed as relative standard error in table 2) was good (<45%).

Table 2: Population pharmacokinetic parameters of ICU-HD patients compared with ICU-85 patients (Gregoire at al.(9))

	ICU-HD patients				ICU-85[d] (Grégoire et al.)(9)	
			Residual Errors			
Parameter [a]	Typical value (RSE%)[a]	IIV[b] CV%[c] (RSE%)	Proportional CV% (RSE%)[c]	Additive (mg/L) (RSE%)	Typical value (RSE%)[c]	IIV CV% (RSE%)[e]
CMS						
V_{CMS} (L)	21 (13)	24 (45)	48 (12)	0.11 (28)	15.7 (7)	44 (14)
CL_{RCMS} (mL/min)	-	-			68.5 (12)	72 (11)
CL_{NRCMS}(mL/min)	113 (14)	31 (35)			43.7 (11)	42 (18)
Colistin						
V_{col}/f_m (L)	28.3 (18)	42 (36)	15 (24)	0.13 (27)	10.2 (16)	81 (15)
CL_{col}/f_m (mL/min)	33.3 (16)	42 (29)			37.7 (10)	37 (15)

V_{CMS}, volume of distribution of CMS; CL_{RCMS}, renal clearance of CMS; CL_{NRCMS}, nonrenal clearance of CMS; V_{col}, volume of distribution of colistin; Cl_{col}, clearance of colistin; f_m, unknown fraction of the nonrenal clearance of CMS that actually forms colistin.
[a] RSE%, relative standard error (expressed as a percentage).
[b] IIV, Interindividual variability.
[c] CV%, coefficient of variation (expressed as a percentage).
[d] typical value for a patient of 70kg with a creatinine clearance of 85mL/min.

Figure 3 shows CMS and colistin plasma concentration-time profiles simulated after single dose of CMS (3 MIU) in the three pre-defined populations. The CMS plasma concentrations profiles simulated in a typical ICU-HD patient and in a typical ICU-85 patient were virtually superimposed and accordingly corresponding $AUC_{0-\infty}$ were almost identical (33.0 mg.h/L and 33.25 mg.h/L respectively) (Figure 3A). But noticeably CMS systemic exposure was increased by almost 2.5 folds in the virtual ICU-00 patient with a corresponding $AUC_{0-\infty}$ at 85.4 mg.h/L (Figure 3A).

Different observations were made for colistin, in particular $AUC_{0-\infty}$ predicted in a typical ICU-HD patient (79.4 mg.h/L) was about three times higher than in a typical ICU-85 patient (27.6 mg.h/L) and close to the value simulated for the virtual ICU-00 individual (70.8 mg.h/L). Yet although colistin exposure was comparable in ICU-HD and in ICU-00 patients, concentrations profiles differed with a lower Cmax in HD patients (3.6 vs. 4.9 mg/L) likely to a larger volume of distribution leading also to a longer half-life (Figure 3B).

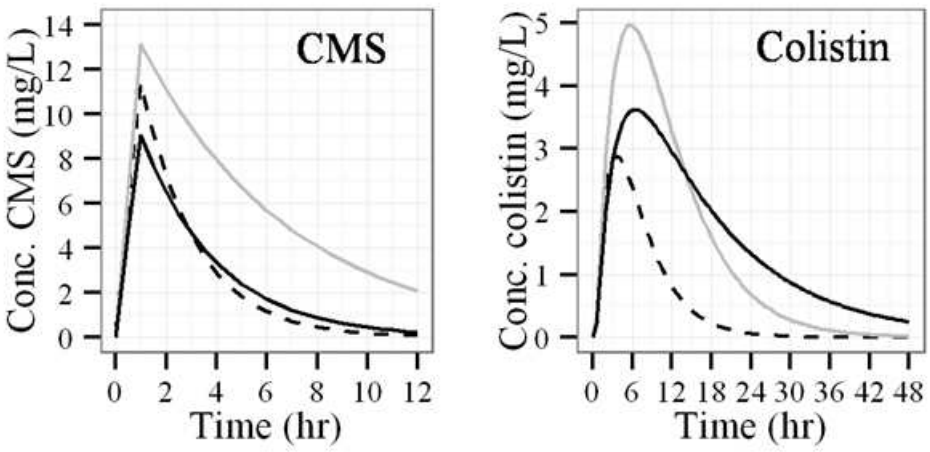

Figure 3: Plasma concentration-time profiles of CMS (left) and colistin (right), after single dose administration of CMS (3 MIU), predicted from PK parameters values corresponding to a typical ICU-HD patient (black full line), a typical ICU-85 patient (black dashed line), and a virtual ICU-00 patient (Grey full line)

Simulations suggest that after multiple administrations of CMS 1.5 MIU q12h in ICU-HD patient, plasma colistin concentrations at steady-state should fluctuate between 3 and 4 mg/L. However at the end of HD sessions colistin concentrations would drop to 1 mg/L. Administration of a 3 MIU "re-loading" dose of CMS instead of the regular 1.5 MIU dose, after each HD sessions, would reduce the time necessary to return at steady-state (Fig. 4). However with these colistin concentrations profiles, high PTA should only be obtained for bacteria with an MIC equal or less than 0.5 mg/L, and providing the 3 MIU "re-loading" dose of CMS is given after each HD session (Fig. 5).

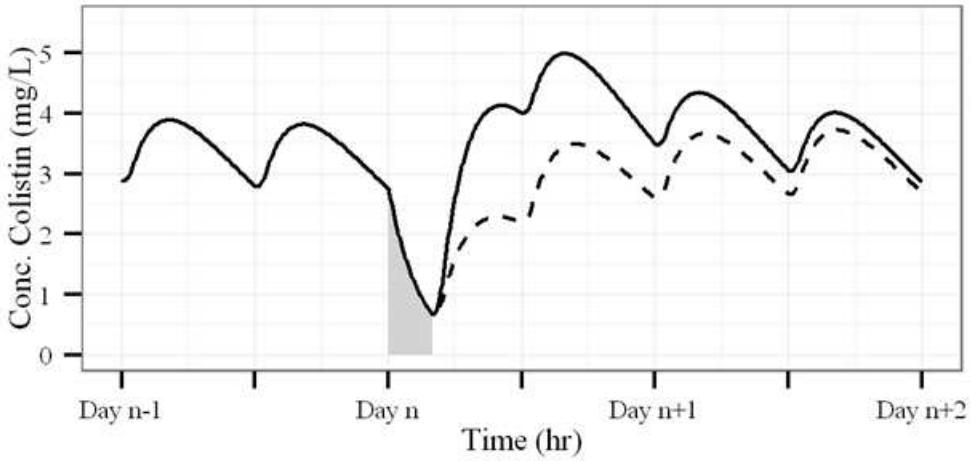

Figure 4: Simulations of colistin plasma concentration-time profiles in ICU-HD patients receiving a 4-hour HD session on Day n and dosed with1.5 MIU q12h of CMS. The CMS dose planned before the HD session was postponed immediately after the session and was either 1.5 MIU (dash line) or 3 MIU (solid line)

Discussion

This study allowed comparisons between CMS and colistin PK in ICU patients with preserved renal function (ICU -85) and with acute renal failure requiring intermittent HD (ICU-HD). But in order to evaluate whether CMS and colistin PK could be similar in ICU-85 and in ICU-HD patients, except for CMS renal excretion, simulations were also carried out in virtual patients (ICU-00) using PK parameters values obtained previously in ICU-85 patients(9), except for CL_{RCMS} set at 0 mL/min. This will be discussed first and the effect of HD on CMS and colistin PK will then be considered to provide practical dosing regimens recommendations in ICU-HD patients.

CMS volume of distribution was moderately increased in ICU-HD patients compared with ICU-85 patients (Table 2) but surprisingly total clearance in ICU-HD patients (typical value: 113 mL/min) was virtually the same as in ICU-85 patients (typical value: 112 mL/min). This result suggests that CMS non-renal clearance (CL_{NRCMS}) is increased by approximately two folds (from 43.7 mL/min to 113 mL/min) in HD patients, compensating for the absence of renal clearance, which has never been reported before (4, 6). Accordingly CMS concentrations versus time profiles in typical ICU-HD and ICU-85 patients are virtually superimposed (Figure 3A). Yet because the exact mechanism of CMS non-renal clearance remains unknown it is difficult to assess the origin of this increased CL_{NRCMS} in ICU-HD patients. Noticeably because CMS PK parameters were estimated between HD sessions, artefacts such as drug adsorption onto HD membranes must be ruled out. Moreover, as plasma sampling and CMS concentrations measurement were handled in the same conditions than for the compared ICU-85 patients (9), a bias of the CL_{NRCMS} estimation for the present study has to be ruled out. It may then be hypothesized that endogenous substances that accumulate in plasma between HD sessions could interfere with the hydrolysis of CMS occurring at physiologic pH and leading eventually to colistin (15, 16). However it should also be reminded that measured CMS concentrations correspond in fact to the sum of various methanesulphonate derivatives intermediates (i.e. all five or only a part of the primary amine group of colistin are methanesulphonated in CMS) eventually converted into colistin (17). Therefore CMS PK parameters, including CL_{NRCMS}, correspond to apparent parameters that must be carefully interpreted. But more importantly for dosing regimen optimization it should be reminded that colistin exposure, or average colistin concentrations at steady-state, is determined by its rate of formation and its rate of elimination. And the former depends upon the fraction of the CMS dose that is eventually converted into colistin and not upon CL_{NRCMS}. Unfortunately this fraction of the CMS dose converted into colistin is unknown. This also raises a terminology issue that requires clarification. It was initially suggested that the fraction of the CMS dose not excreted in urine was entirely converted into colistin(1). This

assumption was made by several authors including Plachouras et al. (8) and ourselves (3), from which it was estimated that in heathy volunteers approximately 2/3 of the administered CMS was directly excreted unchanged in urine and therefore that the remaining 1/3, referred as f_m, was converted into colistin (3). However since that a more complex PK disposition scheme including a 3rd route of elimination, was suggested for CMS by Garonzik et al.(4). Accordingly only a fraction of the CMS not excreted in urine would be converted into colistin, and this was defined as f_m(4). Therefore the meaning of f_m differs between studies since in the reference article published by Plachouras et al. (8) as well as in our initial paper (3), f_m refers to the fraction of the CMS dose converted into colistin, consistent with the usual terminology for metabolites PK (18). Although the 3rd route of CMS elimination is not supported by strong experimental data, at least to our knowledge, it cannot be ruled out.

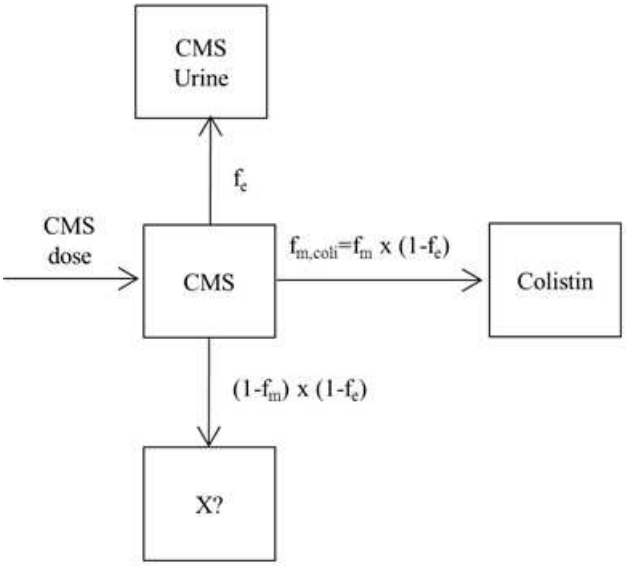

Figure 6: Schematic representation of CMS disposition following its administration. f_e corresponds to the fraction of CMS dose excreted unchanged in urine; f_m to the fraction of CMS dose not excreted unchanged in urine that is eventually converted into colistin; and $f_{m,coli}$ to the fraction of the CMS dose that is converted to colistin.

Therefore in order to avoid confusion and facilitate between studies comparisons, we have decided to take into consideration this extra route of CMS elimination in our most recent studies(9, 12). But for clarification we have also decided to call $f_{m,coli}$ the fraction of the CMS dose eventually converted into colistin. This new disposition scheme with the corresponding new terminology is illustrated on Figure 6 with an X compartment standing for the unknown 3rd route of elimination for CMS. Noticeably $f_{m,coli}$ depends on the fraction of CMS excreted in urine (f_e) and on the fraction of CMS not excreted in urine that is converted into colistin (f_m) as follows:

$$f_{m,coli}=f_m\,(1-f_e). \quad \text{Eq. 1}$$

It should then be acknowledged that for the apparent colistin PK parameters (V_{col}/f_m and CL_{col}/f_m) reported in this paper (Table 2), and previously by Garonzik et al. (4) and Grégoire et al. (9), f_m corresponds the fraction of CMS not excreted in urine that is converted into colistin, as considered in Eq. 1. And it is important to note that colistin plasma versus time concentrations profiles are actually governed by $V_{col}/f_{m,coli}$ and $CL_{col}/f_{m,coli}$ and not by V_{col}/f_m and CL_{col}/f_m. This explains why colistin AUC is almost 3 times higher in a typical ICU-HD patient than in a typical ICU-85 patient, although corresponding typical CL_{col}/f_m values are not much different (Figure 3B and Table 2). Indeed, the ratio of colistin AUC corresponds to the ratio of $CL_{col}/f_{m,coli}$ values (33.3 mL/min vs 96.8 mL/min),which differs from CL_{col}/f_m values due to the 2.6-folds lower fraction of CMS excreted non renally in ICU-85 patients ($1-f_e$=39%) than in ICU-HD patients ($1-f_e$=100%). Therefore the almost 3 times greater AUC of colistin in ICU-HD patients compared with ICU-85 patients is very likely due to a large extent to the abolished CMS renal excretion in ICU-HD patients. Colistin elimination half-life is about 3 times longer in ICU-HD patients than in ICU-85 patients (9.8 h versus 3.1h), but apparently mostly due to an increased volume of distribution (Table 2), of several potential origins that would need to be explored but among which a decreased binding on alpha1-acid glycoprotein (14, 19) or a disease related increased distribution within tissues.

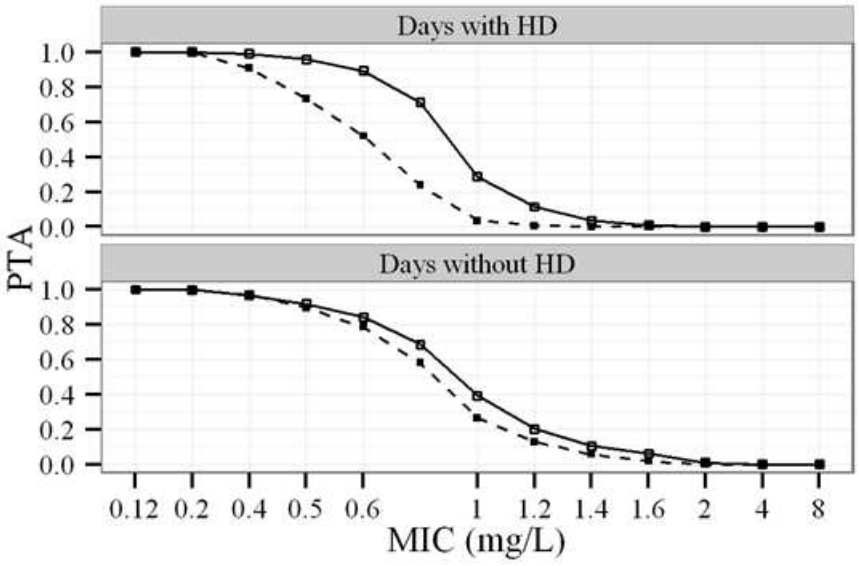

Figure 5: Probability of Target Attainment (PTA) of colistin in ICU-HD patients dosed with 1.5 MIU q12h of CMS on days with (up) and without HD (bottom). On days with HD (top) the CMS dose planned before the HD session was postponed immediately after the session and was either 1.5 MIU (dash line) or 3 MIU (solid line)

CMS dosing regimen in ICU-HD patients must take into account the consequences of renal failure on colistin formation ($f_{m,coli}$) and elimination (CL_{col}) but also CMS and colistin removal during HD.

Although this specific aspect was not investigated during the present study, we have previously shown that both CMS and colistin were efficiently cleared during HD (5). Because HD clearance may vary with the type of HD systems and membranes, we have used CMS and colistin HD clearance values previously determined in similar setting (5), which are consistent with those reported by Garonzik et al. (4) and by Jitmuang et al. (6) for CMS. However the colistin HD clearance estimated by Marchand et al. that we have used (8.2 L/h) is greater than that reported by Garonzik and Jitmuang (3.4 and 3.99 L/h respectively). This discrepancy could be due to the HD apparatus or the brand of CMS administered. Because most of the CMS and colistin present into the body are cleared during HD sessions, it seems appropriate not to administer CMS before HD but rather immediately after HD sessions. Furthermore Garonzik and al. have suggested the addition of 30 to 50% to the daily maintenance on days with HD session (4). Our PTA estimates suggest that providing MIC<0.5 mg/L, an appropriate post-HD “re-loading” CMS dose could be 3 MIU, leading to 4.5 MIU administered on days with HD and 3 MIU on days without HD. In fact this corresponds to a 50% increase of the daily dose on days with HD compared with days without HD, which is consistent with Garonzik et al. recommendation(4) although different methodologies were employed (Monte-Carlo simulations for PTA calculations in the present study vs. regression methods along with a cost function for Garonzik). One concern is the nephrotoxicity of colistin which, for patients with preserved renal function, increases with trough concentrations (>2.4 mg/L) and concomitant treatment with other nephrotoxic drugs (20). As data about nephrotoxicity of colistin for patients with prior acute renal failure are lacking the physician should evaluate the benefit/risk balance and thoroughly monitor the evolution of the renal function.

In conclusion an unexpected and difficult to explain increase of CMS non-renal clearance in HD patients, compensating for its abolished renal clearance, was evidenced for the first time. Its consequences on colistin exposure were discussed together with those of other potentially altered colistin PK parameters values in HD patients. These findings were subsequently used to conduct PK-PD simulations, showing that a dosing regimen with 1.5 MIU of CMS given twice daily, except a supplemental dose of 1.5 MIU administered along with the scheduled 1.5 MIU dose just after the HD session (i.e. total of 4.5 MIU for a HD day)would allow to maintain colistin plasma concentrations between 3 and 4 mg/L for sufficiently long to obtain high PTA values, at least for bacteria with MICs equal or less than 0.5 mg/L in the absence of combination with another antibiotic. This dosing regimen seems a-priori to be the best initial choice for ICU-HD patients.

Funding

This work was supported by the national « ProGramme Hospitalier de Recherche Clinique » (PHRC) N°2302.

M. Jacobs was supported by a doctoral fellowship from the University of Poitiers and the “Conseil regional de Poitou-Charentes”.

References

1. **Li J, Nation RL, Turnidge JD, Milne RW, Coulthard K, Rayner CR, Paterson DL.** 2006. Colistin: the re-emerging antibiotic for multidrug-resistant Gram-negative bacterial infections. Lancet Infect Dis **6:**589-601.
2. **Nation RL, Li J, Cars O, Couet W, Dudley MN, Kaye KS, Mouton JW, Paterson DL, Tam VH, Theuretzbacher U, Tsuji BT, Turnidge JD.** 2015. Framework for optimisation of the clinical use of colistin and polymyxin B: the Prato polymyxin consensus. Lancet Infect Dis **15:**225-234.
3. **Couet W, Gregoire N, Gobin P, Saulnier PJ, Frasca D, Marchand S, Mimoz O.** 2011. Pharmacokinetics of colistin and colistimethate sodium after a single 80-mg intravenous dose of CMS in young healthy volunteers. Clin Pharmacol Ther **89:**875-879.
4. **Garonzik SM, Li J, Thamlikitkul V, Paterson DL, Shoham S, Jacob J, Silveira FP, Forrest A, Nation RL.** 2011. Population pharmacokinetics of colistin methanesulfonate and formed colistin in critically ill patients from a multicenter study provide dosing suggestions for various categories of patients. Antimicrob Agents Chemother **55:**3284-3294.
5. **Marchand S, Frat JP, Petitpas F, Lemaitre F, Gobin P, Robert R, Mimoz O, Couet W.** 2010. Removal of colistin during intermittent haemodialysis in two critically ill patients. J Antimicrob Chemother **65:**1836-1837.
6. **Jitmuang A, Nation RL, Koomanachai P, Chen G, Lee HJ, Wasuwattakul S, Sritippayawan S, Li J, Thamlikitkul V, Landersdorfer CB.** 2015. Extracorporeal clearance of colistin methanesulphonate and formed colistin in end-stage renal disease patients receiving intermittent haemodialysis: implications for dosing. J Antimicrob Chemother **70:**1804-1811.
7. **Luque S, Sorli L, Li J, Collado S, Barbosa F, Berenguer N, Horcajada JP, Grau S.** 2014. Effective removal of colistin methanesulphonate and formed colistin during intermittent haemodialysis in a patient infected by polymyxin-only-susceptible *Pseudomonas aeruginosa*. J Chemother **26:**122-124.
8. **Plachouras D, Karvanen M, Friberg LE, Papadomichelakis E, Antoniadou A, Tsangaris I, Karaiskos I, Poulakou G, Kontopidou F, Armaganidis A, Cars O, Giamarellou H.** 2009. Population pharmacokinetic analysis of colistin methanesulfonate and colistin after intravenous administration in critically ill patients with infections caused by Gram-negative bacteria. Antimicrob Agents Chemother **53:**3430-3436.
9. **Gregoire N, Mimoz O, Megarbane B, Comets E, Chatelier D, Lasocki S, Gauzit R, Balayn D, Gobin P, Marchand S, Couet W.** 2014. New colistin population pharmacokinetic data in critically ill patients suggesting an alternative loading dose rationale. Antimicrob Agents Chemother **58:**7324-7330.
10. **Nation RL, Li J, Cars O, Couet W, Dudley MN, Kaye KS, Mouton JW, Paterson DL, Tam VH, Theuretzbacher U, Tsuji BT, Turnidge JD.** 2014. Consistent global approach on reporting of colistin doses to promote safe and effective use. Clin Infect Dis **58:**139-141.
11. **Gobin P, Lemaitre F, Marchand S, Couet W, Olivier JC.** 2010. Assay of colistin and colistin methanesulfonate in plasma and urine by liquid chromatography tandem mass spectrometry (LC-MS/MS). Antimicrob Agents Chemother **54:**1941-1948.
12. **Boisson M, Jacobs M, Gregoire N, Gobin P, Marchand S, Couet W, Mimoz O.** 2014. Comparison of intrapulmonary and systemic pharmacokinetics of colistin methanesulfonate (CMS) and colistin after aerosol delivery and intravenous administration of CMS in critically ill patients. Antimicrob Agents Chemother **58:**7331-7339.
13. **Dudhani RV, Turnidge JD, Coulthard K, Milne RW, Rayner CR, Li J, Nation RL.** 2010. Elucidation of Pharmacokinetic/Pharmacodynamic Determinant of Colistin

Activity against *Pseudomonas aeruginosa* in Murine Thigh and Lung Infection Models. Antimicrob Agents Chemother **54:**1117-1124.

14. **Mohamed AF, Karaiskos I, Plachouras D, Karvanen M, Pontikis K, Jansson B, Papadomichelakis E, Antoniadou A, Giamarellou H, Armaganidis A, Cars O, Friberg LE.** 2012. Application of a Loading Dose of Colistin Methanesulphonate (CMS) in Critically Ill Patients: Population Pharmacokinetics, Protein Binding and Prediction of Bacterial Kill. Antimicrob Agents Chemother.
15. **Wallace SJ, Li J, Rayner CR, Coulthard K, Nation RL.** 2008. Stability of colistin methanesulfonate in pharmaceutical products and solutions for administration to patients. Antimicrob Agents Chemother **52:**3047-3051.
16. **Bergen PJ, Li J, Rayner CR, Nation RL.** 2006. Colistin methanesulfonate is an inactive prodrug of colistin against *Pseudomonas aeruginosa*. Antimicrob Agents Chemother **50:**1953-1958.
17. **He H, Li JC, Nation RL, Jacob J, Chen G, Lee HJ, Tsuji BT, Thompson PE, Roberts K, Velkov T, Li J.** 2013. Pharmacokinetics of four different brands of colistimethate and formed colistin in rats. J Antimicrob Chemother.
18. **Rowland M, Tozer TN.** 1995. Clinical Pharmacokinetics: Concepts and applications. Lippincott Williams & Wilkins, Philadelphia.
19. **Azad MA, Huang JX, Cooper MA, Roberts KD, Thompson PE, Nation RL, Li J, Velkov T.** 2012. Structure-activity relationships for the binding of polymyxins with human alpha-1-acid glycoprotein. Biochem Pharmacol **84:**278-291.
20. **Sorli L, Luque S, Grau S, Berenguer N, Segura C, Montero MM, Alvarez-Lerma F, Knobel H, Benito N, Horcajada JP.** 2013. Trough colistin plasma level is an independent risk factor for nephrotoxicity: a prospective observational cohort study. BMC Infect Dis **13:**380.

C. *In-silico* evaluation of resistance models

Distinguishing Antimicrobial Models with Different Resistance Mechanisms via Population Pharmacodynamic Modeling.

M. Jacobs[1], N. Grégoire[1], W. Couet[1], J. B. Bulitta[2]

INSERM U1070, Poitiers, France[1]; Centre for medicine Use and Safety, Monash University (Parkville campus), Parkville, Australia[2]

Corresponding author: *nicolas.gregoire@univ-poitiers.fr*

Keywords:

Pharmacokinetics / pharmacodynamics

Semi-mechanistic, mechanism-based modeling

Dynamic in-vitro infection models

Static concentration time-kill studies

Population modeling

Part of this work was previously presented at the European Congress of Clinical Microbiology and Infectious Diseases (ECCMID) 2013 as abstract P913.

Abstract

Semi-mechanistic pharmacokinetic-pharmacodynamic (PK-PD) modeling is increasingly used for antimicrobial drug development and optimization of dosage regimens, but systematic simulation-estimation studies to distinguish between competing PD models are lacking. This study compared the ability of static and dynamic *in-vitro* infection models to distinguish between models with different resistance mechanisms and how accurately and precisely the parameters are estimated. Monte Carlo simulations (MCS) were performed for models with one susceptible bacterial population without (M1) or with a resting stage (M2), one population model with adaptive resistance (M5), pre-existing susceptible and resistant populations without (M3) or with (M4) inter-conversion, and with two pre-existing populations with adaptive resistance (M6). For each model, 200 experimental datasets of the total bacterial population were simulated over 24h using static antibiotic concentrations (0.125 to 32x EC_{50}) or over 48h under dynamic conditions (peak of 8x EC_{50} every 12h for an antibiotic with 1h half-life). Twelve-hundred random datasets (each containing 20 curves for static or 3 curves for dynamic conditions) were generated by Monte-Carlo simulations. Each dataset was estimated by all six models via population PD modeling to compare bias and precision. When the parameters were estimated with the model used for simulations, M1 and M3 gave unbiased estimates (<10%) with a good precision (<30%). However, parameters for adaptive resistance and inter-conversion for M2, M4, M5 and M6 had high bias and large imprecision under static and dynamic conditions. Common statistical criteria and diagnostic plots did not support sound identification of the true resistance mechanism. Therefore, it seems advisable to quantify resistant bacteria and characterize their resistance mechanisms to perform extended simulations and translate from *in-vitro* experiments to animal models and ultimately patients.

Background

Antimicrobial therapy greatly benefits from optimized antibiotic dosage regimens that are supported by pharmacokinetic (PK) and pharmacodynamic (PD) concepts. During several decades, the minimum inhibitory concentration (MIC) was the predominantly used measure to predict antibiotic efficacy and it still is considered as a 'gold standard' for determining the bacterial susceptibility to antimicrobials [1]. As most antibiotics have been available for more than a decade, their development relied on an MIC based approach.

Despite its popularity, the MIC is subject to several limitations. It is determined at only one time point (usually between 16 and 24h), at a low initial bacterial inoculum (i.e. usually in the absence of resistant populations), and utilizes constant (i.e. static) antibiotic concentrations [1]. Therefore, the

MIC neither provides information on the time-course of bacterial killing [2-4] nor on emergence of resistance [5,6].

To address some of the limitations of the MIC approach, many static and dynamic *in-vitro* and *in-vivo* infection model studies have assessed the ability of empirical PK/PD indices to predict the efficacy of antibiotics. Such data have proven useful to optimize antibiotic monotherapy regimens for patients [2,7,8]. The large majority of murine infection model studies only assessed bacterial counts at one time point (usually 24 h) and did not assess the time-course of bacterial killing *in-vivo*.

In-vitro infection model experiments [9] use either static antibiotic concentrations [6,10-13], simulate the dynamic time-course of antibiotic concentrations observed in patients [5,14-16], or utilize both of these approaches[17-19]. These experimental models provide a wealth of time-course data on bacterial growth, killing and resistance and are well suited to develop PK/PD models [20]. The latter mathematical models can characterize bacterial killing and resistance [4] and prospectively optimize antibiotic dosage regimens.

While a series of time-course models for bacterial growth, killing and emergence of resistance has been proposed, it is currently unknown which type of dataset from *in-vitro* studies is required to soundly develop such PK/PD time-course models. We suspected that these models with different resistance mechanisms cannot be discriminated based on “typical” experimental data and that parameter estimates might be biased. We are also not aware of a systematic simulation-estimation study assessing the bias and precision of parameter estimates from *in-vitro* antibacterial models.

Therefore, our objective was to compare the ability of static and dynamic *in-vitro* infection models to identify the PK/PD model with the true resistance mechanism used during simulation and to estimate model parameters accurately and precisely. We used Monte Carlo simulations based on six candidate models and estimated these PK/PD model via the importance sampling algorithm in the S-ADAPT software which is a robust and one of the latest population modeling algorithms.

Materials and methods.

The overview flow chart (Figure 1) summarizes the simulation-estimation procedures.

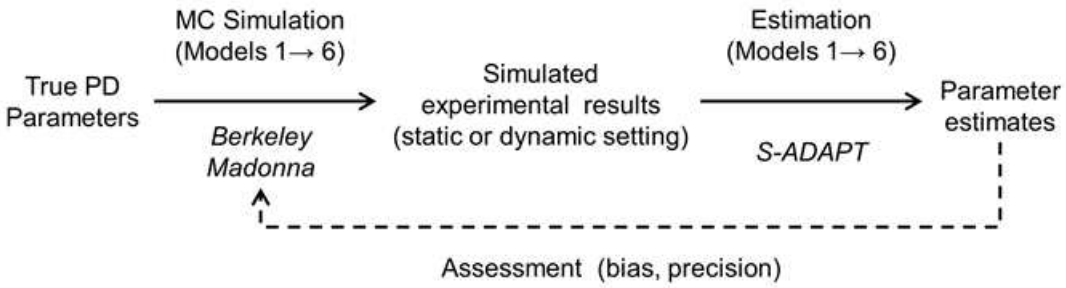

Fig. 1: Simulation-estimation flow chart. Based on a set of true PD parameter values, Monte Carlo (MC) simulations were performed using six PD models to generate experimental datasets under both static and dynamic conditions. Each of these datasets was then analyzed and PK/PD parameters estimated via population modeling in S-ADAPT for each of the six models (yielding 36 simulation-estimation scenarios in total). The parameter estimates for each model were compared to the true parameter values used during simulation to assess bias and precision.

Six different PD models were selected to reflect a range of relevant PD models for antibiotics (Figure 2). These models contained one bacterial population with no emergence of resistance (M1), one population with the capacity to convert into a resting stage (M2), presence in the inoculum of two bacterial populations with different susceptibility to an antibiotic (M3 and M4) and one or two bacterial populations with a reversible adaptation to the antibiotic (M5 and M6). Models M3, M4 and M6 represent heteroresistance of the initial inoculum and models M5 and M6 incorporate adaptive resistance. Adaptive resistance was described by a turnover model to describe the stimulation of adaptive resistance in response to an antibiotic and reversion back to baseline after removal of the antibiotic (Figure 2). Monte Carlo (MC) simulations were performed based on each of these six PD models to generate 1,200 simulated datasets (with multiple curves each) in static or dynamic setting.

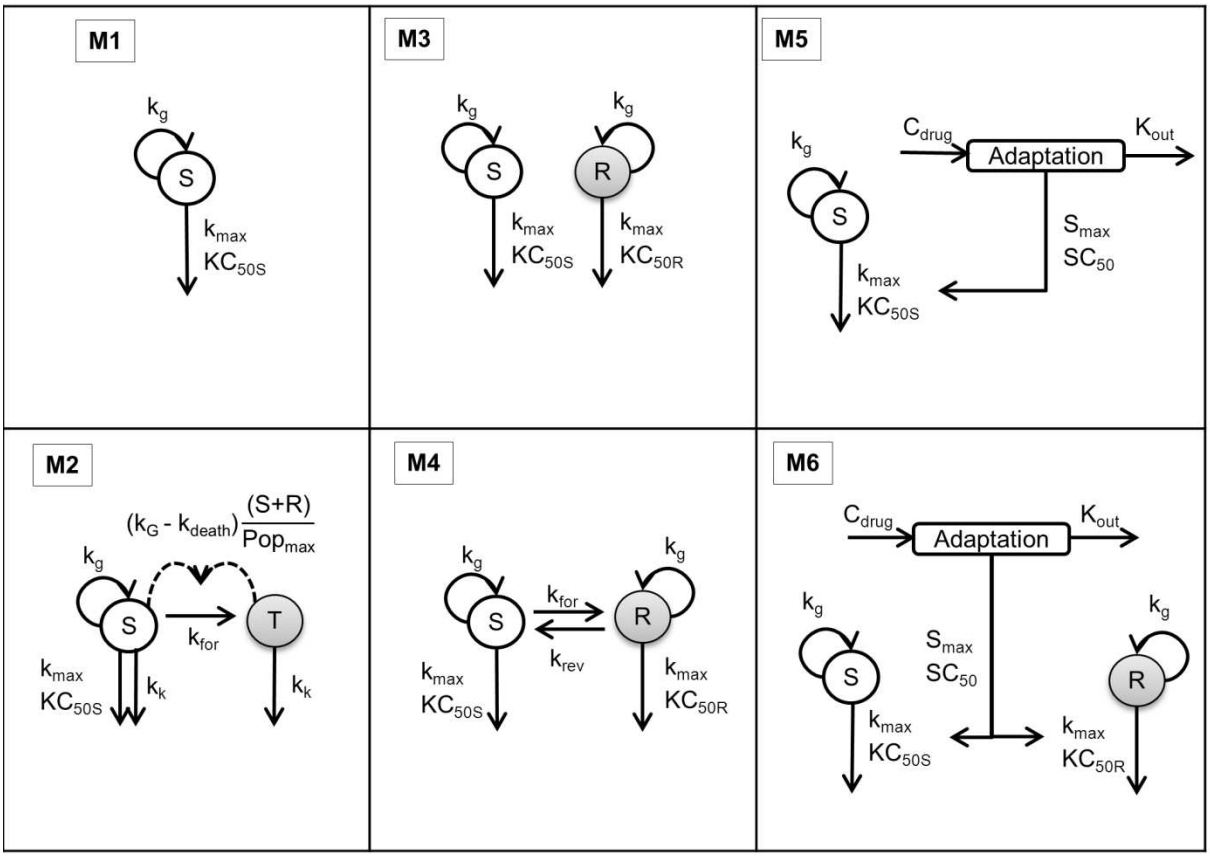

Fig 2: Structure of the PK/PD models. S, drug-susceptible bacteria; T, resting, drug-tolerant bacteria; R, drug-resistant bacteria. Parameters are defined in the method section and in Table 1.

Pharmacodynamic models.

All six models contained a logistic growth function to limit growth to a maximum total bacterial population size (Popmax).

Model 1 (M1) contained one bacterial population and bacterial killing followed an Emax model. This model was originally proposed for antibiotic PD by Zhi et al. [21] and subsequently used by other investigators [3,22]. The differential equation for the number of viable, susceptible bacteria (S) was:

$$\frac{dS}{dt} = \left[k_g \cdot \left(1 - \frac{S}{Popmax}\right) - \frac{kmax \cdot C}{KC_{50} + C} \right] \cdot S \qquad (1)$$

Initial condition (IC): $S_0 = 10^{Inoc}$.

The k_g is the apparent growth rate constant, C the antibiotic concentration, Popmax the maximum concentration of bacteria, k_{max} the maximal rate constant of bacterial killing, and KC_{50} the antibiotic

concentration yielding 50% of k_{max}. The mean generation time (MGT) was calculated as the inverse of kg.

Model 2 was adapted from Nielsen et al.[11] **(Figure 2)**. The total bacterial population is comprised of two populations (i.e. two stages), one proliferating and susceptible stage and one resting and antibiotic tolerant stage. The total bacterial population is assumed to stimulate the transfer of bacteria from the susceptible stage to the tolerant stage. The transfer from resting stage to the susceptible stage is considered to be negligible and was fixed to zero following the original publication [11]. Bacteria in the resting state did not grow and were not killed by the antibiotic. As resting bacteria did not revert back to the proliferating stage, they were only subject to a first-order natural death process. These tolerant bacteria are (slowly) dying and therefore cause a biphasic killing profile. In this model, bacteria in the tolerant stage can however not repopulate the replicating population since the reversion to the susceptible replicating stage was assumed to be zero.

As bacteria were simulated to be in the early logarithmic growth phase, we assumed that only a small fraction (10^{-5}) of bacteria in the starting inoculum was in the resting and antibiotic-tolerant stage (T). This choice had very limited impact on the model, as this fraction (10^{-5}) is equivalent to the number of bacteria that convert from the S to the T stage in approximately 1 min for a 10^6 CFU/mL inoculum.

Both subpopulations were assumed to have the same natural death rate constant (k_{death})**.** The differential equations for the susceptible (S) and resting (T) population of model 2 are:

$$\frac{dS}{dt} = \left[\left(k_g - k_{death}\right) \cdot \left(1 - \frac{S+T}{Popmax}\right) - \frac{kmax \cdot C}{KC_{50} + C} \right] \cdot S \qquad \text{IC: } S_0 = 10^{Inoc} - R_0 \qquad (2)$$

$$\frac{dT}{dt} = \left(k_g - k_{death}\right) \cdot \left(\frac{S+T}{Popmax}\right) \cdot S - k_k \cdot T \qquad \text{IC: } R_0 = 10^{Inoc\ -\ 5} \qquad (3)$$

The mean natural death time (MDT) was calculated as the inverse of k_{death}.

Model 3 **(Figure 2)** was derived from Jumbe *et al.* [23], Gumbo *et al.* [24] and Campion *et al.* [14]. This model included a pre-existing susceptible (S) and a pre-existing resistant (R) population. Both populations did not interconvert. The initial condition of the resistant population is the mutation frequency (mutf) multiplied by the total inoculum and the initial condition of the susceptible population is the remainder of bacteria. Both populations were assumed to have the same maximal killing rate constant (k_{max}) and the same growth rate constant (k_g). These populations differed

however in their drug concentration (KC_{50}) yielding 50% of kmax and the KC_{50} of the resistant population (KC_{50R}) was greater than that of the susceptible population (KC_{50S}). This yields the following differential equations for model 3:

$$\frac{dS}{dt} = \left[k_g \cdot \left(1 - \frac{S+R}{Popmax}\right) - \frac{kmax \cdot C}{KC_{50S} + C} \right] \cdot S \qquad \text{IC: } S_0 = 10^{Inoc} \cdot (1 - 10^{mutf}) \qquad (4)$$

$$\frac{dR}{dt} = \left[k_g \cdot \left(1 - \frac{S+R}{Popmax}\right) - \frac{kmax \cdot C}{KC_{50R} + C} \right] \cdot R \qquad \text{IC: } R_0 = 10^{Inoc - mutf} \qquad (5)$$

In comparison to model 3, model 4 (M4) contained an additional bi-directional inter-conversion between the susceptible and resistant population (Figure 2). Model 4 was derived from Jusko *et al. [25]* and Yano *et al.* [13]. The initial inoculum of the resistant population was assumed to be in equilibrium (i.e. steady-state) with the susceptible population. Therefore, the initial condition of the resistant population was calculated as $CFU_0 \cdot k_{for} / k_{rev}$ and the initial condition of the susceptible population was $CFU_0 \cdot (1 - k_{for} / k_{rev})$. Model 4 was described by the following differential equations:

$$\frac{dS}{dt} = \left[k_g \cdot \left(1 - \frac{S+R}{Popmax}\right) - \frac{kmax \cdot C}{KC_{50S} + C} \right] \cdot S - k_{for} \cdot S + k_{rev} \cdot R \qquad (6)$$

IC: $S_0 = 10^{Inoc} \cdot (1 - k_{for} / k_{rev})$

$$\frac{dR}{dt} = \left[k_g \cdot \left(1 - \frac{S+R}{Popmax}\right) - \frac{kmax \cdot C}{KC_{50R} + C} \right] \cdot R + k_{for} \cdot S - k_{rev} \cdot R \qquad (7)$$

IC: $R_0 = 10^{Inoc} \cdot k_{for} / k_{rev}$

The k_{for} and k_{rev} are the first-order transfer rate constants from the susceptible to the resistant population and *vice versa*.

Model 5 contained one bacterial subpopulation with adaptive resistance. An adaptive resistance model has been proposed previously by Tam *et al.* [26]. In the present study, we propose a new adaptation function that was based on an indirect response model to reflect the situation that bacteria often need to synthesize a protein (and other biomolecules) to overexpress a resistance mechanism. The synthesis and turnover of such molecules can be captured by a turnover model [27,28]. In the present model, the adaptation increases over time as a saturable function of the

antibiotic concentration and decreases following a first order rate constant k_{out}. In order that at steady-state the adaptation was equal to the saturable function mentioned above, the zero-order production rate of adaptation was set to k_{out}. The adaptation affected the KC_{50s} to reflect the up-regulation of an efflux pump. The differential equations for model 5 were:

$$\frac{dS}{dt} = \left[k_g \cdot \left(1 - \frac{S}{Popmax}\right) - \frac{kmax \cdot C}{KC_{50S} + C} \right] \cdot S \qquad \text{IC: } S_0 = 10^{Inoc} \qquad (8)$$

$$\frac{d(Adaptation)}{dt} = \left(\frac{Smax \cdot C}{SC_{50} + C} - Adaptation \right) \cdot k_{out} \qquad \text{IC: } Adaptation_0 = 0 \qquad (9)$$

$$KC_{50S} = KC_{50,base} \cdot (1 + Adaptation) \qquad (10)$$

The adaptation variable defines the extent of change of KC_{50S} in response to a bacterial alteration (such as the expression of an efflux pump; e.g. MexXY-OprM in response to an aminoglycoside)[29]. The $KC_{50,base}$ is the antibiotic concentration causing 50% of kmax at time 0 (i.e. in absence of adaptation), S_{max} the maximum fold-increase of $KC_{50,base}$ due to adaptive tolerance, SC_{50} the drug concentration that yields 50% of S_{max} and k_{out} the first order loss rate constant for adaptation. The mean turnover time (MTT_{loss}) was calculated as the inverse of k_{out}.

Models 3 and 6 both contained two pre-existing subpopulations with different susceptibility. In contrast to model 3, model 6 contained the same adaptation (i.e. tolerance) function as model 5 which affected the KC_{50} of both the susceptible (KC_{50S}) and resistant (KC_{50R}) population in model 6.

$$\frac{dS}{dt} = \left[k_g \cdot \left(1 - \frac{S+R}{Popmax}\right) - \frac{kmax \cdot C}{KC_{50S} + C} \right] \cdot S \qquad \text{IC: } S_0 = 10^{Lg\_Inoc}\,(1\text{-}10^{mutf}) \qquad (11)$$

$$\frac{dR}{dt} = \left[k_g \cdot \left(1 - \frac{S+R}{Popmax}\right) - \frac{kmax \cdot C}{KC_{50R} + C} \right] \cdot R \qquad \text{IC: } R_0 = 10^{Lg\_Inoc} \cdot 10^{mutf} \qquad (12)$$

$$\frac{d(Adaptation)}{dt} = \left(\frac{Smax \cdot C}{SC_{50} + C} - Adaptation \right) \cdot k_{out} \qquad \text{IC: } Adaptation_0 = 0 \qquad (13)$$

$$KC_{50S} = KC_{50S,base} \cdot (1 + Adaptation) \qquad (14)$$

$$KC_{50R} = KC_{50R,base} \cdot (1 + Adaptation) \qquad (15)$$

These six PD models can be readily expanded by including different mean generation times and different maximum killing rate constant for the susceptible and resistant populations. However, for the purposes of this simulation estimation study, the simpler version of these models was preferred to support parameter estimation.

Table 1: Parameter values used for Monte Carlo simulations

Descriptions	Parameters	Units	Used in models	Mean (=true value used during simulations)
Mean generation time	MGT	min	1-6	60
Initial inoculum	Inoc	$\log_{10}$ (CFU/mL)	1-6	6
Maximum population size	Popmax	$\log_{10}$ (CFU/mL)	1-6	9.5
Maximum killing rate constant	kmax	h^{-1}	1-6	4
Antibiotic concentration yielding 50% of k_{max} in susceptible population	KC50S	mg/L	1-6	1
Antibiotic concentration yielding 50% of k_{max} in resistant population	KC50R	mg/L	3, 4, 6	4
Mean natural death time	MDT	min	2	400
Mutation frequency	Log_{10} Mutf		3, 4, 6	-5
First-order transfer rate constant from susceptible to resistant population	k_{for}	$\log_{10}$ (1/h)	4	-6
First-order transfer rate constant from resistant to susceptible population	k_{rev}	$\log_{10}$ (1/h)	4	-1
Maximum fold-increase of KC_{50} due to adaptive tolerance ('resistance')	Smax		5, 6	4
Antibiotic concentration that yields 50% of S_{max}	SC50	mg/L	5, 6	0.4
Mean turnover time for adaptive tolerance	MTT_{loss}	h	5, 6	20

[a]: All parameters were simulated with a small between curve variability to represent generally well reproducible *in-vitro* curves. Parameter were assumed to follow a log-normal distribution and were simulated with a 10% coefficient of variation for the between curve variability. Parameters estimated on $\log_{10}$ scale (see unit column) were simulated via a normal distribution on $\log_{10}$ scale and had a standard deviation of 0.05.

Monte Carlo simulations for static and dynamic in-vitro infection models

Population mean estimates: Informed by the range of published parameter values for different antibiotics and bacterial strains [3,6,10,13,16,17,19,30-33] (Table 1), we selected sets of parameter values that yielded comparable CFU vs. time profiles over 24 h for simulation from the six models. A starting inoculum of 10^6 CFU/mL was applied for all simulations.

Between curve variability and residual error: For these well-controlled *in-vitro* studies, between curve variability was set to a small coefficient of variation of 10% for log-normally distributed parameters and to a standard deviation of 0.05 on log_{10} scale for normally distributed parameters. All models were simulated and estimated using a major-diagonal variance-covariance matrix. The residual error of log_{10} CFU/mL counts was additive with a standard deviation of 0.2 on log_{10} scale. A limit of quantification (LLOQ) of 10 CFU/ml was chosen [17] (equivalent to one colony per agar plate for a volume of 100 uL bacterial suspension per agar plate).

Simulated experimental designs: To mimic typical experimental conditions, ten different constant antibiotic concentrations were simulated for each static time-kill experiment. These concentrations were 0 mg/L (control), and 0.125, 0.25, 0.5, 1, 2, 4, 8, 16, and 32 time the KC_{50} of the susceptible population (assumed to be 1 mg/L). Each concentration was simulated in duplicate yielding 20 curves per static time-kill dataset. Viable counts were observed at 0 (pre-dose), 0.5, 1, 2, 4, 8, 12 and 24 h.

For dynamic one-compartment *in-vitro* models, we simulated one dose level with dosing every 12 h in duplicate and a growth control. The simulated antibiotic peak concentration was 8x the KC_{50} of the susceptible population and antibiotic concentrations decreased with a pharmacokinetic half-life of 1 h. Bacterial counts were simulated in duplicates and for a growth control at 0, 1, 2, 4, 8, 12, 24, 28, 32, 36 and 48 h. A short half-life has been used to allow antibiotic concentrations to vary over a large range with peak concentrations yielding significant killing and trough concentrations being essentially ineffective. This was expected to support estimation of model parameters and emphasize the features of a dynamic infection model.

Monte Carlo Simulations: Our simulation-estimation studies (Figure 1) included the generation of 200 datasets for each candidate model via Monte Carlo simulations for static or dynamic antibiotic concentration-time profiles. This included 100 datasets simulated under static and another 100 datasets simulated under dynamic conditions. Each dataset comprised 20 viable count profiles of the total bacterial population for static antibiotic concentration experiments and 2 profiles for 1-compartment dynamic infection models. These Monte Carlo simulations were performed for 6 candidate models yielding 1,200 datasets in total. Berkeley Madonna (version 8.3.18, University of California) was used for all simulations (Table 2).

Table 2: Conditions used for Monte Carlo simulations of static and dynamic *in-vitro* infection models

Experi-mental condition	Initial antibiotic concentration (x KC50)	Sampling times (h)	Simulated elimination half-life (h)	Dosing interval (h)	Number of models used for simulation	Number of experiments simulated for each model	Number of replicates
Static	0, 0.125, 0.25, 0.5, 1, 2, 4, 8, 16, 32	0, 0.5, 1, 2, 4, 8, 12 and 24			6	100 [a]	Duplicate
Dynamic	8	0, 1, 2, 4, 8, 12, 24, 28, 32, 36 and 48	1	12h	6	100 [b]	Duplicate + 1 growth control

a: Each dataset for a static time-kill model contained 20 viable count profiles (including that of the growth control).
b: Each dataset for a dyamic infection model study contained 2 viable count profiles .

Estimation of population PD parameters: Each simulated dataset was estimated via population PK/PD modeling using the true model as well as the five other models yielding 6 x 1,200 = 7,200 estimation runs in total. Estimation was performed using nonlinear mixed-effects modeling in the S-ADAPT software via the importance sampling algorithm (pmethod = 4 in S-ADAPT) [34]. Modeling was facilitated by the SADAPT-TRAN tool and utilized estimation settings that were previously qualified for robust estimation of mechanism-based models[35,36]. Viable counts were fitted on $\log_{10}$ scale and viable counts below the limit of counting were handled by using Beal M3 method as implemented in S-ADAPT[37]. In order to avoid local minima initial values for estimation were set to the true values.

PD model selection: The majority of combinations of the six studied models are nested. The more complex model converge to the simpler models, if the mutation frequency of the resistant population is zero, if the maximum extent of adaptation (Smax) is zero, if there is no conversion of bacteria to a resting stage, or if there is no inter-conversion between the susceptible and resistant subpopulation. The objective function value (OFV, -1x log-likelihood in S-ADAPT) was calculated by S-ADAPT for each of the 7,200 estimation runs. For comparison of two nested models, the LRT with a chi-square distribution and one degree of freedom per additional model parameter was used with a p-value of 0.05. For comparison of two non-nested models, we chose the model with the lower objective function as the better model.

Precision and bias of parameters estimates: The parameter estimates from each of the estimation runs were compared with true parameter values used during simulation from the true model. The bias was calculated as.

$$\text{Bias} = \frac{\text{Estimate} - \text{true value}}{\text{true value}} \quad (17)$$

The precision was calculated as:

$$\text{Precision (CV\%)} = \frac{\text{Standard deviation(Estimates)}}{\text{Mean(Estimates)}} \quad (18)$$

Simulation of viable count profiles: To visualize the differences between competing models for the chosen experimental conditions, viable count profiles were simulated from the true parameter estimates over 96 h.

Results

The models aimed to provide comparable profiles based on the same experimental design. However the simulated viable counts profiles for static time-kill experiments yielded two general shapes of profiles (Figure 3A). The first type showed bacterial killing without regrowth (M1 and M2) with model 2 containing a slower terminal phase representing natural death of bacteria in the resting stage. The second group yielded initial bacterial killing followed by regrowth (M3, M4, M5 and M6) due to a resistant bacterial population, adaptation, or both. Figure 3B shows the viable count profiles simulated under dynamic conditions.

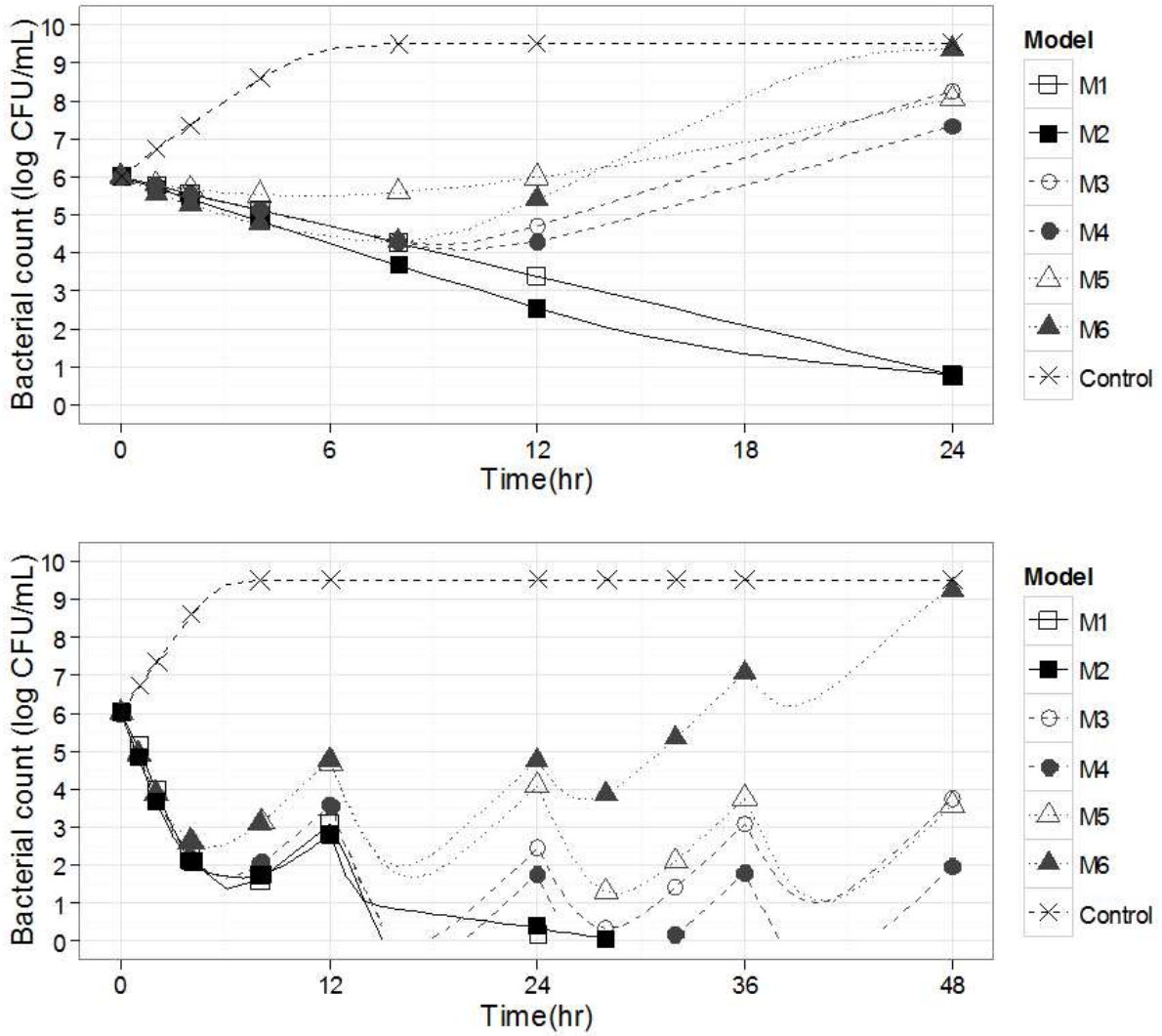

Figure 3: Typical viable count profiles simulated. Profiles are presented for the six different models with either a static antibiotic concentration of 1 mg/L (up) or with a dynamic concentration mimicking administration every 12h of an antibiotic with a 1 h half-life and a peak concentration of 8 times KC_{50S} (bottom). Symbols indicate sampling times for CFU counting.

Model selection: Each column in Table 3 refers to one true model used for simulation under static or dynamic conditions. The lines in Table 3 show the frequency of selecting the respective model as the best model based on the LRT. If M1 was the true model, both static and dynamic conditions identified M1 as the true model in 99 or 100% of the cases. For the model with one population with a resting stage (M2), model 2 was correctly identified as the best model in 96% of cases for the static scenario but only in 2% of the cases for the dynamic scenario.

When model 3 was used as true model for simulations, static conditions correctly identified M3 as the best model in 92% and dynamic conditions in 84% of the cases (Table 3).

Interestingly, when the model with two subpopulations and a slow inter-conversion (M4) was the true model, M3 was incorrectly selected as the best model in 92% (static) or 96% (dynamic setting) of the cases. Identification of both models with adaptive tolerance (M5 and M6) as the true model failed in at least 68% of the cases under both scenarios.

Table 3: Probability of selecting a model Mi by the likelihood ratio test (LRT; different rows) for six different true models (columns) used for simulation under dynamic or static conditions. The probability to correctly select the true model as the best model is represented by the diagonal.

		Actual (i.e. true) model											
Condition		Static time-kill						Dynamic infection model					
Models		M1	M2	M3	M4	M5	M6	M1	M2	M3	M4	M5	M6
LRT Selected model (%)	M1	93	.	.	.	.	.	89	87	.	.	.	.
	M2	7	96	.	.	.	.	3	8	.	.	.	.
	M3	.	3	82	81	84	44	6	3	97	96	84	90
	M4	.	.	17	18	2	2	.	1	.	1	2	.
	M5	.	.	.	.	11	.	2	1	.	1	13	.
	M6	.	1	1	1	3	54	.	.	3	2	1	10

(ex. In dynamic setting, model M3 was selected at 66% when model M5 was used to simulate).

Bias and imprecision of parameter estimates: Table 4 (all six models) and Figure 4 (models 1, 3 and 5) compare the true parameter values with the median parameter estimates under static and dynamic conditions (from the 100 datasets for each model and case).

The median estimates were within 10% of the true value and the imprecision was <20% CV for most parameters of M1 and M2 under both static and dynamic conditions (Table 4). A noticeable exception was the estimated mean time of natural death (MDT) of resting bacteria in M2 which was considerably biased by 326% in the dynamic setting and biased by 20% in the static setting.

For the model with a susceptible and resistant population without inter-conversion (M3), the vast majority of median estimates were within 10% of the true value with exception of KC_{50S} (estimated 34% higher) and KC_{50R} (estimated 82% higher than the true value) in the static setting. Both for models 3 and 4, the dynamic setting provided less biased parameter estimates, although the slow inter-conversion rate constants (k_{for} and k_{rev}) of M4 were difficult to estimate under both settings.

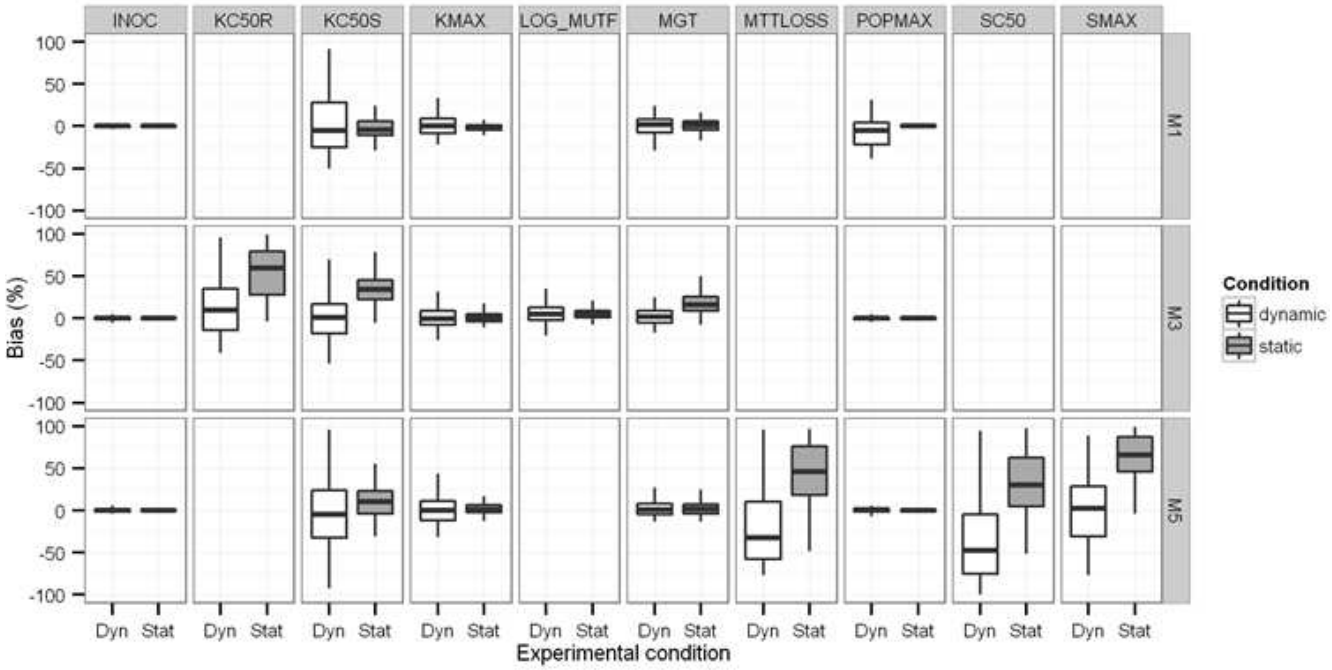

Fig. 4: Bias between true and estimated parameters. Boxplots of the bias between true and estimated parameter values under static and dynamic conditions for 3 different models (M1, M3 and M5).

For models with adaptive resistance (M5 and M6), most model parameters were estimated close to their true values and with good precision. However, the parameters related to the adaptation process (i.e. Smax, SC_{50} and MTTloss) were considerably biased and estimated with poor precision for both scenarios and both models (M5 and M6).

Overall, the precision of parameter estimates was better for static compared to dynamic conditions for all models.

Impact of biased parameter estimates on viable counts: The viable count profiles predicted from the median estimates under static and dynamic conditions (Figure 5) matched the predicted profiles from the true parameter estimates closely during the first 48 h. For models 3, 4 and 5, the deviations were moderate between 48 and 96 h and tended to be larger for the model predictions under static compared to dynamic conditions. Predictions were better for the two population model without adaptation (M3) than those for the model containing one population with adaptation (M5). Although some of the parameter estimates were biased for the more complex model M6 (two populations with adaptation), good predictions were observed.

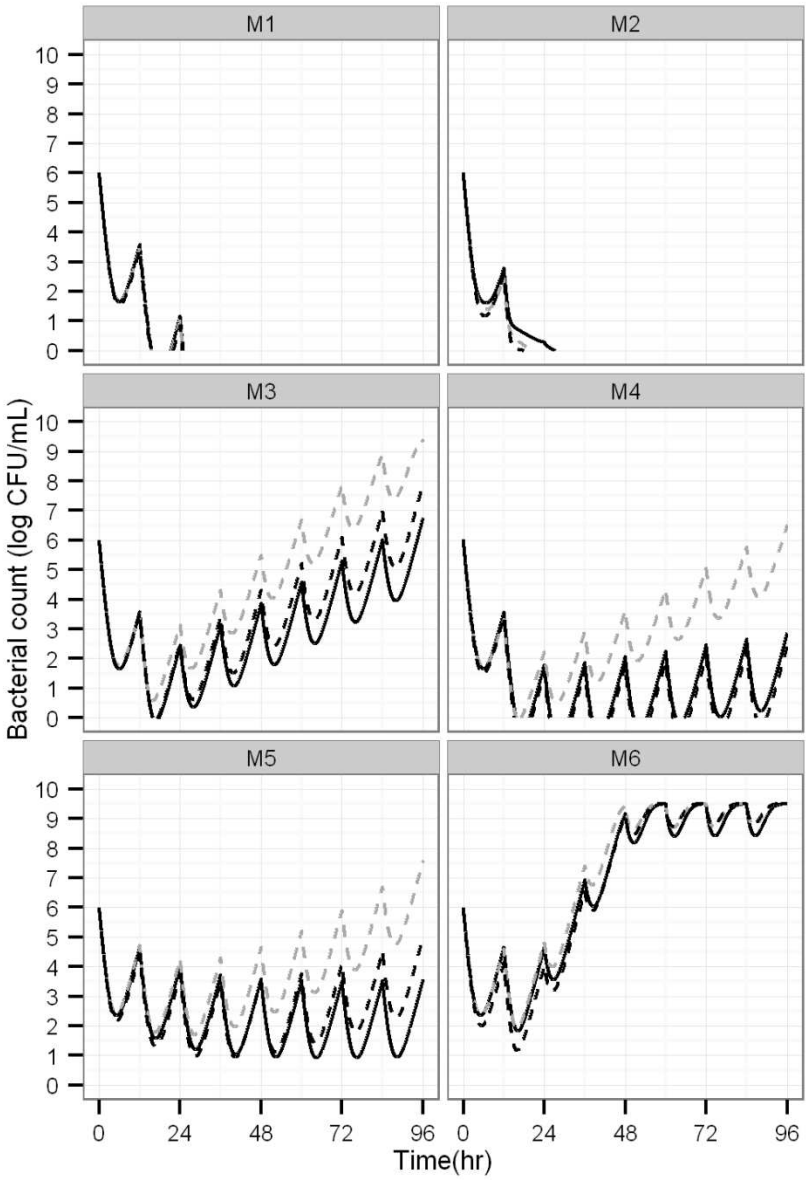

Fig 5: Comparison between true and CFU profiles extrapolated over time from parameter estimates. Typical CFU profiles in dynamic conditions, using the true parameter values (solid black lines) or parameter estimates from the dynamic (dashed black) or static (dashed grey) setting for the 6 models.

Table 4: Median and coefficient of variation (CV%) of parameter estimates when the parameters were estimated with the model used for simulations (n=1200; i.e. 100 replicates for each setting and each model) under static or dynamic condition.

			Model 1		Model 2		Model 3		Model 4		Model 5		Model 6	
Parameter	**True value**	**Unit**	Static	Dynamic	Static	Dynamic	Static	Dynamic	Static	Dynamic	Static	Dynamic	Static	Dynamic
MGT	**60.0**	**min**	60.6 (8)	61.0 (11)	60.5 (9)	68.5 (20)	69.4 (13)	61.2 (9)	73.0 (12)	60.9 (10)	61.0 (12)	60.7 (10)	61.5 (6)	62.2 (12)
Inoc	**6.00**	**Log_{10} CFU/mL**	6.00 (0.5)	6.00 (2)	6.00 (0.4)	6.01 (2)	6.00 (0.4)	5.99 (2)	6.01 (0.5)	6.02 (2)	6.01 (0.6)	5.99 (2)	6.00 (0.6)	5.99 (2)
Popmax	**9.50**	**Log_{10} CFU/mL**	9.53 (1)	8.96 (20)	9.52 (1)	10.9 (16)	9.50 (0.9)	9.49 (4)	9.49 (0.9)	9.54 (10)	9.51 (0.7)	9.51 (9)	9.51 (0.78)	9.51 (1)
kmax	**4.00**	**h^{-1}**	3.94 (4)	4.00 (11)	4.02 (8)	4.09 (15)	4.03 (6)	3.98 (12)	4.00 (5)	4.20 (12)	4.03 (6)	4.01 (16)	3.98 (4)	4.11 (19)
KC_{50S}	**1.00**	**mg/L**	0.950 (15)	0.97 (35)	0.980 (16)	1.03 (41)	1.34 (14)	1.01 (38)	1.33 (17)	1.12 (17)	1.10 (20)	0.98 (59)	1.13 (17)	1.15 (59)
MDT	**400**	**min**			321 (18)	1280 (177)								
Log_{10} Mutf	**-5.00**				-5.77 (14)	-6.36 (16)	-5.24 (6)	-5.25 (17)	-5.22 (9)	-4.89 (20)			-5.20 (8)	-5.81 (25)
KC_{50R}	**4.00**	**mg/L**					7.26 (40)	4.54 (36)	6.35 (42)	3.56 (73)			5.24 (28)	6.12 (350)
k_{for}	**-6.00**	**Log_{10} (1/h)**							-7.63 (8)	-7.11 (5)				
k_{rev}	**-1.00**	**Log_{10} (1/h)**							-56700 (450)	-4.3 (310)				
Smax	**4.00**										9.60 (29)	5.68 (110)	5.88 (44)	6.95 (190)
SC_{50}	**0.40**	**mg/L**									0.86 (52)	0.25 (120)	0.510 (106)	0.28 (200)
MTT_{LOSS}	**20.0**	**h**									46.6 (38)	35.4 (130)	40.5 (33)	81.8 (92)

Discussion

During the last five decades, a considerable variety of structures for models with irreversible drug effects has been proposed in antimicrobial and antineoplastic chemotherapy. These published models include both empiric descriptions of viable count profiles and mechanism-based models. The latter model were developed to characterize relevant aspects of the mechanisms of antibiotic action, bacterial resistance and tolerance for antibiotic mono- and combination therapy and are highly useful to predict the time-course of bacterial growth, killing and resistance and to thereby optimize antibiotic dosage regimens. The vast majority of these antibacterial PK/PD models [3,38] were developed using data on the total bacterial population and did not model viable counts from antibiotic containing agar plates. However, some models co-modelled both the total and resistant subpopulations.

In this context, it seems surprising that no systematic simulation-estimation study has yet been published to assess the ability to distinguish between competing antimicrobial PD models with different resistance mechanisms. This lack of knowledge affects the vast majority of mathematical models in antibacterial PD. We addressed this gap by performing parametric Monte Carlo simulations with in total 1,200 simulated datasets that were estimated using six relevant structural models and two common designs for *in-vitro* infection models. These models reflected genotypically stable resistance mechanisms, phenotypic tolerance (*i.e.* adaptation), inter-conversion between bacterial populations, or multiple of these mechanisms (Figure 2). The 1,200 datasets were estimated for both the true model and the other five models (i.e. 6 x 1,200 = 7,200 estimation runs in total) to assess the ability to distinguish between competing models.

While models M1 and M2 yielded bacterial killing and death without regrowth, M3 to M6 could all describe viable count profiles with initial killing followed by regrowth due to emergence of resistance. It was therefore interesting to assess, whether a robust population PK/PD estimation algorithm (i.e. importance sampling) can adequately distinguish between competing models. Despite the use of one of the latest population modeling algorithms, standard statistical criteria could only identify the true model under both static and dynamic conditions in more than 80% of the cases for models M1 and M3. Importantly, M3 was incorrectly selected as the best model in the large majority of cases even if models M4, M5 or M6 were the true model used during simulation. Despite frequently sampled viable counts of the total population over time, statistical modeling criteria could therefore not reliably identify the true model in case of regrowth due to bacterial resistance. Viable count data on the resistant population(s) from antibiotic-containing agar plates at 0 and 24 h, for

example, would provide direct experimental evidence to accept or reject several candidate models (Figure 2) and seems therefore highly valuable and warranted.

This difficulty to select the most appropriate mechanism of resistance based on modelling methods alone is supported by experience from our previously study on *P. aeruginosa* exposed to static concentrations of ciprofloxacin [6]. In this study, we leveraged insights on the presumably most relevant mechanism of resistance to select the final model for ciprofloxacin. Therefore a good understanding of the mechanism governing the interaction between the antibiotic and the bacteria is beneficial for selection of the most appropriate model. Ideally, such selection should be supported by quantitative viable counts of resistant subpopulations by plating bacterial strains onto agar containing antibiotics. The selection of the appropriate model can be guided with the characterization of subpopulations either at the beginning of the experiment with the determination of the mutational frequency to resistance [39] or during the experiment [10,40], thus allowing the choice between models with or without initial subpopulations and with or without inter-conversions amongst them.

Despite considerable bias for some parameter estimates, the discrepancies between predicted and actual CFU profiles (Figure 5) were limited and may possibly be considered acceptable. This applies particularly for the small discrepancies during the first 24 h to 48 h which is likely the most critical time in the management of infections in critically-ill patients. Model predictions over longer time periods (i.e. extrapolation) led to more biased predictions. The parameter estimates showed less bias for the dynamic compared to the static setting for models with heteroresistance or adaptation. Moreover our predictions were based on the median of the parameters values. As these simulations did not account for parameter imprecision, the discrepancies between the predicted and the actual viable count profiles are likely larger for some sets of estimated parameters.

As expected, the dynamic setting yielded less precise, *i.e.* with larger coefficient of variation, parameter estimates most likely due to the considerably smaller number of observations for the dynamic setting (containing 2 curves + one control) compared to the static setting (containing 20 curves per dataset). In practice the statistical gain of the dynamic design can also be offset by the significantly increased workload for dynamic experimental conditions. In order to improve the precision of parameter estimates under the dynamic conditions we tested some more intensive experimental designs, i.e. with 4 replicates (instead of 2) or with two different doses (8x EC_{50} + 32x EC_{50}) administered during the experiment (data not shown). However these more intensive experiments did not improve significantly the precision of parameter estimates under dynamic

conditions. This means that in order to obtain precise estimation of parameters with a dynamic system, it would necessitate a much more informative design, *e.g.* either much longer or with much more bacterial counts over time or with much more replicates.

Static concentration time-kill studies [9] are very efficient and cost-effective and allow studying a large range of antibiotic concentrations. Most published studies did not exchange the growth medium regularly (e.g. every 24 h) and therefore toxic bacterial metabolites may accumulate and nutrients get depleted over time. Also, degradation (e.g. of β-lactam antibiotics) over longer experimental conditions would need to be accounted for. Therefore, performing static concentration time-kill studies over more than 24 h requires a considerably increased amount of work.

Dynamic *in-vitro* infection models such as the one-compartment and hollow-fiber system can mimic human PK [4], by changing drug concentrations and turnover of fresh broth medium using various pumps. The control of these flow rates permits to simulate different half-lives of drugs and also provides washout of toxic bacterial metabolites elimination. Therefore, these dynamic experiments are often run over multiple days to week and longer [26], [41] and typically use multiple dosing [42]. These dynamic *in-vitro* models require though a significantly enhanced workload and therefore complement and extend the more efficient static concentration time-kill studies for translation to animal studies and ultimately to patients.

In conclusion, for datasets based only on the total bacterial population, standard statistical modeling criteria based on latest estimation algorithms failed to correctly identify the PD model with the true resistance mechanism(s) in the large majority of cases. These datasets did not contain data on antibiotic-resistant populations. This finding is highly important, as most published models in antibacterial PD were developed based only on data corresponding to the total population. For our simulation scenario, the dynamic infection model provided more accurate parameter estimates than static concentration time-kill studies. Yet the latter yielded more precise parameter estimates compared to dynamic models likely due to the much larger dataset. For both static and dynamic conditions, parameter related to adaptive resistance and inter-conversion of bacterial populations was poorly estimated. Predicted viable counts over the experimentally studied duration (*i.e.* 24 to 48 h) were reasonably accurate despite biased parameter estimates. However, simulations over longer durations showed more pronounced deviations and should be interpreted conservatively. Overall, it seems highly beneficial to utilize quantitative viable count data of resistant subpopulations and insights on their resistance mechanisms to support the choice of the most appropriate model for bacterial resistance.

Fundings

M.J. is supported by a doctoral fellowship from the University of Poitiers and the “Conseil regional de Poitou-Charentes”.

References

1. Andrews JM (2001) Determination of minimum inhibitory concentrations. J Antimicrob Chemother 48 Suppl 1: 5-16.
2. Craig WA (1998) Pharmacokinetic/pharmacodynamic parameters: rationale for antibacterial dosing of mice and men. Clin Infect Dis 26: 1-10; quiz 11-12.
3. Czock D, Keller F (2007) Mechanism-based pharmacokinetic-pharmacodynamic modeling of antimicrobial drug effects. J Pharmacokinet Pharmacodyn 34: 727-751.
4. Mueller M, de la Pena A, Derendorf H (2004) Issues in pharmacokinetics and pharmacodynamics of anti-infective agents: kill curves versus MIC. Antimicrob Agents Chemother 48: 369-377.
5. Chung P, McNamara PJ, Campion JJ, Evans ME (2006) Mechanism-based pharmacodynamic models of fluoroquinolone resistance in *Staphylococcus aureus*. Antimicrob Agents Chemother 50: 2957-2965.
6. Gregoire N, Raherison S, Grignon C, Comets E, Marliat M, et al. (2010) Semimechanistic pharmacokinetic-pharmacodynamic model with adaptation development for time-kill experiments of ciprofloxacin against *Pseudomonas aeruginosa*. Antimicrob Agents Chemother 54: 2379-2384.
7. Mouton JW, Dudley MN, Cars O, Derendorf H, Drusano GL (2005) Standardization of pharmacokinetic/pharmacodynamic (PK/PD) terminology for anti-infective drugs: an update. J Antimicrob Chemother 55: 601-607.
8. Craig WA (1998) Choosing an antibiotic on the basis of pharmacodynamics. Ear Nose Throat J 77: 7-11; discussion 11-12.
9. Gloede J, Scheerans C, Derendorf H, Kloft C (2010) *In-vitro* pharmacodynamic models to determine the effect of antibacterial drugs. J Antimicrob Chemother 65: 186-201.
10. Bulitta JB, Yang JC, Yohonn L, Ly NS, Brown SV, et al. (2010) Attenuation of colistin bactericidal activity by high inoculum of *Pseudomonas aeruginosa* characterized by a new mechanism-based population pharmacodynamic model. Antimicrob Agents Chemother 54: 2051-2062.
11. Nielsen EI, Viberg A, Lowdin E, Cars O, Karlsson MO, et al. (2007) Semimechanistic pharmacokinetic/pharmacodynamic model for assessment of activity of antibacterial agents from time-kill curve experiments. Antimicrob Agents Chemother 51: 128-136.
12. Schmidt S, Rock K, Sahre M, Burkhardt O, Brunner M, et al. (2008) Effect of protein binding on the pharmacological activity of highly bound antibiotics. Antimicrob Agents Chemother 52: 3994-4000.
13. Yano Y, Oguma T, Nagata H, Sasaki S (1998) Application of logistic growth model to pharmacodynamic analysis of *in-vitro* bactericidal kinetics. J Pharm Sci 87: 1177-1183.
14. Campion JJ, McNamara PJ, Evans ME (2005) Pharmacodynamic modeling of ciprofloxacin resistance in *Staphylococcus aureus*. Antimicrob Agents Chemother 49: 209-219.
15. Katsube T, Yano Y, Yamano Y, Munekage T, Kuroda N, et al. (2008) Pharmacokinetic-pharmacodynamic modeling and simulation for bactericidal effect in an *in-vitro* dynamic model. J Pharm Sci 97: 4108-4117.
16. Meagher AK, Forrest A, Dalhoff A, Stass H, Schentag JJ (2004) Novel pharmacokinetic-pharmacodynamic model for prediction of outcomes with an extended-release formulation of ciprofloxacin. Antimicrob Agents Chemother 48: 2061-2068.
17. Nielsen EI, Cars O, Friberg LE (2011) Predicting *in-vitro* antibacterial efficacy across experimental designs with a semimechanistic pharmacokinetic-pharmacodynamic model. Antimicrob Agents Chemother 55: 1571-1579.
18. Schmidt S, Sabarinath SN, Barbour A, Abbanat D, Manitpisitkul P, et al. (2009) Pharmacokinetic-pharmacodynamic modeling of the *in-vitro* activities of oxazolidinone antimicrobial agents against methicillin-resistant *Staphylococcus aureus*. Antimicrob Agents Chemother 53: 5039-5045.

19. Liu P, Rand KH, Obermann B, Derendorf H (2005) Pharmacokinetic-pharmacodynamic modelling of antibacterial activity of cefpodoxime and cefixime in *in-vitro* kinetic models. Int J Antimicrob Agents 25: 120-129.
20. Mouton JW, Vinks AA (2005) Pharmacokinetic/pharmacodynamic modelling of antibacterials *in-vitro* and in-vivo using bacterial growth and kill kinetics: the minimum inhibitory concentration versus stationary concentration. Clin Pharmacokinet 44: 201-210.
21. Zhi JG, Nightingale CH, Quintiliani R (1988) Microbial pharmacodynamics of piperacillin in neutropenic mice of systematic infection due to *Pseudomonas aeruginosa*. J Pharmacokinet Biopharm 16: 355-375.
22. Mouton JW, Vinks AA, Punt NC (1997) Pharmacokinetic-pharmacodynamic modeling of activity of ceftazidime during continuous and intermittent infusion. Antimicrob Agents Chemother 41: 733-738.
23. Jumbe N, Louie A, Leary R, Liu W, Deziel MR, et al. (2003) Application of a mathematical model to prevent in-vivo amplification of antibiotic-resistant bacterial populations during therapy. J Clin Invest 112: 275-285.
24. Gumbo T, Louie A, Deziel MR, Parsons LM, Salfinger M, et al. (2004) Selection of a moxifloxacin dose that suppresses drug resistance in *Mycobacterium tuberculosis*, by use of an *in-vitro* pharmacodynamic infection model and mathematical modeling. J Infect Dis 190: 1642-1651.
25. Jusko W (1973) J Pharmacokinet Biopharm 1: 175-200.
26. Tam VH, Kabbara S, Vo G, Schilling AN, Coyle EA (2006) Comparative pharmacodynamics of gentamicin against *Staphylococcus aureus* and *Pseudomonas aeruginosa*. Antimicrob Agents Chemother 50: 2626-2631.
27. Felmlee MA, Morris ME, Mager DE (2012) Mechanism-based pharmacodynamic modeling. Methods Mol Biol 929: 583-600.
28. Hassan M, Svensson US, Ljungman P, Bjorkstrand B, Olsson H, et al. (1999) A mechanism-based pharmacokinetic-enzyme model for cyclophosphamide autoinduction in breast cancer patients. Br J Clin Pharmacol 48: 669-677.
29. Hocquet D, Vogne C, El Garch F, Vejux A, Gotoh N, et al. (2003) MexXY-OprM efflux pump is necessary for a adaptive resistance of *Pseudomonas aeruginosa* to aminoglycosides. Antimicrob Agents Chemother 47: 1371-1375.
30. de la Pena A, Grabe A, Rand KH, Rehak E, Gross J, et al. (2004) PK-PD modelling of the effect of cefaclor on four different bacterial strains. Int J Antimicrob Agents 23: 218-225.
31. Treyaprasert W, Schmidt S, Rand KH, Suvanakoot U, Derendorf H (2007) Pharmacokinetic/pharmacodynamic modeling of *in-vitro* activity of azithromycin against four different bacterial strains. Int J Antimicrob Agents 29: 263-270.
32. Nikolaou M, Tam VH (2006) A new modeling approach to the effect of antimicrobial agents on heterogeneous microbial populations. J Math Biol 52: 154-182.
33. Bulitta JB, Ly NS, Yang JC, Forrest A, Jusko WJ, et al. (2009) Development and qualification of a pharmacodynamic model for the pronounced inoculum effect of ceftazidime against *Pseudomonas aeruginosa*. Antimicrob Agents Chemother 53: 46-56.
34. Bauer RJ, Guzy S, Ng C (2007) A survey of population analysis methods and software for complex pharmacokinetic and pharmacodynamic models with examples. AAPS J 9: E60-83.
35. Bulitta JB, Landersdorfer CB (2011) Performance and robustness of the Monte Carlo importance sampling algorithm using parallelized S-ADAPT for basic and complex mechanistic models. AAPS J 13: 212-226.
36. Bulitta JB, Bingolbali A, Shin BS, Landersdorfer CB (2011) Development of a new pre- and post-processing tool (SADAPT-TRAN) for nonlinear mixed-effects modeling in S-ADAPT. AAPS J 13: 201-211.
37. Beal SL (2001) Ways to fit a PK model with some data below the quantification limit. J Pharmacokinet Pharmacodyn 28: 481-504.
38. Nielsen EI, Friberg LE (2013) Pharmacokinetic-pharmacodynamic modeling of antibacterial drugs. Pharmacol Rev 65: 1053-1090.

39. Drusano GL, Bonomo RA, Bahniuk N, Bulitta JB, Vanscoy B, et al. (2012) Resistance emergence mechanism and mechanism of resistance suppression by tobramycin for cefepime for *Pseudomonas aeruginosa*. Antimicrob Agents Chemother 56: 231-242.
40. Bowker KE, Noel AR, Tomaselli SG, Elliott H, Macgowan AP (2012) Pharmacodynamics of the antibacterial effect of and emergence of resistance to doripenem in *Pseudomonas aeruginosa* and Acinetobacter baumannii in an *in-vitro* pharmacokinetic model. Antimicrob Agents Chemother 56: 5009-5015.
41. Louie A, Heine HS, Kim K, Brown DL, VanScoy B, et al. (2008) Use of an *in-vitro* pharmacodynamic model to derive a linezolid regimen that optimizes bacterial kill and prevents emergence of resistance in *Bacillus anthracis*. Antimicrob Agents Chemother 52: 2486-2496.
42. Blaser J, Stone BB, Zinner SH (1985) Two compartment kinetic model with multiple artificial capillary units. J Antimicrob Chemother 15 Suppl A: 131-137.

D. PK/PD of colistin and bacterial resistance

Pharmacokinetic – Pharmacodynamics modelling of the quickly occurring and partially reversible adaptive resistance of *Pseudomonas aeruginosa* to colistin using a bioluminescent strain *in-vitro*

Jacobs M.[1,2], Grégoire N.[1,2], Chauzy A.[1,2], Jeannot K.[3], Nielsen E.I.[4], Marchand S.[1,2,5], Friberg L.E.[4], Plésiat P.[3], Couet W.[1,2,5]

[1] Inserm U1070, Poitiers, France

[2] Université de Poitiers, UFR Médecine-Pharmacie, Poitiers, France

[3] Laboratory of Bacteriology, French National Reference Center for Antibiotic Resistance, University Hospital of Besançon, France

[4] Department of Pharmaceutical Biosciences, Uppsala University, Uppsala, Sweden

[5] CHU Poitiers, Service de Toxicologie-Pharmacocinétique, Poitiers, France

Keywords:

Pharmacokinetics / pharmacodynamics

Semi-mechanistic, mechanism-based modeling

Static concentration time-kill studies

Bioluminescence

Bacterial resistance

Introduction

Over the last years, colistin (polymyxin E) was increasingly used as a last option for the treatment of infections caused by multi-drug resistant Gram-negative bacteria as *Pseudomonas aeruginosa, Acinetobacter baumannii* and *Klebsiella pneumonia*[1,2]. The effect of colistin against *Pseudomonas aeruginosa* has been correlated with the area under the unbound concentration–time curve over 24h divided by the minimum inhibitory concentration (fAUC/MIC) both *in-vitro*[3] and in-vivo[4]. The target breakpoint has been estimated between 22.6 and 30.4 depending on the strain in *in-vitro*[3]. The fAUC/MIC target required to achieve 2-log kill was estimated to vary between 27.6 and 36.1, in an thigh infection model, and between 36.9 and 45.9 in an lung infection model[4]. Although these index and target values may facilitate the selection of appropriate dosing regimens for optimal antibacterial effect, they do not describe the rapid loss of efficacy due to the emergence of resistance described with *Pseudomonas aeruginosa* as opposed to mechanistic or semi-mechanistic pharmacokinetic/pharmacodynamic PK/PD) modeling. The resistance toward polymyxins in *Pseudomonas aeruginosa* is due to the modification of the lipid A with 4-amino-4-deoxy-L-arabinose (L-Ara4N) on the LPS[5] by activation of the PhoP/PhoQ system[6] or the PmrA/PmrB system [5,7-10]. A mechanistic PK/PD modeling study has been performed to describe this changing activity of colistin with time by Bulitta et al[11]. The authors have built a model that describes the competitive binding between colistin, Mg^{2+} and Ca^{2+} to the outer bacterial membrane of *Pseudomonas aeruginosa.* They describe the resistance to colistin by the presence of multiple subpopulations in the inoculum. In another study Mohamed et al.[12] described the loss of colistin efficacy with time as an adaptive process. Development of mutants and adaptive resistance may both lead to reduced antimicrobial efficacy and it may be difficult to discriminate between various types of PK/PD models simply from modeling criterion. In case of adaptive resistance the phenomenon reverses when the antimicrobial exposure is suspended whereas in case of multiple subpopulations the reversion can occur if the resistant populations have a fitness cost. Therefore in order to characterize the rapid decrease of *Pseudomonas aeruginosa* sensitivity to colistin with time, an original experimental design focusing on these phenomenon reversibility and using a bioluminescent strain was developed. The bioluminescence technique is a non-destructive, real-time reporter of bacterial metabolism that can be used to monitor the effect of antimicrobials and to quantify the bacteria[13,14]. This technique uses microorganisms expressing the lux operon which are able to emit light, as a result of the activity of bacterial luciferase in metabolically active bacteria[15,16].

Materials and methods

Strain and media

Reference strain *P.aeruginosa* PAO1 was rendered bioluminescent by insertion of operon *luxCDABE* into the chromosomal site *att*Tn*7*, by using the recombinant plasmid pUC18-mini-Tn*7*T-Gm^{R}-*lux* modified. The *lac* promoter region of plasmid pCR2.1-TOPO® (Invitrogen) was PCR amplified with primers PlacA1 (5'-CGGACTAGTCGATTCATTAATGCAGCTGG-3') and PlacA2 (5'-CGGGGATCCTGTGTGAAATTGTTATCCGCT-3'). The resulting amplicon was digested with *Spe*I and *Bam*H1 endonucleases, and then was cloned upstream of the *luxCDABE* coding sequence in pUC18-mini-Tn*7*T-Gm^{r}-*lux*. The new construct, pUC18-mini-Tn*7*T-Gm^{R}-P$_{lac}$*lux,* was transferred into PAO1 by electroporation, allowing the integration of mini-Tn*7* into the bacterial genome, as previously described[17]. Bacteria were grown in Mueller-Hinton broth (MHB) (Fluka BioChemika; Sigma-Aldrich, France)with adjusted concentrations of Ca^{2+} and Mg^{2+} (MH Ca^{2+}/Mg^{2+}) at 37°C.

Relationship between CFUs and relative luminescence units

The *P. aeruginosa* inoculum was prepared by suspension of the bacteria from an 18-h logarithmic-growth-phase culture in Muller-Hinton broth, adjusted to a final concentration of ~10^{6} CFU/ml, in 10mL glass tubes. Colistin was added to obtain concentrations of 0.5, 2, 4, 16, 32 and 64 mg/L. For all experiments, a growth control experiment was conducted in which no colistin was added, and three replicates were performed. All tubes were incubated at 37°C.

At 0, 2, 5, 8, 24 and 30h, bioluminescence was measured by a photon counter (IVIS, Caliper Life Sciences, Hopkinton, MA) and CFUs were counted manually on Muller-Hinton agar after an 18h-24h incubation at 37°C. Bioluminescence was determined with a 5-min acquisition time and a large bining by the photon counter. For image analysis a rectangular region of interest (ROI) was drawn over the tubes. The surface area of the ROI was kept constant. Bioluminescence was expressed as radiance/mL (photons/sec/cm²/steradian/mL) with a lower limit of quantification (LLOQ) at 175 radiance/mL.

To determine the relationship between bioluminescence and viable counts, the two measurements were plotted against each other and a univariate regression analysis was performed (regression analysis function, Excel 2007, Microsoft, USA).

Consecutive Kill-curves

For all experiments, the *P. aeruginosa* inoculum was prepared by suspension of the bacteria from a 18-24h logarithmic-growth-phase culture in Muller-Hinton broth, adjusted to a final concentration of ~10^6 CFU/ml, in 10mL glass tubes.

Initial kill-curves: For the first experiment, Colistin was added to obtain concentrations of 0.5, 2, 4, 16, 32 and 64 mg/L. At 0, 2, 5, 8, 24 and 30h, bioluminescence was measured as described above.

Subsequent kill-curves: At 30h the bacteria exposed to 2 mg/L of colistin were harvested by centrifugation (5000 t/min, 10min) and washed 2 times with NaCL isotonic solution. The resulting bacteria were plated on free-drug Muller-Hinton agar for a washout period of 0 (no plating), 18, 42 or 66 h. Muller-Hinton Agar was incubated at 37°C and bacteria were plated on a new Muller-Hinton agar every 24h.

After the corresponding washout period, a new bacterial suspension was prepared. Colistin was added to obtain concentration of 32, 64, 128, 256, 512 mg/L. Bioluminescent was measured before (time 0) and at 2, 5, 8, 24 and 30h after adding colistin (Figure 1).

For all experiments, a growth control experiment was conducted in which no colistin was added, and three replicates were performed. All tubes were incubated at 37°C.

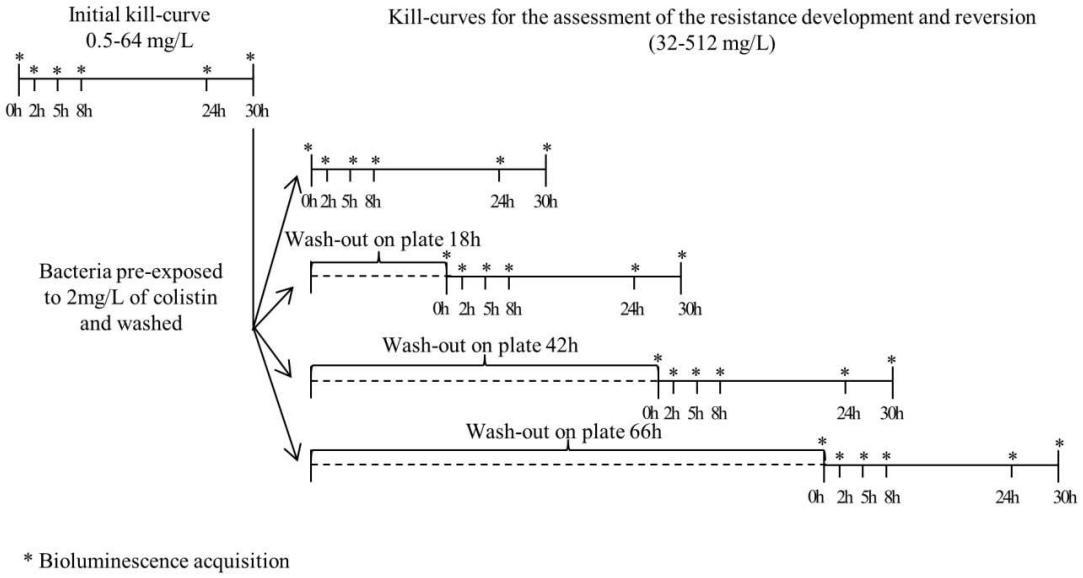

Figure 1: Schematic illustration of the experimental design

Determination of colistin concentration in broth

Determination of colistin concentrations in broth was performed by a LC-MS/MS method adapted from a method in plasma previously described [18]. A Waters Alliance 2695 separation module equipped with a binary pump and an autosampler thermostated at 4°C and a Waters Micromass Quattro micro API tandem mass spectrometer were used. A solid-liquid extraction (SPE) was used to isolate the compounds of interest from the complex biological matrix. After an elution with methanol containing 0.5% formic acid, the organic solvent was evaporated to dryness under a nitrogen steam and injected after reconstitution in formic acid 0.1%. Separation was performed on a reversed-phase XBrigde® C18 analytical column using an isocratic elution consisting of 25% acetonitril in formic acid 0.1%. The compounds were detected in the turbo ion spray positive mode. Seven points calibration curves were constructed at colistin concentrations ranging from 0.039 to 10 mg/L. Using 250 µL volume the lower limit of quantification was 0.024 µg /mL for colistin A and 0.015 µg /mL for colistin B. The between-day variability was characterized at three concentrations: 0.024, 0.384 and 6.144 µg /mL with a precision and accuracy less than 15%.

Selection and characterization mutants resistant to colistin

Resistant mutants to colistin were systematically screened in bacterial cultures after 24h exposure to 0.6 mg/L. Bacterial samples were plated onto MHA plates without antibiotic and grown during 18-24h at 35°C. Every day for 6 days, the bacteria were resuspended in drug-free medium and plated onto MHA plates, and the MIC of colistin was determined by macrodilution MHB procedures and interpreted according to the CLSI guidelines. Genomic DNA from the parental strain PAO1lux and the mutants resistant to colistin were extracted from cells using the QIAamp DNA Mini kit (Qiagen). Amplification and sequencing of genes pmrB, phoQ, parS, parR, cprS, and cprR were performed using specific primers as previously reported[9,19,20].

Modelling

Bioluminescence data were converted into equivalent CFU with the regression equation experimentally determined. All data were log-transformed and fitted using NONMEM 7.2 software (ICON Development solutions, Hanover, MD, USA) with LAPLACIAN algorithm and M3 method for handling data below the limit of quantification[21].

The structure of the semi-mechanistic model used was based on the experimental characterization of the mechanisms of resistance (multiple subpopulations + adaptative resistance) and on statistical comparison between models (cf below). It was adapted from the model developed by Mohamed et al[12,22] to describe the development of adaptive resistance of E.coli in the presence of gentamicin. Two sub-populations were included in the model, corresponding to drug-susceptible bacteria (S) and a drug-resistant bacteria (R), growing with different first-order rate constants (k_{gS} and k_{gR} for S and R bacteria respectively). Without antibiotic, the bacteria grow exponentially until maximal concentration counts (PopmaxS and PopmaxR for S and R bacteria respectively) are reached and a stationary level is attained. A logistic function was used to model this self-limiting growth. The conversion from the S population to the R population was modelled with a first-order rate constant for mutation (mutf). The starting inoculum was supposedly composed only of S bacteria. The equations below (Equations 1 and 2) describe the concentration of viable bacteria over time, without antibiotic:

$$\frac{dS}{dt} = k_{gS} * \left(1 - \frac{S+R}{PopmaxS}\right) * S - mutf * S \qquad \text{Equation 1}$$

$$\frac{dR}{dt} = k_{gR} * \left(1 - \frac{S+R}{PopmaxR}\right) * R + mutf * S \qquad \text{Equation 2}$$

In the absence of resistance the effect of colistin on bacterial killing (k_{col}) was tested to follow a linear, power (Equation 3), Emax or sigmoid function. The effect of colistin was supposed to differ between S and R forms.

$$k_{col} = slope * C^{\alpha} \qquad \text{Equation 3}$$

The differential equations become then (Equations 4 and 5):

$$\frac{dS}{dt} = k_{gS} * \left(1 - \frac{S+R}{PopmaxS}\right) * S - mutf * S - slopeS * C^{\alpha} * S \qquad \text{Equation 4}$$

$$\frac{dR}{dt} = k_{gR} * \left(1 - \frac{S+R}{PopmaxR}\right) * R + mutf * S - slopeR * C^{\alpha} * R \qquad \text{Equation 5}$$

where C is colistin concentration.

The presence of colistin initiated adaptive resistance development. Initially the hypothetical amount associated to the absence of adaptation, ARoff, was fixed to 1 whereas the amount associated to the adaptation, Aron, was fixed to 0. Upon colistin exposure transfers occurred between these two

amounts, which affects the fraction of amounts in the two compartments. The transfers between AROff and ARon for adaptive resistance are described in Equations 7 and 8. K_{on} and k_{off} describe the rate of development and reversal of adaptive resistance, respectively. K_{on} was tested to be a linear, power (Equation 6), Emax or a sigmoid function of colistin concentration or as a zero order constant transfer independent of colistin concentration. $K_{onslope}$ is the resistance rate constant in the presence of colistin.

$$k_{on} = k_{onslope} * C^{\gamma} \quad \text{Equation 6}$$

$$\frac{dAR_{off}}{dt} = k_{off} * AR_{on} - k_{on} * AR_{off} \quad \text{Equation 7}$$

$$\frac{dAR_{on}}{dt} = k_{on} * AR_{off} - k_{off} * AR_{on} \quad \text{Equation 8}$$

The adaptive resistance was modelled to occur only for S bacteria, R bacteria or for both (with different parameter estimates).

In case of adaptive resistance the rate constant of bacterial killing (k_{col}) is reduced by a function of the proportion of resistance development (Aron) powered by a parameter β (Equation 9 and 10). The parameter β was evaluated to be identical or different between the S and the R bacteria.

$$\frac{dS}{dt} = k_g * \left(1 - \frac{S+R}{PopmaxS}\right) * S - mutf * S - slopeS * C^{\alpha} * (1 - AR_{on}{}^{\beta}) * S \quad \text{Equation 9}$$

$$\frac{dR}{dt} = k_g * \left(1 - \frac{S+R}{PopmaxR}\right) * R + mutf * S - slopeR * C^{\alpha} * \left(1 - AR_{on}{}^{\beta}\right) * R \quad \text{Equation 10}$$

The residual variability was modelled to be additive in log scale. An inter-experiment variability was tested on all parameters. A bootstrap of 200 samples was used to estimate the uncertainty of the parameter estimates. Models were discriminated by their difference of objective function value (OFV): a reduction of at least 10.83 (corresponding to a P-value <0.001 for 1 degree of freedom) was required to choose the more complex model.

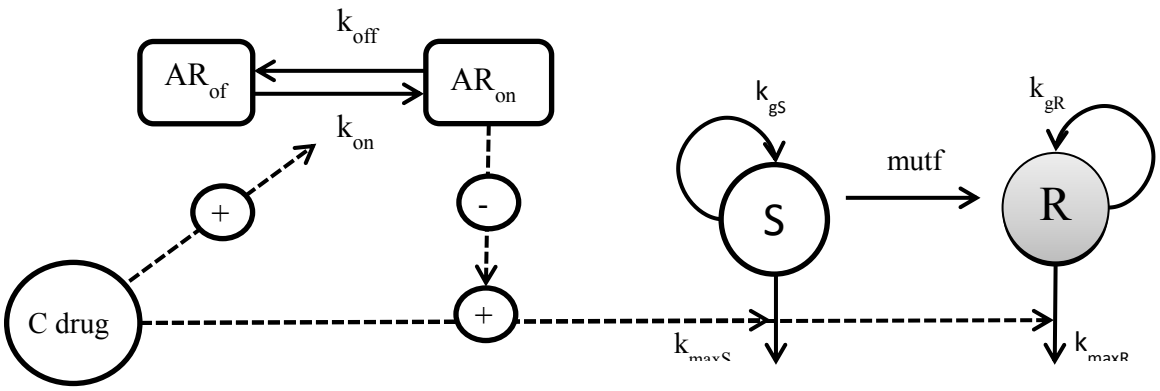

Figure 2: Schematic illustration of the final PK/PD model

Predictions of colistin effect versus time in a typical critically ill patient (creatinine clearance =86 mL/min and body weight=76 kg) were performed on the basis of a pharmacokinetic model previously developed [23] and the PK-PD model developed here. The fraction of colistin concentration unbound in plasma, which was considered as the active form, was estimated according to equations reported by Mohamed et al. [24] for a ratio of colistin A to colistin B of 3.1. Simulations were performed with Berkeley Madonna (Version 8.3.18, university of California) on a 24h time period by comparing treatment with colistin methanesulfonate (CMS, the prodrug of colistin) 4.5 MIU administered as 1-h infusions twice daily without and with a 9MIU loading dose .

Results

Colistin Concentrations

Colistin concentrations measured at starting time of kill-curves experiments were on average equal to 0.33, 0.6, 2.0, 9.5, 21.0, 43.1, 94.2, 207.2 and 405.7mg/L when corresponding theoretical concentrations were 0.5, 2, 4, 16, 32, 64, 128, 256 and 512 mg/L.

Relationship between CFUs and bioluminescence imaging

There were 126 data points for which both viable counts and bioluminescence were measured. A correlation (r^2=0.94) was observed when all points for viable counts and bioluminescence were plotted against each other (Figure 2).This correlation was described by the following equation (Equation 11):

$$\text{Bacterial counts} = 0.289 * \text{bioluminescence}^{1.3452} \qquad \text{Equation 11}$$

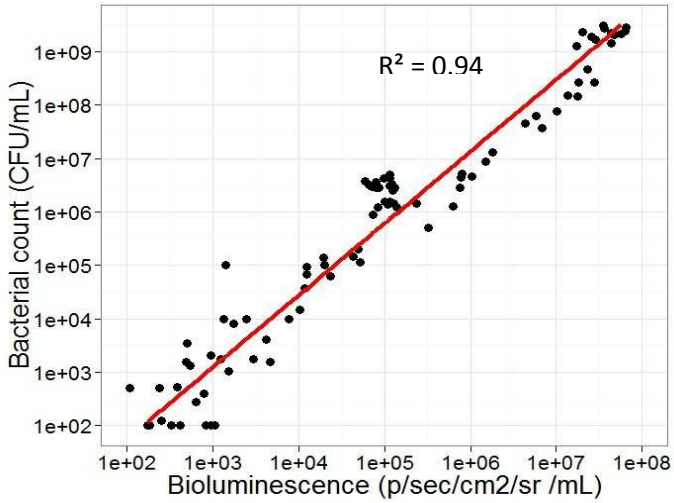

Figure 3: Linear regression analysis illustrating the correlation between viable counts and bioluminescence

Consecutives Kills curves experiments

Mean time-kill curves are shown on Figure 3: Observed CFU versus time after exposure at various colistin concentrations during an initial (top - a) and subsequent kill-curve (bottom - b) without washout.. Initial kill-curves, that is without prior exposure to colistin, showed a decay of CFU for colistin concentrations equal or higher than 0.3 mg/L, followed by a rapid regrowth typically observed after 6h for colistin concentrations up to 2 mg/L of colistin (Figure 3). Yet after previous 30h exposure at colistin 0.6 mg/L, the initial decay of CFU with time was only observed for concentrations greater than 94 mg/L. Yet bacteria were still able to regrow in the presence of colistin at a concentration of 207 mg/L (Figure 3).

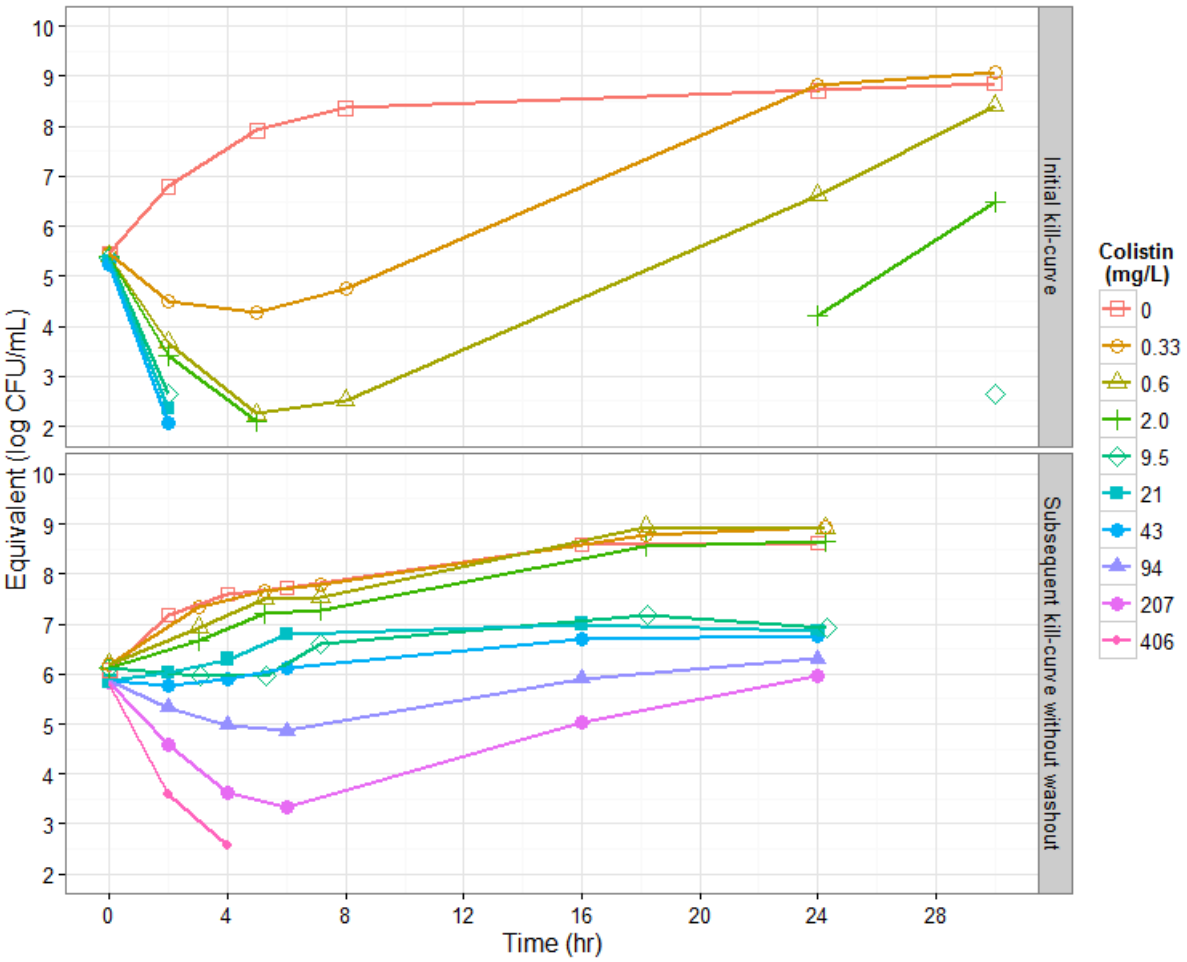

Figure 4: Observed CFU versus time after exposure at various colistin concentrations during an initial (top - a) and subsequent kill-curve (bottom - b) without washout.

The effect of washout duration on antimicrobial effect recovery is illustrated on Figure 4. The shortest washout period (18 h) was sufficient to recover part of the initial bactericidal effect, but complete recovery was not observed even after the longest (66h) washout period.

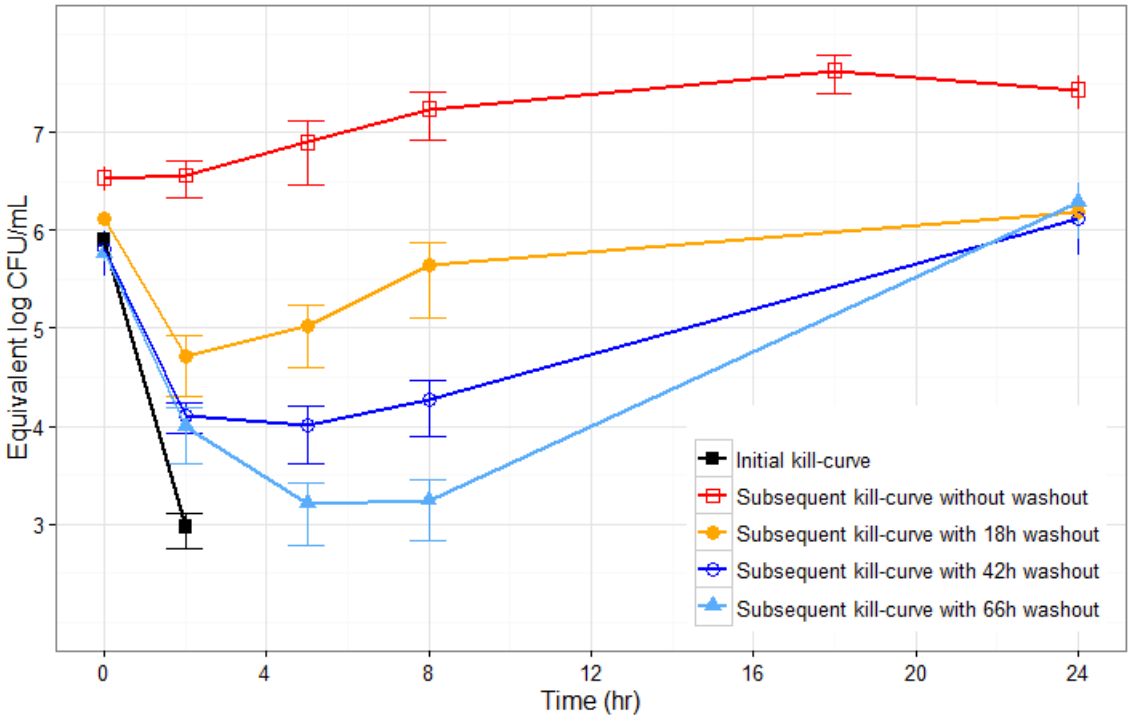

Figure 5: Observed (Mean±SD) CFU versus time after exposure at a colistin concentration measured at 21 mg/L on average, during the initial and the subsequent kill curves with 18, 42 and 66 hours of washout.

Selection and characterization mutants resistant to colistin.

To evaluate the emergence of mutants resistant during the experiments, the MIC of colistin was determined in each bacterial culture at time 0 and 24h of drug-exposure (0.6 mg/L). Interestingly, a mutant resistant to colistin (8 mg/L) was selected 24 hour after colistin-exposure. Sequencing of the PAO1*lux* strain and its mutant revealed two amino-acid substitutions (Ser68Gly, and Val147Gly) in the PmrB protein in the mutant, confirming the acquisition of colistin resistance. Note that none additional mutation was identified in the other genes involved in acquired resistance to colistin.

Modeling.

In a first step, only the initial kill-curves were considered. Several models were able to well describe the data, such as a model with two distinct subpopulations (OFV= 186) or a model with an adaptive population (OFV=334) or two distinct adaptive subpopulations (OFV=386). In this case, the model with 2 populations without adaptation was statistically better (likelihood ratio test). Moreover this model was in accordance with the presence of a stable mutant 24 h after the start of the experiment. However in a second step, when all the data were used (initial kill curves and subsequent kill curves

with different times of washout), the model with 2 populations without adaptation could not describe the second regrowth observed during the second kill curves. Yet a model with 2 distinct populations with an adaptive resistance on both of them was able to describe the full dataset.

Table 1: Population parameter estimates for the final model

		Typical value (RSE%)	
Parameter	Description	Sensitive (S) population	Resistant (R) population
k_g (h^{-1})	rate constant of bacterial growth	0.605 (15.1%)	
Popmax (log10 CFU/mL)	bacterial count at the stationary phase	8.87 (15.1%)	6.9 (4.8%)
mutf (log10 h^{-1})	Mutation rate constant from sensitive to resistance subpopulation	-4.02 (1.5%)	
Slope (L /mg/h)	linear factor for drug effect	5.16 (24.1%)	0.246 (22.6%)
α	Power factor for drug effect	1 Fixed	0.57 (16.3%)
kon_{slope} (L/mg/h)	resistance rate constant in the presence of colistin	0.321 (18.1%)	0.063 (24%)
γ	Power factor for concentration influence on adaptation rate	0 Fixed	
k_{off} (h^{-1})	rate constant for bacteria to return to the susceptible state	0.001 (16.4%)	
β	Power factor for reduction of drug effect by adaptation	1 Fixed	
RES	Residual error on log scale	1.12 (10.04%)	

Finally the bactericidal effect of colistin was best described by a linear model (α=1) for the sensitive sub-population and a power model (α=0.57) for the resistant sub-population. The observed emergence of adaptive resistance was best described by a first order kinetics, independently of the colistin concentration (γ=0). Bacterial adaptive resistance was described by a reduction of colistin bactericidal effect with parameter β fixed to 1. The reversal of the resistance was described by a first order rate constant (k_{off}). The final model is presented on Figure 5 and corresponding parameter estimates are reported in Table 1. Goodness of data fit plots was satisfactory (Figure 6). WRES values were less than 2 and no obvious bias was observed (Figure 7). The residual variability (Table 1) was reasonably low (1.2 log10 CFU/mL additive). Addition of an inter-experiment variability did not improve significantly OFV.

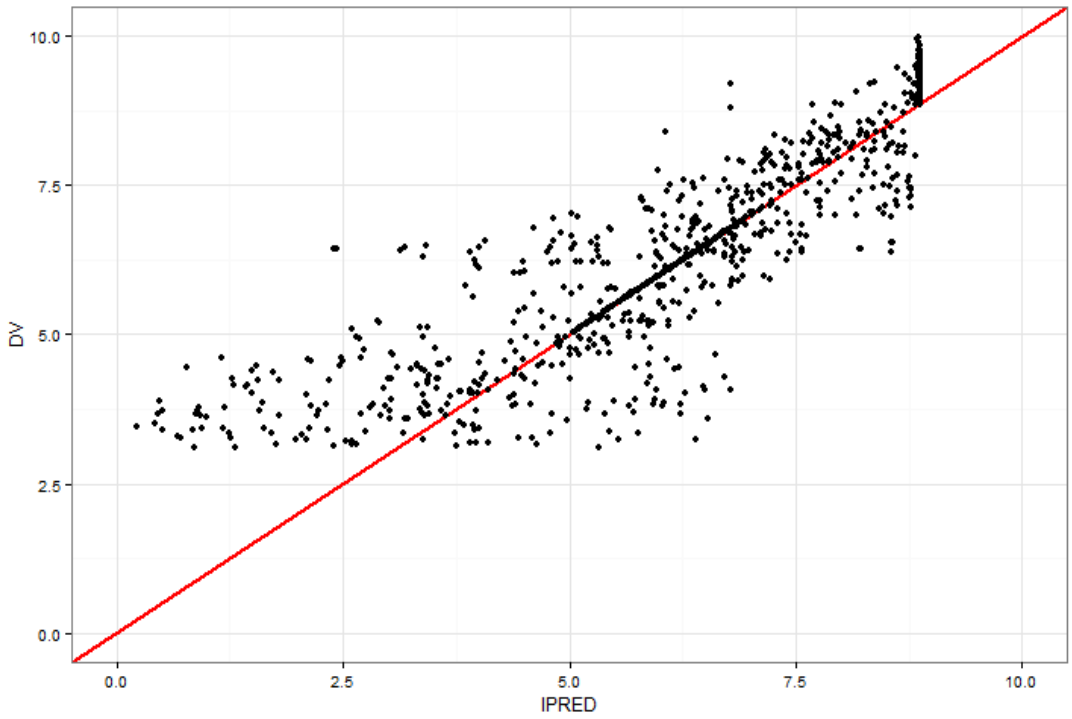

Figure 6: Diagnostic plots: DV versus IPRED

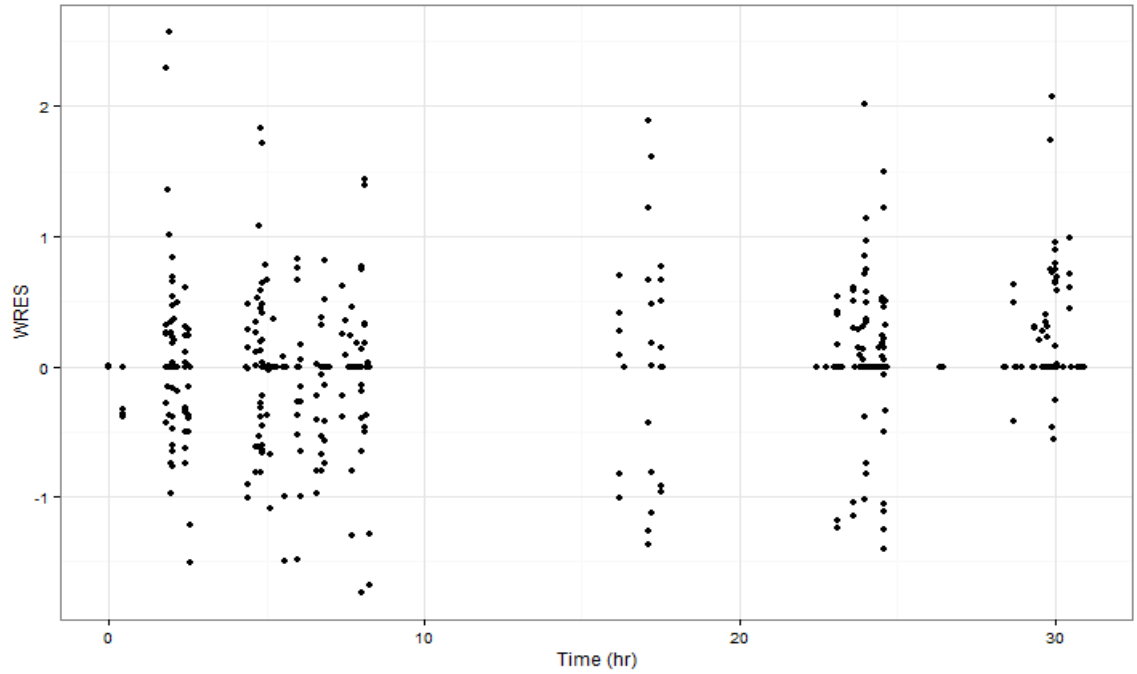

Figure 7: Diagnostic plots: WRES versus time

Discussion

These new results are consistent with previous findings obtained with static *in-vitro* time-kill curve experiments [11,12,25]. In particular we observed a rapid bactericidal effect of colistin on *Pseudomonas aeruginosa* followed by a regrowth typically after 6h, at colistin concentrations within the range of values encountered in clinical practice. Noticeably measured colistin concentrations were lower (19%–70%) than theoretical values, with a relatively larger loss at lower concentrations, possibly due to unspecific binding of colistin to the material, but this complicating factor has already been described.

As opposed to the two previous PK/PD modeling studies[11,12] experiments were prolonged after the initial kill-curve, by performing a second time-kill curve immediately or after different washout periods. This unusual design brought information on the kinetics of resistance development by various mechanisms with time in the presence of colistin, and on their reversibility after the antibiotic was withdrawn. But it also allowed better characterization of the relatively high colistin concentrations necessary to kill bacteria after they lost their initial susceptibility. Interestingly a regrowth of CFU after an initial decay was also observed during the second time-kill experiments (Figures 3 and 4), indicating a two steps resistance development with a regrowth during the first time-kill curve in presence of clinically relevant colistin concentrations, and a second re-growth during the second time-kill at much higher concentrations, up to 200 mg/L. In clinical practice this would suggest that except for host defenses provided by the immune system, colistin monotherapy would rapidly become inefficient, at least to eradicate this particular strain of *Pseudomonas aeruginosa*. This may be viewed as a limitation of this study based on bioluminescence imaging as a substitute for the traditional bacterial counting. However bioluminescence imaging is a non-destructive, real-time reporter of bacterial metabolism that can be used to monitor the rapidly changing bacteria susceptibility with time much more easily than by measuring CFU (17,18), which is perfectly suited for the purpose of developing semi-mechanistic PK/PD models and in particular to monitor the rapid rate of appearance and possibly disappearance of adaptative resistance phenomenon.

The resistance disappearance was quite spectacular although relatively slow compared to its appearance and still not complete after 66h of wash-out (Figure 4). Two mutations in the *pmrB* gene were identified after 24h of exposure to colistin conferring high resistance level to colistin by addition of Ara4N to the lipid A. The mutated sub-population persisted during the experiment indicating, that two populations of bacteria (wild type/*pmrB* mutant) were present during the time

course of the experiment. However these mutations alone could not explain the experimental data and in particular the observation of re-growths during the initial but also the subsequent kill-curve experiment at different concentrations of colistin (Figure 3) and the partial reversibility of this acquired resistance (Figure 4). Therefore an adaptive model of resistance was added, consistent with the fact that the extent of bacteria loss of sensivity with time in presence of colistin.

As previously mentioned during this study the focus was placed on the rate of resistance reversibility after colistin withdrawal which could have practical consequences. Interestingly even if the growth rate was estimated to be identical for the S and R forms, the model predicts a fitness cost for the R bacteria due to a maximal number of R bacteria at the stationary phase (Popmax) which was estimated to be lower than that of S bacteria. As a consequence the proportion of S bacteria would increase during the wash-out periods after colistin has been withdrawn. However using a protocol with wash-out periods of various durations to better characterize the sensitivity rate of recovery, it was possible to estimate that the reversibility of the adaptation phenomenon was very slow with a half-life of about 700 h, meaning that it should not be possible to take advantage of this in clinical practice. Yet this half-life value is much longer than that reported by Mohamed et al. (7.6 h)[12] and the respective parts of fitness cost and adaptation reversion in the efficacy recovery should be further explored.

This PK/PD model with two types of resistance phenomenon suggests that even within a relatively narrow range of clinically relevant values, a relatively modest change in colistin concentrations has a major effect on the antimicrobial effect. For example at a colistin concentration equal to 0.5 mg/L, an initial decrease of CFU with time is predicted during the initial time-kill curve, corresponding essentially to the disappearance of susceptible bacteria (S) initially present. But this is followed by a regrowth starting after approximately 6h and corresponding to a mixture of S that became adapted and resistant mutants (R) (Figure 8a). Therefore in these conditions the overall efficacy is rather limited with an approximately 1000 fold greater CFU value at 24h than at time zero due to both an adaptation of the S forms that still correspond to the majority of the germs and to the development of the R. A totally different picture is observed at a colistin concentration of 2.0 mg/L since in this case the initial CFU decay is faster and greater but still followed by a regrowth (Figure 8b). Yet after 24h total CFU predicted by the model are in the same range of value than at time zero, indicating a much greater overall effect than after exposure of colistin 0.5 mg/L. However the model predicts that the observed regrowth corresponds almost exclusively due to R bacteria that are virtually totally resistant to colistin even before adaptation. In other words at a colistin concentration of 2.0 mg/L (and in fact higher than 1mg/L), the S form should not have a chance to adapt and would disappear,

but the R form should still develop. Moreover a loss of efficacy with time would still be observed due to the adaptation of the R form, with a half-life of about 11 h. Noticeably according to the model, adaptation of the S is quicker than that of the R bacteria, consistent with the value reported by Mohamed et al. for two different strains of *Pseudomonas aeruginosa* (16).. Colistin concentrations greater than 16 mg/L were predicted to prevent the emergence of R bacteria, however such high colistin concentrations in plasma are likely to be toxic and therefore unexpected in clinical practice, except possibly within the lung after aerosol delivery[25]. Interestingly these reversible adaptation phenomenon suspected for both the S and R forms, should only be relevant for the S form in clinical practice, since at plasma concentrations measured in patients, colistin should be efficient against the S form before but not after adaptation, whereas in these conditions the R form is almost totally resistant even without adaptation.

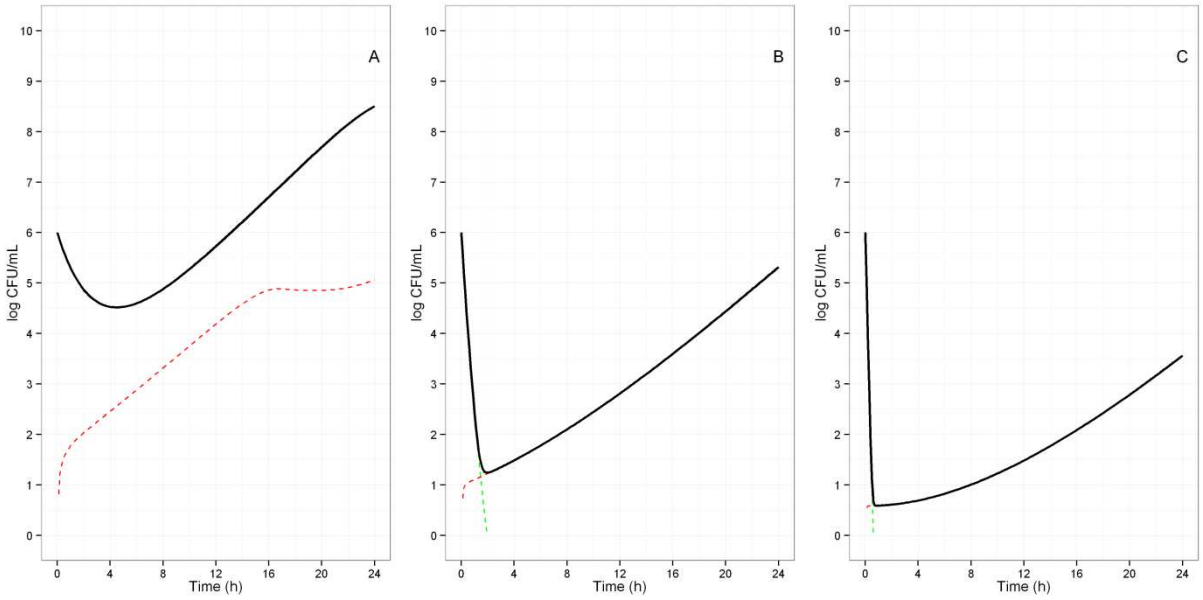

Figure 8: Model predicted number of bacteria versus time, in the S (dashed green line), R (dashed red line) and total (solid black line) forms, in the presence of colistin at a concentration equal to 0.5 mg/L (A), 2.0 mg/L (B) or 5.0 mg/L (C) corresponding to an initial kill-curve

During kill-curves experiments colistin concentrations do not vary with time which may not be a problem for proper PK/PD model characterization and estimation of parameters values. However colistin concentrations were simulated to vary in order to mimic the clinical situation for a typical critically ill patient and unbound concentrations were considered. The PK/PD model predicts that administration of a 9 MIU loading dose of CMS (the prodrug of colistin) should allow a much better elimination of the S subpopulation of bacteria (Figure 9), especially by preventing its adaptation. However the administration of the loading dose is predicted to have only a minimal impact on the R

subpopulation of bacteria. This suggests that a loading dose of CMS should be recommanded in order to reduce the adaptation of *Pseudomonas aeruginosa* against colistin but a combination therapy seems necessary to prevent the apparition of resistant mutants. These simulations should be considered with their limitations, notably those related to *in-vitro-in-vivo* extrapolations and the fact that only one strain of *Pseudomonas aeruginosa* was studied. However, despite this unique strain, it should be representative of many others initially susceptible to colistin (the MIC of the strain was 1 mg/L) but eliciting resistance over time.

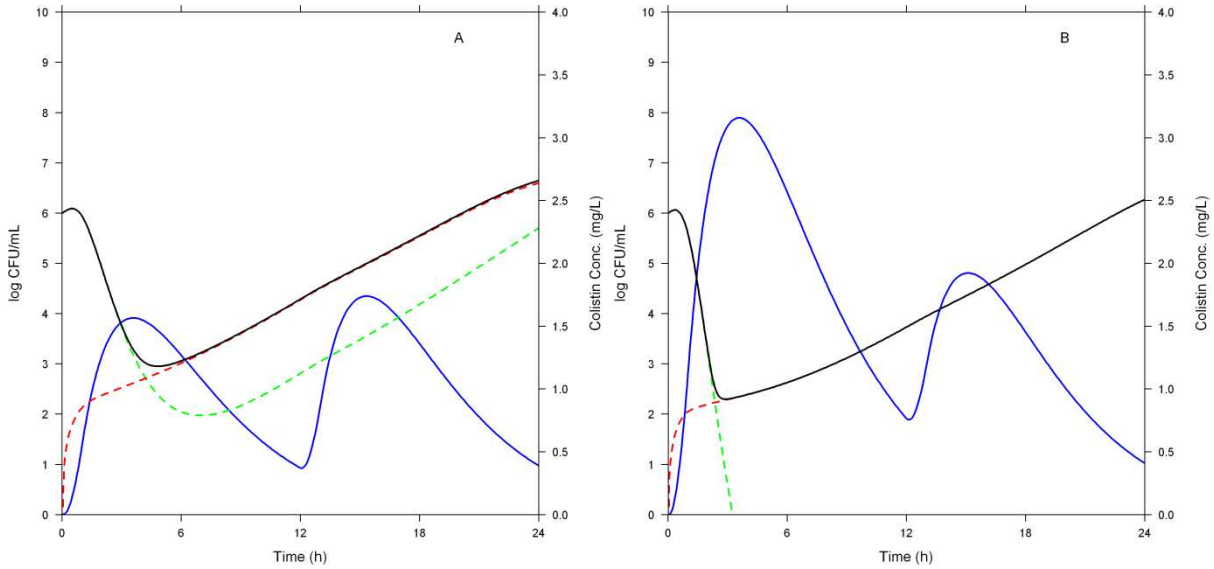

Figure 9: Model predicted plasma unbound concentrations (blue solid line) and number of bacteria - in the S (dashed green line), R (dashed red line) and total (solid black line) forms- versus time (0-24 h), after treatment with colistin methanesulfonate (CMS) 4.5 MIU twice daily without (A) and with a loading dose (9MIU)

This PK/PD modeling was capable to bring useful information on the complex relationship between colistin concentration and the development of a rapid and partially reversible reduction of colistin antimicrobial efficacy against *Pseudomonas aeruginosa.* Yet this model presents several limitations. Bulitta et al. described an inoculum effect that was not taken into consideration at this stage. Yet this effect is expected and this extra-complexity should be implemented in the near future. These same authors used a model of hetero-resistance consisting of three different subpopulations whereas two subpopulations were sufficient to provide an adequate description of our experimental data. But our objective was not to develop an extensive mechanistic model the most simple PK/PD model with some mechanistic support to properly describe our experimental data.

Overall this study may suggest a number of practical recommendations for the clinicians. It was observed that the initial population of bacteria was sensitive to colistin but that it adapted rapidly (half-life of 2h) to become much less sensitive since in our experimental conditions, efficient antimicrobial concentrations after 30h of exposure, should be close to 40 mg/mL, at least for this particular strain, which would be toxic and therefore not clinically achievable. Therefore front-loading strategies would be recommended as already done. However stable mutants appearing consistently during the first 24 h of exposure to colistin at therapeutic concentrations, present a very high level of resistance. Colistin alone cannot eradicate these mutants, and although the immune system defenses should not be neglected, combination therapies seem absolutely necessary.

In conclusion the *in-vitro* pharmacodynamics of colistin on *Pseudomonas aeruginosa* was assessed through an innovative bioluminescent technology associated with an original experimental design. A PK/PD model, incorporating both adaptive and mutational resistance consistent with the actual mechanism responsible for the rapid loss of colistin efficacy, was used to describe the data. Resistance developed fast and high, suggesting that a loading dose, associated with combination therapy, should be necessary to prevent its apparition.

Funding

M. Jacobs is supported by a doctoral fellowship from the University of Poitiers and the “Conseil regional de Poitou-Charentes”.

1. Li J, Nation RL, Turnidge JD, et al. Colistin: the re-emerging antibiotic for multidrug-resistant Gram-negative bacterial infections. *Lancet Infect Dis* 2006;6:589-601.

2. Nation RL, Li J, Cars O, et al. Framework for optimisation of the clinical use of colistin and polymyxin B: the Prato polymyxin consensus. *Lancet Infect Dis* 2015;15:225-234.

3. Bergen PJ, Bulitta JB, Forrest A, et al. Pharmacokinetic/pharmacodynamic investigation of colistin against *Pseudomonas aeruginosa* using an *in-vitro* model. *Antimicrob Agents Chemother* 2010;54:3783-3789.

4. Dudhani RV, Turnidge JD, Coulthard K, et al. Elucidation of the pharmacokinetic/pharmacodynamic determinant of colistin activity against *Pseudomonas aeruginosa* in murine thigh and lung infection models. *Antimicrob Agents Chemother* 2010;54:1117-1124.

5. Chen HD, Groisman EA. The biology of the PmrA/PmrB two-component system: the major regulator of lipopolysaccharide modifications. *Annu Rev Microbiol* 2013;67:83-112.

6. Miller AK, Brannon MK, Stevens L, et al. PhoQ mutations promote lipid A modification and polymyxin resistance of *Pseudomonas aeruginosa* found in colistin-treated cystic fibrosis patients. *Antimicrob Agents Chemother* 2011;55:5761-5769.

7. Lee JY, Chung ES, Na IY, et al. Development of colistin resistance in pmrA-, phoP-, parR- and cprR-inactivated mutants of *Pseudomonas aeruginosa*. *J Antimicrob Chemother* 2014.

8. Moskowitz SM, Ernst RK, Miller SI. PmrAB, a two-component regulatory system of *Pseudomonas aeruginosa* that modulates resistance to cationic antimicrobial peptides and addition of aminoarabinose to lipid A. *J Bacteriol* 2004;186:575-579.

9. Barrow K, Kwon DH. Alterations in two-component regulatory systems of phoPQ and pmrAB are associated with polymyxin B resistance in clinical isolates of *Pseudomonas aeruginosa*. *Antimicrob Agents Chemother* 2009;53:5150-5154.

10. Moskowitz SM, Brannon MK, Dasgupta N, et al. PmrB mutations promote polymyxin resistance of *Pseudomonas aeruginosa* isolated from colistin-treated cystic fibrosis patients. *Antimicrob Agents Chemother* 2012;56:1019-1030.

11. Bulitta JB, Yang JC, Yohonn L, et al. Attenuation of colistin bactericidal activity by high inoculum of *Pseudomonas aeruginosa* characterized by a new mechanism-based population pharmacodynamic model. *Antimicrob Agents Chemother* 2010;54:2051-2062.

12. Mohamed AF, Cars O, Friberg LE. A pharmacokinetic/pharmacodynamic model developed for the effect of colistin on *Pseudomonas aeruginosa in-vitro* with evaluation of population pharmacokinetic variability on simulated bacterial killing. *J Antimicrob Chemother* 2014;69:1350-1361.

13. Greer LF, 3rd, Szalay AA. Imaging of light emission from the expression of luciferases in living cells and organisms: a review. *Luminescence* 2002;17:43-74.

14. Thorn RM, Nelson SM, Greenman J. Use of a bioluminescent *Pseudomonas aeruginosa* strain within an *in-vitro* microbiological system, as a model of wound infection, to assess the antimicrobial efficacy of wound dressings by monitoring light production. *Antimicrob Agents Chemother* 2007;51:3217-3224.

15. Beard SJ, Salisbury V, Lewis RJ, et al. Expression of lux genes in a clinical isolate of *Streptococcus pneumoniae*: using bioluminescence to monitor gemifloxacin activity. *Antimicrob Agents Chemother* 2002;46:538-542.

16. Gahan CG. The bacterial lux reporter system: applications in bacterial localisation studies. *Curr Gene Ther* 2012;12:12-19.

17. Choi K-H, Schweizer HP. mini-Tn7 insertion in bacteria with single attTn7 sites: example *Pseudomonas aeruginosa*. *Nat Protoc* 2006;1:153-161.

18. Gobin P, Lemaitre F, Marchand S, et al. Assay of colistin and colistin methanesulfonate in plasma and urine by liquid chromatography tandem mass spectrometry (LC-MS/MS). *Antimicrob Agents Chemother* 2010;54:1941-1948.

19. Muller C, Plésiat P, Jeannot K. A two-component regulatory system interconnects resistance to polymyxins, aminoglycosides, fluoroquinolones, and β-lactams in *Pseudomonas aeruginosa*. *Antimicrob Agents Chemother* 2011;55:1211-1221.

20. Gutu AD, Sgambati N, Strasbourger P, et al. Polymyxin resistance of *Pseudomonas aeruginosa* phoQ mutants is dependent on additional two-component regulatory systems. *Antimicrob Agents Chemother* 2013;57:2204-2215.

21. Beal SL. Ways to fit a PK model with some data below the quantification limit. *J Pharmacokinet Pharmacodyn* 2001;28:481-504.

22. Mohamed AF, Nielsen EI, Cars O, et al. Pharmacokinetic-pharmacodynamic model for gentamicin and its adaptive resistance with predictions of dosing schedules in newborn infants. *Antimicrob Agents Chemother* 2012;56:179-188.

23. Gregoire N, Mimoz O, Megarbane B, et al. New colistin population pharmacokinetic data in critically ill patients suggesting an alternative loading dose rationale. *Antimicrob Agents Chemother* 2014;58:7324-7330.

24. Mohamed AF, Karaiskos I, Plachouras D, et al. Application of a Loading Dose of Colistin Methanesulphonate (CMS) in Critically Ill Patients: Population Pharmacokinetics, Protein Binding and Prediction of Bacterial Kill. *Antimicrob Agents Chemother* 2012.

25. Boisson M, Jacobs M, Gregoire N, et al. Comparison of intrapulmonary and systemic pharmacokinetics of colistin methanesulfonate (CMS) and colistin after aerosol delivery and intravenous administration of CMS in critically ill patients. *Antimicrob Agents Chemother* 2014;58:7331-7339.

IV. Discussion

The starting point of this thesis was the study performed by Grégoire et al.[139], who investigated the PK of colistin and its prodrug CMS, in critically ill patients receiving multiple doses of CMS. Results of this study challenged the PK rational for a loading dose and confirmed that the maintenance dose could be adjusted to creatinine clearance. However colistin PK was characterized by large inter and intra-individual variabilities that could render a priori dosage adjustments insufficient to accurately control colistin exposure and would suggest individual therapeutic drug monitoring over the treatment period. Because colistin PK is partly driven by the excretion of unchanged CMS in urine, it is expected to be altered in some specific populations, such as patients with renal impairment undergoing hemodialysis or not. Moreover because colistin is used in intensive care units to treat ventilator associated pneumonia or for cystic fibrosis patients with chronic colonization by *Pseudomonas aeruginosa*[174], the administration of CMS as aerosol is of potential interest to increase local pulmonary concentrations and reduce the risk of systemic toxicity.

We firstly investigated the pharmacokinetics of colistin after CMS aerosol delivery for treating pulmonary infections in critically ill patients[175]. Aerosol delivery gained interest for the treatment of pulmonary infections since this route of administration permits to deliver drug directly at the site of infection[176-179]. Therefore, compared with intravenous administration, higher local concentrations and thus better efficiency, but also lower systemic toxicity are expected. In this study, CMS and colistin concentrations were measured on two separate occasions within the plasma and epithelial lining fluid (ELF) of critically ill patients (n=12) who had received 2 MIU of CMS either by aerosol delivery or by intravenous (IV) administration.

A major finding was that both CMS and colistin concentrations in ELF are much higher (in the range of 100-1000 folds) after CMS aerosol delivery than IV administration, which is fully consistent with observations in rats[180,181]. The major difference with rats experiments was that after aerosol delivery in patients, most of the CMS was lost with expired airflow since on average only 9% of the CMS dose could eventually reach the systemic circulation, compared with approximately 69% in rats [180,181] using the Pen Century system for deep intrapulmonary delivery.

Both ELF and plasma profiles of colistin and CMS were successfully described by using the PK model previously used by Grégoire et al. for systemic PK [139], completed by one ELF compartment for colistin and one ELF compartment for CMS. This PK model linked to an *in-vitro* PD model of colistin on *Pseudomonas aeruginosa* was used to simulate bactericidal effect of colistin in ELF depending on the route of administration. These simulations predicted a dramatic superiority of CMS aerosol delivery

compared with IV administration in terms of antimicrobial activity. Therefore a major effect of the route of administration on the antimicrobial effect was predicted using this *Pseudomonas aeruginosa* PAO1 strain. Yet in clinical practice a single aerosol delivery with the usual 2 MIU of CMS is unlikely to clear all bacteria in an irreversible manner as suggested by these simulations.

An explanation could be that colistin may not distribute evenly within lung and could hardly reach some specific areas such as hypo-oxygenated tissue where bacteria could develop. Multiple studies have been made to determine the respiratory tract deposition of airborne particles for risk assessment of air pollution or inhaled drug delivery[182-185]. The authors demonstrated that lung deposition is governed by a multitude of parameters including the breathing pattern, particle characteristics, flow dynamics and morphological structure of the lung[182-185]. Deposition measurements are based on complex analysis of the inhaled and exhaled gas and statistics methods[185] that provide information about the heterogeneity of the drug deposition but not about ELF concentrations.

Bronchoalveolar lavage is the most common method used to investigate ELF concentrations. It is commonly used by physicians to diagnose infections and pulmonary pathologies[186-188]. However the interpretations of ELF concentration obtained by BAL can be biased due to various cofounding factors such as described by Kiem and Shentag[189]. The most important factor is the dilution of ELF by the saline volume used for lavage. The administration of this liquid can disturb the homeostasis of the cells contained in ELF, mostly alveolar macrophages, and induced their lysis. If the measured antibiotic distributes intracellularly, the lysis of the macrophage liberates the drug into the extracellular environment and artificially increases ELF concentrations[190]. Yet this problem is likely to be encountered with antibiotics such as fluoroquinolones with extensive intracellular penetration[191,192] but not so much with colistin which considering its physico-chemical characteristics (average *molecular weight* of 1,163 Da, polar surface area of 490 Å, log *P* of 3.42)[180] is unlikely to penetrate extensively within cells[181]. The volumetric dilution of ELF by the liquid of lavage needs also to be taken into account; usually ELF concentrations (C_{ELF}) are obtained according to the equation $C_{ELF}=C_{BAL}$ ($Urea_{plasma}/Urea_{BAL}$), where C_{BAL} corresponds to the concentration measured in BAL fluid, and $Urea_{BAL}$ and $Urea_{plasma}$ correspond to the concentrations of urea determined in BAL fluid and plasma, respectively[151]. Urea is a small, relatively nonpolar, endogenous compound that freely cross physiological membranes[189]. Consequently the urea concentration in ELF is considered to be same as in plasma, and the ratio $Urea_{plasma}/Urea_{BAL}$ is used to correct for the volumetric dilution caused by the BAL[151,189,193]. Yet Marcy et al.[194] and Effros et al.[195] have demonstrated that the ratio of plasma / BAL urea concentrations can vary over time due to the rapid diffusion of urea into BAL fluid during the

lavage procedure that leads to underestimated C_{ELF}[193]. Kiem et al. recommend a quick lavage procedure of less than 1 min to limit this bias[189]. Bronchoscopic microsampling[196] (also called micro-Bal, used in our study[175]) is an alternative to the traditional BAL using a lower volume of saline (20 mL vs 100-300mL) and consequently limiting the ELF dilution and its constraints (cell lysis, urea equilibrium). This method can also be performed with a double sterile catheter[175] that prevents sampling contamination during intubation by the antibiotic present in upper airways. Another alternative is microdialysis[197,198], but this is an invasive method requiring surgery and therefore that can be used only under specific circumstances and drugs. Colistin in particular sticks to membranes and for that reason is not a good candidate for microdialysis.

Antibiotic concentrations estimated within ELF are therefore global and although better than plasma concentrations, they may not be fully representative of concentrations at the site of action. Accordingly PK modeling of these concentrations with a single compartment representing ELF, that assumes an even distribution of colistin in the lung over time, constitutes a simplification of what actually happens physiologically. In order to take into account the physiology of the lung, from the trachea to alveolar sacs and from ELF to parenchyma, a more complex modeling is needed. Physiological based pharmacokinetics (PBPK) models can be used to describe more precisely the distribution in tissues by considering the physiological architecture of the tissue[199], the diffusion of the drug through the different cell layers[200] and the physiology of the body[201]. These models are frequently used by pharmaceutical industry to predict oral disposition of drug candidates[202] but rarely for lung disposition[203]. However PBPK models are difficult to develop because they necessitate a large amount of physiological and physico-chemical data. Furthermore the computational resources necessary are large and hardly achievable with common desktop computers. Yet PBPK models seem a good alternative to empirical models and need to be further investigated for the characterization of drug disposition within the lung after systemic or aerosol delivery.

In this “aerosol study” , plasma concentrations profiles of colistin obtained after giving CMS IV were also in full agreement with those obtained by our group using the same brand of CMS in the same type of patients[139] but only partially consistent with results previously published by others[154,155]. CMS and colistin concentrations were assayed in all modern studies by validated methods. Gregoire and Plachouras used a liquid chromatography-tandem mass spectrometry (LC-MS/MS) method[144,145], whereas Garonzik used a liquid chromatography coupled with mass spectrometry (LC-MS) method[143]. These methods are two-step determination procedures with in a first time the assay of colistin concentrations, then sulfuric acid is added to hydrolyze CMS and its intermediates (described in next

chapter) into colistin. CMS concentrations are determined indirectly by subtracting the colistin concentrations determined in biological samples from the whole colistin concentrations determined after hydrolysis. Thus CMS concentrations determined correspond to the sum of the concentrations of CMS and of all its intermediates that hydrolyze into colistin with sulfuric acid. All authors reported also that blood samples were immediately chilled, centrifuged and that plasma were kept frozen from -20°C to -80°C until being assayed to preserve stability of CMS[140,204,205]. CMS degradation into colistin after sampling or/and during bioanalytical proceeding is unlikely to have contributed to discrepancies observed between some of our results and those of Plachouras[154] or Garonzik[155], because an artefact due to uncontrolled CMS hydrolysis would have an impact principally at early times when CMS concentrations are high, and not at later times when CMS has been totally cleared, which was the case in our study. Therefore a bioanalytical issue explaining inter-studies discrepancies between colistin PK in plasma is rather unlikely.

Among the potential explanations of these inter-studies discrepancies, it may then be hypothesized that they were due to a brand effect as mentioned during the 1st International Conference on Polymyxins in Prato[206] and documented in a controlled experiment in rats[136]. CMS is composed of at least 30 different compounds, mainly CMS A and CMS B[135,136]. In 2013, He et al.[136] investigated the pharmacokinetics of four different brands and reported that the colistin PK varied from one to the other. They also reported a ratio of CMS B to CMS A (hydrolyzed into respectively colistin B and colistin A) varying from 15 % to 98 % depending on the brand. Colistin A and B differ only in the structure of their N-terminal fatty acyl chains[136], however this difference is susceptible to alter some PK parameters of colistin such as the protein binding. Mohamed et al.[207] have shown that the unbound fraction of colistin A (fuA) was concentration dependent with a maximum fuA estimated to 31.2 %, whereas the unbound fraction of colistin B (fuB) was found to be constant (average, 43 %). The overall unbound fraction of colistin is therefore dependent on the ratio of colistin A and colistin B. In an other hand, Couet et al.[156] mentioned, in a study in healthy volunteers, that plasma PK parameters of CMS A and CMS B were virtually identical, as well as PK parameters of colistin A and colistin B. Therefore a difference of ratio between colistin A and colistin B explaining inter-studies discrepancies between colistin PK in plasma is doubtful.

He et al. also investigated the formation of colistin from CMS depending on the brand[136]. In addition to be a mixture of CMS A and CMS B, various intermediates of methanesulfonate derivatives (i.e. all five or only a part of the primary amine groups of colistin are methanesulphonated in CMS) are present in commercial formulations of CMS. The non-renal clearance of CMS ($CLnr_{CMS}$) is usually considered as the clearance of transformation of CMS into colistin. Thus the $CLnr_{CMS}$ is the clearance

of multiple compounds, which through various reactions and intermediates, form colistin A or B[208]. CMS is supposed to be converted into colistin by chemical hydrolysis at physiological pH[141,205] according to a first order process[139,154,175]. Consequently similar concentrations profiles of CMS may give similar concentrations profiles of colistin, since the conversion is supposed to be describe as a first order process. However a clear difference in the colistin profiles of different products was observed despite similar CMS profiles[136]. The conversion from CMS to colistin seems to be more complex that a first order hydrolysis and also seems to differ with the brand. It was hypothesized that the difference of methanesulphonation observed chromatographically between brands could have led to these differences[136].

Surprisingly, whereas about 60% of CMS is excreted unchanged in urine in ICU patients[139] during our study in HD patients, the total clearance of CMS in ICU-HD patients (typical value: 113 mL/min) was virtually the same as in ICU-85 patients (typical value: 112mL/min). The only possible explanation is an increase of CMS non-renal clearance at 113 mL/min to "compensate" for the absence of the renal clearance (0 mL/min). The exact underlying mechanism is unknown but among potential explanations, it may be hypothesized that endogenous substances that accumulate in plasma between HD sessions could interfere with the hydrolysis of CMS occurring at physiological pH and eventually increase the formation rate of colistin[141,205,209,210]. However this increase of $CLnr_{CMS}$ has never been reported before[155,211].

A more complex PK disposition scheme including a 3rd route of elimination was suggested for CMS by Garonzik et al.[155] Accordingly only a fraction, defined as f_m, of the CMS not excreted in urine would be converted into colistin[155]. This 3rd route remains hypothetical, but strengthens the complexity of the mechanisms involved in the conversion of CMS into colistin. Further investigations would be needed to describe more precisely this 3rd route in order to adequately predict colistin PK. One option would be to develop an analytical method to measure the concentrations of the different intermediates between CMS and colistin. This reasoning remains true for all products that need to be converted into an active form.

As discussed in the previous part, colistin PK can differ depending on the route of administration, the type of patients and also the brand. With appropriate data, PK modeling can be used to optimize dosing regimen. However it should be kept in mind that dosing regimens have to be simple enough to be applicable in clinical practice. Therefore it would be important to recommend dosing regimens that do not depend on the CMS brand. Two different profiles of colistin PK have been reported, possibly associated with differences of brands. One is described by Couet and Gregoire using

Colymicin® brand (from Sanofi-Aventis) that induces relatively high concentrations of colistin less than 4 h after CMS administration and which challenges the need for a loading dose, on the contrary to the PK described by Garonzik using Colistate® and Plachouras using Colistin/Norma®. However as a loading dose of Colymicin® brand allows to reach high colistin concentrations without adverse effects it seems adequate to recommend the administration of a loading dose to ICU patients whatever the brand, either to rapidly reach steady-state or as part of a front loading strategy.

The second part of this thesis was conducted in order to investigate the pharmacodynamics of colistin against *Pseudomonas aeruginosa*, in particular the development of resistance. The effect of colistin against *Pseudomonas aeruginosa* has been correlated with the area under the unbound concentration–time curve over 24h divided by the minimum inhibitory concentration (fAUC/MIC) both *in-vitro*[95] and in-vivo[164]. The target breakpoint has been estimated between 22.6 and 30.4 depending on the strain *in-vitro*[95]. The fAUC/MIC target required to achieve 2-log kill at H24 was estimated to vary between 27.6 and 36.1 in a thigh infection model, and between 36.9 and 45.9 in a lung infection model[164]. Although these indexes and target values may facilitate the selection of appropriate dosing regimens for optimal antibacterial effect, they do not describe the rapid loss of efficacy due to the emergence of resistance described with *Pseudomonas aeruginosa. A*fter an initial decay, a bacterial regrowth is frequently observed both in *in-vitro* and *in-vivo* experiments [75,83,90,129,130]. Bacterial regrowth can be due either to the decrease of the drug concentrations below the efficient threshold as eventually happens *in-vivo* or to the development of resistance, both mechanisms can happen simultaneously. When the antibiotic concentration does not vary with time, as it is the case for time-kill experiments *in-vitro*, the development of resistance is the more likely phenomenon explaining a bacterial regrowth, although the possible degradation or non-specific binding of the antimicrobial should be considered. Whereas the first phenomenon can be handled by increasing the dosage or re-administer the drug, the second may be more complicated to manage. Description and quantification of the emergence of resistance over time is quite challenging but PK-PD modeling approaches are more and more frequently used in that purpose [64,70,74,133,212-214]. Different structural models have been used, with apparently the same efficiency to fit the data[74,133], indicating that modeling criterion alone may not be able to discriminate between different models and that the best model may be selected from proper understanding of mechanism involved in resistance acquisition and development. This issue was addressed by comparing the performances of different structural PK-PD models using a simulation approach and then the *in-vitro* pharmacodynamics of colistin against *Pseudomonas aeruginosa* was investigated using a well-defined bioluminescent strain of bacteria.

Before performing an *in-vitro* study, the ability of different PK-PD models to fit data were assessed and static[70,74-77] (constant concentration with time) and dynamic[69,83-85] (variable concentrations with time) experimental designs were compared. Experimental data reflecting different theoretical mechanisms of resistance were simulated in static and dynamic conditions. These simulated data were then analyzed with different PK-PD models. In summary, standard statistical modeling criteria failed to correctly identify the PK-PD model corresponding to the true resistance mechanism(s), whatever the static or dynamic design of the experiment. Moreover, even if the actual model was used to fit the data the parameter estimates were often biased. These results have several implications. In a descriptive purpose many models can be adequately used to make comparisons between antimicrobials, bacterial strains or dosing regimens…. However extrapolations from these models, *e.g.* over a longer period of time or from *in-vitro* to *in-vivo*, seem very risky. Indeed, the use of a "wrong" model or of biased parameter estimates led to predictions that might differ strongly from actual data. This was an important finding since most of the published PD models for antibiotics were developed from usual time-kill experiments and derived simulations results are questionable. For example, the resistance of *Pseudomonas aeruginosa* towards colistin has been described with two different models. A mechanistic PK/PD modeling study has been performed to describe the changing activity of colistin with time by Bulitta et al[74]. The authors have built a model that describes the competitive binding between colistin, Mg^{2+} and Ca^{2+} to the outer bacterial membrane of *Pseudomonas aeruginosa.* They resumed the resistance to colistin by the presence of multiple subpopulations in the inoculum. In another study Mohamed et al.[133] resumed the loss of colistin efficacy with time as an adaptive process. In both studies data were collected from static concentrations experimental designs, and both models provided a satisfactory fit of bacterial counts over the 24 h experiment. However extrapolations over a longer period of time from these two distinct models will lead to different outputs and therefore different dosing recommendations. Therefore in the presence of complex adaptation or/and resistance phenomenon it seems important to have information about the mechanism of resistance in order to select the most relevant PD model. Nevertheless extrapolations should always be careful and confirmed by experimental/clinical trials.

We have applied the conclusions of our previous *in-silico* study to design our *in-vitro* experiment. A usual kill-curves experiment performed with static concentrations of colistin was prolonged in time with subsequent kill curves performed immediately after the first one or after different durations of drug-free bacterial growth. Moreover the mechanisms of resistance appearing during the experiment were microbiologically characterized and implemented –converted into mathematical equations- in the PK-PD model used to fit the data. Interestingly a regrowth of CFU after an initial decay was also

observed during the second time-kill experiments, indicating a two steps resistance development with a regrowth during the first time-kill curve in presence of clinically relevant colistin concentrations, and a second re-growth during the second time-kill at much higher concentrations, up to 200 mg/L. The resistance disappearance on drug-free plate was quite spectacular although relatively slow compared to its appearance and still not complete after 66 h of wash-out. Overall this study may suggest a number of practical recommendations for the clinicians. It was observed that the initial population of bacteria was sensitive to colistin but that it adapted rapidly (half-life of 2h) to become much less sensitive since in our experimental conditions, efficient antimicrobial concentrations after 30h of exposure, should be close to 40 mg/mL, at least for this particular strain, which would be toxic and therefore not clinically achievable. These observations confirm that the first 24 h of treatment are the most critical time in the management of infections in critically-ill patients. Therefore front-loading strategies would be recommended, as already done[139,207], in order to prevent the rapid adaptation of bacteria to colistin. Moreover stable mutants highly resistant to colistin also appeared during the first 24 h of exposure to colistin at therapeutic concentrations. Colistin alone cannot eradicate these mutants, and although the immune system defenses should not be neglected, combination therapies seem necessary [58,68]. This study confirm also the need of experimental design longer that 24-h in order to characterize the development of resistance over time. It would be now interesting to investigate the combination of colistin with another antimicrobial in order to prevent mutually the emergence of resistances.

Most of the PK/PD models for antibacterial drugs are developed with PD data obtained from *in-vitro* experiments and PK data separately obtained in human. PK is usually defined as “how the body handles the drug”, whereas PD is defined as “how the drug affects the body” [215]. However antibiotics differ from other drugs in that the antibiotics do not affects the body (with the exception of side effects) but bacteria inside. *In-vitro* studies present several advantages as the lower cost, a more controlled environment, a better repeatability…. However *in-vitro* experiments generally do not take into account physiological processes such as the impact of the immune system, the development of biofilms or the drug concentration at the site of action (e.g. lungs). This explains why *in-vitro*/*in-vivo* extrapolations are particularly difficult in the field of infectiology.

A vast number of animal models have been developed to describe antibacterial therapy. Most of the infection models have been developed in rats and mice and mimics multiple types of infections, such as thigh infection models[129,216], pneumonia models[216,217], peritonitis models[218], meningitis models[219]

or skin infection models[220]. The effect of the immune system can be assessed by comparing the PD endpoint in immunocompetent animals versus animals rendered partially or completely neutropenic after administrations of cyclophosphamide[221]. The most commonly used PD endpoint is the count of CFU after 24 h of treatment which can be expressed as the relative change of log CFU compared to a non-treated control animal. The endpoint is usually associated with PK data to identify which of the PK/PD indices best predicts the efficiency of the drug[216]. PK/PD models characterizing the full time course of drug effects in animal are still scarce[129,222]. One plausible cause is that to quantify bacterial in tissue, animal has to be sacrificed, tissues of interest harvested, grinded, and spread on agar plates before CFU counting. Therefore a large number of animals are needed since only one measure of the PD endpoint can be obtained per animal. Moreover the inter-individual variability cannot be distinguished from the residual error when estimating the drug PD with only one endpoint estimate per animal and therefore statistical tests lack of power to demonstrate significant effects. Imagery methods such as bioluminescence allow performing multiple measures on the same animal, even if this method has a lower sensitivity than CFU counting. The measure of bioluminescence is realized with a charge coupled device (CCD) camera that count the photons emitted by the reaction of the luciferine with the luciferase inside the transfected bacteria[103,104]. During *in-vitro* experiments the ray light goes through the broth and glasses before to be captured by the camera but during an *in-vivo* experiment the ray light need also to go through tissues than can absorb it and then reduce the sensitivity. This partial absorption of the signal is one of the major drawbacks of the bioluminescence method. Bioluminescence is used in infectious studies, to evaluate the dissemination of the pathogens [223-225] and to evaluate the antibacterial effects[108]. To our knowledge no PK/PD study has been performed to describe the full time course of drug effects using bioluminescence in pulmonary infection models. During this thesis, in addition to the results presented herein, I also developed a model of lung infection in mouse. The objective was to assess the impact of the route of administration (*SC* versus aerosol delivery) in mice pulmonary infected with bioluminescent *Pseudomonas aeruginosa*. In their respective reviews, Mizgerd[226], Bakker-Woudenberg[227] and Hernández[228] mentioned that the development of an animal model takes times, mostly because multiple preliminary studies are needed to assure the survival of the animal. We have performed some of these studies during our development, and a brief review of the principal steps will be presented in the next paragraph.

Firstly we tested two different species of mice, since susceptibility to a pathogen can vary from one species of experimental animal to another. Lipscomp et al.[229] investigated the infection of *Cryptococcus neoformans* in C.B-17, BALB/c and C57BL/6 mice, and showed that bacteria were more persistent in C57BL/6 mice. In our case, we investigated the infection of *Pseudomonas aeruginosa* in

swiss and C57BL/6 mice. C57BL/6 mice presented a longer survival over time and were chosen for the next experiments. We also tested several bacterial inoculum sizes. There are more constraints compared to *in-vitro* since a high inoculum can kill the mouse whereas an inoculum too low may be insufficient to infect immuno-competent animals[226]. We tested 3 different inoculums: 0.5 x 10^7, 1 x $10^7$and 3 x 10^7 CFU per mice. The former was too low to obtain a bioluminescent signal and the latter led to a rapid death of mice. Therefore an inoculum of 1*10^7 CFU per mice was used, identical to those reported for similar studies[230-232]. Different ways to inoculate bacteria pulmonary were also tested: intranasal[164 233], intratracheal[234] or via a microsprayer[151] in the trachea. Intranasal inoculations were easy to perform but resulted in a heterogeneous deposition of bacteria[227] and the remaining bacteria on the nose biased the bioluminescence measurement. Intratracheal inoculations were less variable[227] but needed a surgery and the scar on the trachea interfered with aerosol delivery of the treatment. The aerosol delivery of bacteria via a microsprayer was the route of administration that permitted the most efficient inoculation of bacteria without compromising the treatment delivery, however an important technical practice was necessary[151]. All these preparations are mandatory before the beginning of usual *in-vivo* PK/PD studies. In our case an additional step was necessary for the development of the animal model since with the bioluminescence technique of imagery animals had to be anesthetized at each measurement. Therefore the type (SC or aerosol) of anesthesia, the anesthetic used (more or less respiratory depressor), the dose and the frequency of administration were investigated in preliminary studies in order to assure the mouse survival between consecutive measurements. Finally housing conditions needed also to take into account the consequences of the infection such as the change in body temperature and the dehydration. Our animal model has shown some promising preliminary results, but further investigations are still needed to assure the repeatability of this experiment.

In-vivo studies better mimic the conditions encountered during a human infection than *in-vitro* studies. However the workload is much more important and the development of an infection model take a long time before to be reproducible and routinely usable. Nevertheless, associated to PK/PD modeling for the analysis of the antimicrobial effects, *in-vivo* experiments are very helpful for the understanding of the infection time-course during treatments and the determination of optimized dosing regimens.

V. Conclusion

Antibiotics are among the most commonly prescribed drugs. Although the majority of these drugs were developed several decades ago, optimal dosages (dose, dosing interval and treatment duration) have still not been well defined. The aim of this thesis was to develop pharmacokinetic (PK) and pharmacokinetic-pharmacodynamics (PK/PD) models that characterize the time course of drug concentration and the effects of antibiotics on bacterial growth, killing and resistance over time, and to apply these models to guide optimization of dosing regimens of antimicrobial therapies.

A population PK model for colistin and its prodrug, colistin methanesulfonate (CMS) was developed in critically ill patient receiving colistin by nebulization and/or undergoing an intermittent hemodialysis and dosing regimen were recommended accordingly for these patients. Simulations showed the benefits of using aerosol delivery of 2 MUI CMS dose for the treatment of pulmonary infections in critical care patients. For patients with HD session dosing regimen of CMS should be 1.5 MIU twice daily for a non-HD day, CMS should be administered after HD sessions with a dose increase of 1.5 MIU compared to the dose scheduled on non-HD day (i.e. 3+1.5 = total of 4.5 MIU for HD day).

A semi-mechanistic PK/PD model that incorporates the growth, killing kinetics, mutation rate and adaptive resistance development of *Pseudomonas aeruginosa* against colistin was developed based on *in-vitro* time-kill curve data. This study and our assessment on the performances of different structural PK-PD models by using a simulation approach showed the importance of longer study design and complementary microbiological data. A high, quick and partially reversible resistance was described. This study also confirmed that the first 24 h of treatment are the most critical period of time in the management of infections in critically-ill patients and that colistin alone cannot eradicate completely mutants of *Pseudomonas aeruginosa*, and that combination therapies seem necessary.

This thesis contributes to the optimization of dosing regimen for the treatment of infections in critical ill patient, and help to describe the development of resistance in *Pseudomonas aeruginosa* towards colistin. Further investigations have been suggested to improve these findings, such as the development of physiological based models to investigate lung delivery of drugs, assessment of combination therapies with colistin and development of *in-vivo* PK/PD studies.

VI. References

1. Ligon BL. Penicillin: its discovery and early development. *Semin Pediatr Infect Dis* 2004;15:52-57.

2. Fleming A. PENICILLIN IN VENEREAL DISEASES-1. *Br J Vener Dis* 1944;20:133-136.

3. ECDC/EFSA/EMA first joint report on the integrated analysis of the consumption of antimicrobial agents and occurrence of antimicrobial resistance in bacteria from humans and food-producing animals. *EFSA Journal* 2015;13:4006.

4. Fleming A. Nobel Lecture. 1945.

5. WHO. WHO's first global report on antibiotic resistance reveals serious, worldwide threat to public health. 2014.

6. Alekshun MN, Levy SB. Molecular mechanisms of antibacterial multidrug resistance. *Cell* 2007;128:1037-1050.

7. Bellamy WD, Klimek JW. Some Properties of Penicillin-resistant Staphylococci. *J Bacteriol* 1948;55:153-160.

8. Bondi A, Jr., Dietz CC. Penicillin resistant staphylococci. *Proc Soc Exp Biol Med* 1945;60:55-58.

9. Brown AG, Butterworth D, Cole M, et al. Naturally-occurring beta-lactamase inhibitors with antibacterial activity. *J Antibiot (Tokyo)* 1976;29:668-669.

10. Bush K, Jacoby GA. Updated functional classification of beta-lactamases. *Antimicrob Agents Chemother* 2010;54:969-976.

11. Bush K, Jacoby GA, Medeiros AA. A functional classification scheme for beta-lactamases and its correlation with molecular structure. *Antimicrob Agents Chemother* 1995;39:1211-1233.

12. Ambler RP. The structure of beta-lactamases. *Philos Trans R Soc Lond B Biol Sci* 1980;289:321-331.

13. Walsh TR, Toleman MA. The emergence of pan-resistant Gram-negative pathogens merits a rapid global political response. *J Antimicrob Chemother* 2012;67:1-3.

14. Fernandez L, Hancock RE. Adaptive and mutational resistance: role of porins and efflux pumps in drug resistance. *Clin Microbiol Rev* 2012;25:661-681.

15. Jaktaji RP, Heidari F. Study the Expression of ompf Gene in *Esherichia coli* Mutants. *Indian J Pharm Sci* 2013;75:540-544.

16. Kishii R, Takei M. Relationship between the expression of ompF and quinolone resistance in Escherichia coli. *J Infect Chemother* 2009;15:361-366.

17. Paltansing S, Tengeler AC, Kraakman ME, et al. Exploring the contribution of efflux on the resistance to fluoroquinolones in clinical isolates of Escherichia coli. *Microb Drug Resist* 2013;19:469-476.

18. El Amin N, Giske CG, Jalal S, et al. Carbapenem resistance mechanisms in *Pseudomonas aeruginosa*: alterations of porin OprD and efflux proteins do not fully explain resistance patterns observed in clinical isolates. *APMIS* 2005;113:187-196.

19. Li H, Luo YF, Williams BJ, et al. Structure and function of OprD protein in *Pseudomonas aeruginosa*: from antibiotic resistance to novel therapies. *Int J Med Microbiol* 2012;302:63-68.

20. Maseda H, Yoneyama H, Nakae T. Assignment of the substrate-selective subunits of the MexEF-OprN multidrug efflux pump of *Pseudomonas aeruginosa*. *Antimicrob Agents Chemother* 2000;44:658-664.

21. Mesaros N, Glupczynski Y, Avrain L, et al. A combined phenotypic and genotypic method for the detection of Mex efflux pumps in *Pseudomonas aeruginosa*. *J Antimicrob Chemother* 2007;59:378-386.

22. Pradel E, Pagès J-M. The AcrAB-TolC efflux pump contributes to multidrug resistance in the nosocomial pathogen Enterobacter aerogenes. *Antimicrob Agents Chemother* 2002;46:2640-2643.

23. Venter H, Mowla R, Ohene-Agyei T, et al. RND-type drug e ffl ux pumps from Gram-negative bacteria: molecular mechanism and inhibition. *Front Microbiol* 2015;6:377.

24. Du D, Wang Z, James NR, et al. Structure of the AcrAB-TolC multidrug efflux pump. *Nature* 2014;509:512-515.

25. Zhang T, Hu S, Li G, et al. Evaluation of the MeltPro TB/STR assay for rapid detection of streptomycin resistance in *Mycobacterium tuberculosis*. *Tuberculosis (Edinb)* 2015;95:162-169.

26. El'Garch F, Jeannot K, Hocquet D, et al. Cumulative effects of several nonenzymatic mechanisms on the resistance of *Pseudomonas aeruginosa* to aminoglycosides. *Antimicrob Agents Chemother* 2007;51:1016-1021.

27. Jacoby GA. Mechanisms of resistance to quinolones. *Clin Infect Dis* 2005;41 Suppl 2:S120-126.

28. Meireles D, Leite-Martins L, Bessa LJ, et al. Molecular characterization of quinolone resistance mechanisms and extended-spectrum beta-lactamase production in Escherichia coli isolated from dogs. *Comp Immunol Microbiol Infect Dis* 2015.

29. Thomas CM, Nielsen KM. Mechanisms of, and barriers to, horizontal gene transfer between bacteria. *Nat Rev Microbiol* 2005;3:711-721.

30. Eaves DJ, Randall L, Gray DT, et al. Prevalence of mutations within the quinolone resistance-determining region of gyrA, gyrB, parC, and parE and association with antibiotic resistance in quinolone-resistant Salmonella enterica. *Antimicrob Agents Chemother* 2004;48:4012-4015.

31. Friedman SM, Lu T, Drlica K. Mutation in the DNA gyrase A Gene of Escherichia coli that expands the quinolone resistance-determining region. *Antimicrob Agents Chemother* 2001;45:2378-2380.

32. Martinez JL, Baquero F. Mutation frequencies and antibiotic resistance. *Antimicrob Agents Chemother* 2000;44:1771-1777.

33. Gillespie T, Masterton RG. Investigation into the selection frequency of resistant mutants and the bacterial kill rate by levofloxacin and ciprofloxacin in non-mucoid *Pseudomonas aeruginosa* isolates from cystic fibrosis patients. *Int J Antimicrob Agents* 2002;19:377-382.

34. Hughes D, Andersson DI. Carbon starvation of Salmonella typhimurium does not cause a general increase of mutation rates. *J Bacteriol* 1997;179:6688-6691.

35. Brimacombe CA, Ding H, Johnson JA, et al. Homologues of genetic transformation DNA import genes are required for Rhodobacter capsulatus gene transfer agent recipient capability regulated by the CtrA response regulator. *J Bacteriol* 2015.

36. Bearson BL, Brunelle BW. Fluoroquinolone induction of phage-mediated gene transfer in multidrug-resistant Salmonella. *Int J Antimicrob Agents* 2015.

37. Moon BY, Park JY, Hwang SY, et al. Phage-mediated horizontal transfer of a *Staphylococcus aureus* virulence-associated genomic island. *Sci Rep* 2015;5:9784.

38. LEDERBERG J, TATUM EL. Gene recombination in Escherichia coli. *Nature* 1946;158:558.

39. Brolund A, Sandegren L. Characterization of ESBL disseminating plasmids. *Infect Dis (Lond)* 2015:1-8.

40. Hocquet D, Vogne C, El Garch F, et al. MexXY-OprM efflux pump is necessary for a adaptive resistance of *Pseudomonas aeruginosa* to aminoglycosides. *Antimicrob Agents Chemother* 2003;47:1371-1375.

41. Lee JY, Chung ES, Na IY, et al. Development of colistin resistance in pmrA-, phoP-, parR- and cprR-inactivated mutants of *Pseudomonas aeruginosa*. *J Antimicrob Chemother* 2014.

42. El-Halfawy OM, Valvano MA. Antimicrobial heteroresistance: an emerging field in need of clarity. *Clin Microbiol Rev* 2015;28:191-207.

43. Li J, Rayner CR, Nation RL, et al. Heteroresistance to colistin in multidrug-resistant Acinetobacter baumannii. *Antimicrob Agents Chemother* 2006;50:2946-2950.

44. Yau W, Owen RJ, Poudyal A, et al. Colistin hetero-resistance in multidrug-resistant Acinetobacter baumannii clinical isolates from the Western Pacific region in the SENTRY antimicrobial surveillance proGramme. *J Infect* 2009;58:138-144.

45. Skiada A, Markogiannakis A, Plachouras D, et al. Adaptive resistance to cationic compounds in *Pseudomonas aeruginosa*. *Int J Antimicrob Agents* 2011;37:187-193.

46. Yamane K, Wachino J, Suzuki S, et al. New plasmid-mediated fluoroquinolone efflux pump, QepA, found in an Escherichia coli clinical isolate. *Antimicrob Agents Chemother* 2007;51:3354-3360.

47. Hansen LH, Johannesen E, Burmolle M, et al. Plasmid-encoded multidrug efflux pump conferring resistance to olaquindox in Escherichia coli. *Antimicrob Agents Chemother* 2004;48:3332-3337.

48. Moskowitz SM, Brannon MK, Dasgupta N, et al. PmrB mutations promote polymyxin resistance of *Pseudomonas aeruginosa* isolated from colistin-treated cystic fibrosis patients. *Antimicrob Agents Chemother* 2012;56:1019-1030.

49. Melnyk AH, Wong A, Kassen R. The fitness costs of antibiotic resistance mutations. *Evol Appl* 2015;8:273-283.

50. Lenski RE. The cost of antibiotic resistance--from the perspective of a bacterium. *Ciba Found Symp* 1997;207:131-140; discussion 141-151.

51. Schulz zur Wiesch P, Engelstadter J, Bonhoeffer S. Compensation of fitness costs and reversibility of antibiotic resistance mutations. *Antimicrob Agents Chemother* 2010;54:2085-2095.

52. Zünd P, Lebek G. Generation time-prolonging R plasmids: correlation between increases in the generation time of Escherichia coli caused by R plasmids and their molecular size. *Plasmid* 1980;3:65-69.

53. Andersson DI. The biological cost of mutational antibiotic resistance: any practical conclusions? *Curr Opin Microbiol* 2006;9:461-465.

54. Gustafsson I, Cars O, Andersson DI. Fitness of antibiotic resistant Staphylococcus epidermidis assessed by competition on the skin of human volunteers. *J Antimicrob Chemother* 2003;52:258-263.

55. Stickland HG, Davenport PW, Lilley KS, et al. Mutation of nfxB causes global changes in the physiology and metabolism of *Pseudomonas aeruginosa*. *J Proteome Res* 2010;9:2957-2967.

56. Sundqvist M. Reversibility of antibiotic resistance. *Ups J Med Sci* 2014;119:142-148.

57. Komp Lindgren P, Marcusson LL, Sandvang D, et al. Biological cost of single and multiple norfloxacin resistance mutations in Escherichia coli implicated in urinary tract infections. *Antimicrob Agents Chemother* 2005;49:2343-2351.

58. Sander P, Springer B, Prammananan T, et al. Fitness cost of chromosomal drug resistance-conferring mutations. *Antimicrob Agents Chemother* 2002;46:1204-1211.

59. Schrag SJ, Perrot V, Levin BR. Adaptation to the fitness costs of antibiotic resistance in Escherichia coli. *Proc Biol Sci* 1997;264:1287-1291.

60. Bjorkman J, Nagaev I, Berg OG, et al. Effects of environment on compensatory mutations to ameliorate costs of antibiotic resistance. *Science* 2000;287:1479-1482.

61. MacLean RC, Vogwill T. Limits to compensatory adaptation and the persistence of antibiotic resistance in pathogenic bacteria. *Evol Med Public Health* 2014;2015:4-12.

62. Ambrose PG, Bhavnani SM, Rubino CM, et al. Pharmacokinetics-pharmacodynamics of antimicrobial therapy: it's not just for mice anymore. *Clin Infect Dis* 2007;44:79-86.

63. Drusano GL. Antimicrobial pharmacodynamics: critical interactions of 'bug and drug'. *Nat Rev Microbiol* 2004;2:289-300.

64. Tam VH, Louie A, Deziel MR, et al. The relationship between quinolone exposures and resistance amplification is characterized by an inverted U: a new paradigm for optimizing pharmacodynamics to counterselect resistance. *Antimicrob Agents Chemother* 2007;51:744-747.

65. Andrews JM. Determination of minimum inhibitory concentrations. *J Antimicrob Chemother* 2001;48 Suppl 1:5-16.

66. Craig WA. Pharmacokinetic/pharmacodynamic parameters: rationale for antibacterial dosing of mice and men. *Clin Infect Dis* 1998;26:1-10; quiz 11-12.

67. Mueller M, de la Pena A, Derendorf H. Issues in pharmacokinetics and pharmacodynamics of anti-infective agents: kill curves versus MIC. *Antimicrob Agents Chemother* 2004;48:369-377.

68. Czock D, Keller F. Mechanism-based pharmacokinetic-pharmacodynamic modeling of antimicrobial drug effects. *J Pharmacokinet Pharmacodyn* 2007;34:727-751.

69. Chung P, McNamara PJ, Campion JJ, et al. Mechanism-based pharmacodynamic models of fluoroquinolone resistance in *Staphylococcus aureus*. *Antimicrob Agents Chemother* 2006;50:2957-2965.

70. Gregoire N, Raherison S, Grignon C, et al. Semimechanistic pharmacokinetic-pharmacodynamic model with adaptation development for time-kill experiments of ciprofloxacin against *Pseudomonas aeruginosa*. *Antimicrob Agents Chemother* 2010;54:2379-2384.

71. Tato M, Lopez Y, Morosini MI, et al. Characterization of variables that may influence ozenoxacin in susceptibility testing, including MIC and MBC values. *Diagn Microbiol Infect Dis* 2014;78:263-267.

72. Dong Y, Zhao X, Domagala J, et al. Effect of fluoroquinolone concentration on selection of resistant mutants of Mycobacterium bovis BCG and *Staphylococcus aureus*. *Antimicrob Agents Chemother* 1999;43:1756-1758.

73. Drlica K, Zhao X. Mutant selection window hypothesis updated. *Clin Infect Dis* 2007;44:681-688.

74. Bulitta JB, Yang JC, Yohonn L, et al. Attenuation of colistin bactericidal activity by high inoculum of *Pseudomonas aeruginosa* characterized by a new mechanism-based population pharmacodynamic model. *Antimicrob Agents Chemother* 2010;54:2051-2062.

75. Nielsen EI, Viberg A, Lowdin E, et al. Semimechanistic pharmacokinetic/pharmacodynamic model for assessment of activity of antibacterial agents from time-kill curve experiments. *Antimicrob Agents Chemother* 2007;51:128-136.

76. Schmidt S, Rock K, Sahre M, et al. Effect of protein binding on the pharmacological activity of highly bound antibiotics. *Antimicrob Agents Chemother* 2008;52:3994-4000.

77. Yano Y, Oguma T, Nagata H, et al. Application of logistic growth model to pharmacodynamic analysis of *in-vitro* bactericidal kinetics. *J Pharm Sci* 1998;87:1177-1183.

78. Dilworth TJ, Leonard SN, Vilay AM, et al. Vancomycin and piperacillin-tazobactam against methicillin-resistant *Staphylococcus aureus* and vancomycin-intermediate *Staphylococcus aureus* in an *in-vitro* pharmacokinetic/pharmacodynamic model. *Clin Ther* 2014;36:1334-1344.

79. Luther MK, Arvanitis M, Mylonakis E, et al. Activity of daptomycin or linezolid in combination with rifampin or gentamicin against biofilm-forming Enterococcus faecalis or E. faecium in an *in-vitro* pharmacodynamic model using simulated endocardial vegetations and an in-vivo survival assay using Galleria mellonella larvae. *Antimicrob Agents Chemother* 2014;58:4612-4620.

80. Bowker KE, Garvey MI, Noel AR, et al. Comparative antibacterial effects of moxifloxacin and levofloxacin on *Streptococcus pneumoniae* strains with defined mechanisms of resistance: impact of bacterial inoculum. *J Antimicrob Chemother* 2013;68:1130-1138.

81. Brown MR, Melling J. Role of divalent cations in the action of polymyxin B and EDTA on *Pseudomonas aeruginosa*. *J Gen Microbiol* 1969;59:263-274.

82. Gloede J, Scheerans C, Derendorf H, et al. *In-vitro* pharmacodynamic models to determine the effect of antibacterial drugs. *J Antimicrob Chemother* 2010;65:186-201.

83. Campion JJ, McNamara PJ, Evans ME. Pharmacodynamic modeling of ciprofloxacin resistance in *Staphylococcus aureus*. *Antimicrob Agents Chemother* 2005;49:209-219.

84. Katsube T, Yano Y, Yamano Y, et al. Pharmacokinetic-pharmacodynamic modeling and simulation for bactericidal effect in an *in-vitro* dynamic model. *J Pharm Sci* 2008;97:4108-4117.

85. Meagher AK, Forrest A, Dalhoff A, et al. Novel pharmacokinetic-pharmacodynamic model for prediction of outcomes with an extended-release formulation of ciprofloxacin. *Antimicrob Agents Chemother* 2004;48:2061-2068.

86. Nielsen EI, Cars O, Friberg LE. Predicting *in-vitro* antibacterial efficacy across experimental designs with a semimechanistic pharmacokinetic-pharmacodynamic model. *Antimicrob Agents Chemother* 2011;55:1571-1579.

87. Schmidt S, Sabarinath SN, Barbour A, et al. Pharmacokinetic-pharmacodynamic modeling of the *in-vitro* activities of oxazolidinone antimicrobial agents against methicillin-resistant *Staphylococcus aureus*. *Antimicrob Agents Chemother* 2009;53:5039-5045.

88. Liu P, Rand KH, Obermann B, et al. Pharmacokinetic-pharmacodynamic modelling of antibacterial activity of cefpodoxime and cefixime in *in-vitro* kinetic models. *Int J Antimicrob Agents* 2005;25:120-129.

89. Mouton JW, Vinks AA. Pharmacokinetic/pharmacodynamic modelling of antibacterials *in-vitro* and in-vivo using bacterial growth and kill kinetics: the minimum inhibitory concentration versus stationary concentration. *Clin Pharmacokinet* 2005;44:201-210.

90. Tam VH, Kabbara S, Vo G, et al. Comparative pharmacodynamics of gentamicin against *Staphylococcus aureus* and *Pseudomonas aeruginosa*. *Antimicrob Agents Chemother* 2006;50:2626-2631.

91. Louie A, Heine HS, Kim K, et al. Use of an *in-vitro* pharmacodynamic model to derive a linezolid regimen that optimizes bacterial kill and prevents emergence of resistance in *Bacillus anthracis*. *Antimicrob Agents Chemother* 2008;52:2486-2496.

92. Blaser J, Stone BB, Zinner SH. Two compartment kinetic model with multiple artificial capillary units. *J Antimicrob Chemother* 1985;15 Suppl A:131-137.

93. Brugger SD, Baumberger C, Jost M, et al. Automated counting of bacterial colony forming units on agar plates. *PLoS One* 2012;7:e33695.

94. Chiang PJ, Tseng MJ, He ZS, et al. Automated counting of bacterial colonies by image analysis. *J Microbiol Methods* 2015;108:74-82.

95. Bergen PJ, Bulitta JB, Forrest A, et al. Pharmacokinetic/pharmacodynamic investigation of colistin against *Pseudomonas aeruginosa* using an *in-vitro* model. *Antimicrob Agents Chemother* 2010;54:3783-3789.

96. Fuursted K, Schumacher H. Significance of low-level resistance to ciprofloxacin in *Klebsiella pneumoniae* and the effect of increased dosage of ciprofloxacin in-vivo using the rat granuloma pouch model. *J Antimicrob Chemother* 2002;50:421-424.

97. Drusano GL, Bonomo RA, Bahniuk N, et al. Resistance emergence mechanism and mechanism of resistance suppression by tobramycin for cefepime for *Pseudomonas aeruginosa*. *Antimicrob Agents Chemother* 2012;56:231-242.

98. Castillo M, Martin-Orue SM, Manzanilla EG, et al. Quantification of total bacteria, enterobacteria and lactobacilli populations in pig digesta by real-time PCR. *Vet Microbiol* 2006;114:165-170.

99. Holm C, Mathiasen T, Jespersen L. A flow cytometric technique for quantification and differentiation of bacteria in bulk tank milk. *J Appl Microbiol* 2004;97:935-941.

100. Kerstens M, Boulet G, Tritsmans C, et al. Flow cytometric enumeration of bacteria using TO-PRO(R)-3 iodide as a single-stain viability dye. *J Lab Autom* 2014;19:555-561.

101. Greer LF, 3rd, Szalay AA. Imaging of light emission from the expression of luciferases in living cells and organisms: a review. *Luminescence* 2002;17:43-74.

102. Thorn RM, Nelson SM, Greenman J. Use of a bioluminescent *Pseudomonas aeruginosa* strain within an *in-vitro* microbiological system, as a model of wound infection, to assess the antimicrobial efficacy of wound dressings by monitoring light production. *Antimicrob Agents Chemother* 2007;51:3217-3224.

103. Beard SJ, Salisbury V, Lewis RJ, et al. Expression of lux genes in a clinical isolate of *Streptococcus pneumoniae*: using bioluminescence to monitor gemifloxacin activity. *Antimicrob Agents Chemother* 2002;46:538-542.

104. Gahan CG. The bacterial lux reporter system: applications in bacterial localisation studies. *Curr Gene Ther* 2012;12:12-19.

105. Galluzzi L, Karp M. Intracellular redox equilibrium and growth phase affect the performance of luciferase-based biosensors. *J Biotechnol* 2007;127:188-198.

106. Alloush HM, Salisbury V, Lewis RJ, et al. Pharmacodynamics of linezolid in a clinical isolate of *Streptococcus pneumoniae* genetically modified to express lux genes. *J Antimicrob Chemother* 2003;52:511-513.

107. Rocchetta HL, Boylan CJ, Foley JW, et al. Validation of a noninvasive, real-time imaging technology using bioluminescent Escherichia coli in the neutropenic mouse thigh model of infection. *Antimicrob Agents Chemother* 2001;45:129-137.

108. Massey S, Johnston K, Mott TM, et al. In-vivo Bioluminescence Imaging of Burkholderia mallei Respiratory Infection and Treatment in the Mouse Model. *Front Microbiol* 2011;2:174.

109. Bergmann S, Beard PM, Pasche B, et al. Influence of internalin a murinisation on host resistance to orally acquired listeriosis in mice. *BMC Microbiol* 2013;13:90.

110. Bergmann S, Rohde M, Schughart K, et al. The bioluminescent Listeria monocytogenes strain Xen32 is defective in flagella expression and highly attenuated in orally infected BALB/cJ mice. *Gut Pathog* 2013;5:19.

111. Henken S, Bohling J, Ogunniyi AD, et al. Evaluation of biophotonic imaging to estimate bacterial burden in mice infected with highly virulent compared to less virulent *Streptococcus pneumoniae* serotypes. *Antimicrob Agents Chemother* 2010;54:3155-3160.

112. Eagle H. THE THERAPEUTIC ACTIVITY OF PENICILLINS F, G, K, AND X IN EXPERIMENTAL INFECTIONS WITH PNEUMOCOCCUS TYPE I AND STREPTOCOCCUS PYOGENES. *J Exp Med* 1947;85:175-186.

113. Eagle H, Fleischman R, Levy M. "Continuous" vs. "discontinuous" therapy with penicillin; the effect of the interval between injections on therapeutic efficacy. *N Engl J Med* 1953;248:481-488.

114. Eagle H, Fleischman R, Musselman AD. Effect of schedule of administration on the therapeutic efficacy of penicillin; importance of the aggregate time penicillin remains at effectively bactericidal levels. *Am J Med* 1950;9:280-299.

115. Vogelman B, Gudmundsson S, Leggett J, et al. Correlation of antimicrobial pharmacokinetic parameters with therapeutic efficacy in an animal model. *J Infect Dis* 1988;158:831-847.

116. Mouton JW, Dudley MN, Cars O, et al. Standardization of pharmacokinetic/pharmacodynamic (PK/PD) terminology for anti-infective drugs: an update. *J Antimicrob Chemother* 2005;55:601-607.

117. Craig WA. Interrelationship between pharmacokinetics and pharmacodynamics in determining dosage regimens for broad-spectrum cephalosporins. *Diagn Microbiol Infect Dis* 1995;22:89-96.

118. Gustafsson I, Löwdin E, Odenholt I, et al. Pharmacokinetic and pharmacodynamic parameters for antimicrobial effects of cefotaxime and amoxicillin in an *in-vitro* kinetic model. *Antimicrob Agents Chemother* 2001;45:2436-2440.

119. Andes D, Craig WA. Pharmacodynamics of the new fluoroquinolone gatifloxacin in murine thigh and lung infection models. *Antimicrob Agents Chemother* 2002;46:1665-1670.

120. Drusano GL, Johnson DE, Rosen M, et al. Pharmacodynamics of a fluoroquinolone antimicrobial agent in a neutropenic rat model of Pseudomonas sepsis. *Antimicrob Agents Chemother* 1993;37:483-490.

121. Katsube T, Wajima T, Yamano Y, et al. Pharmacokinetic/pharmacodynamic modeling for concentration-dependent bactericidal activity of a bicyclolide, modithromycin. *J Pharm Sci* 2014;103:1288-1297.

122. (EMA) EMA. Guideline on the use of pharmacokinetics and pharmacodynamics in the development of antibacterial medicinal products.

123. Zhi JG, Nightingale CH, Quintiliani R. Microbial pharmacodynamics of piperacillin in neutropenic mice of systematic infection due to *Pseudomonas aeruginosa*. *J Pharmacokinet Biopharm* 1988;16:355-375.

124. Campion JJ, Chung P, McNamara PJ, et al. Pharmacodynamic modeling of the evolution of levofloxacin resistance in *Staphylococcus aureus*. *Antimicrob Agents Chemother* 2005;49:2189-2199.

125. Harigaya Y, Bulitta JB, Forrest A, et al. Pharmacodynamics of vancomycin at simulated epithelial lining fluid concentrations against methicillin-resistant *Staphylococcus aureus* (MRSA): implications for dosing in MRSA pneumonia. *Antimicrob Agents Chemother* 2009;53:3894-3901.

126. Venisse N, Grégoire N, Marliat M, et al. Mechanism-based pharmacokinetic-pharmacodynamic models of *in-vitro* fungistatic and fungicidal effects against Candida albicans. *Antimicrob Agents Chemother* 2008;52:937-943.

127. Mouton JW, Vinks AA, Punt NC. Pharmacokinetic-pharmacodynamic modeling of activity of ceftazidime during continuous and intermittent infusion. *Antimicrob Agents Chemother* 1997;41:733-738.

128. Nolting A, Dalla Costa T, Rand KH, et al. Pharmacokinetic-pharmacodynamic modeling of the antibiotic effect of piperacillin *in-vitro*. *Pharm Res* 1996;13:91-96.

129. Jumbe N, Louie A, Leary R, et al. Application of a mathematical model to prevent in-vivo amplification of antibiotic-resistant bacterial populations during therapy. *J Clin Invest* 2003;112:275-285.

130. Gumbo T, Louie A, Deziel MR, et al. Selection of a moxifloxacin dose that suppresses drug resistance in *Mycobacterium tuberculosis*, by use of an *in-vitro* pharmacodynamic infection model and mathematical modeling. *J Infect Dis* 2004;190:1642-1651.

131. Bulitta JB, Ly NS, Yang JC, et al. Development and qualification of a pharmacodynamic model for the pronounced inoculum effect of ceftazidime against *Pseudomonas aeruginosa*. *Antimicrob Agents Chemother* 2009;53:46-56.

132. Nielsen EI, Cars O, Friberg LE. Pharmacokinetic/pharmacodynamic (PK/PD) indices of antibiotics predicted by a semimechanistic PKPD model: a step toward model-based dose optimization. *Antimicrob Agents Chemother* 2011;55:4619-4630.

133. Mohamed AF, Cars O, Friberg LE. A pharmacokinetic/pharmacodynamic model developed for the effect of colistin on *Pseudomonas aeruginosa in-vitro* with evaluation of population pharmacokinetic variability on simulated bacterial killing. *J Antimicrob Chemother* 2014;69:1350-1361.

134. Udekwu KI, Parrish N, Ankomah P, et al. Functional relationship between bacterial cell density and the efficacy of antibiotics. *J Antimicrob Chemother* 2009;63:745-757.

135. Couet W, Gregoire N, Marchand S, et al. Colistin pharmacokinetics: the fog is lifting. *Clin Microbiol Infect* 2012;18:30-39.

136. He H, Li JC, Nation RL, et al. Pharmacokinetics of four different brands of colistimethate and formed colistin in rats. *J Antimicrob Chemother* 2013;68:2311-2317.

137. Li J, Nation RL, Turnidge JD, et al. Colistin: the re-emerging antibiotic for multidrug-resistant Gram-negative bacterial infections. *Lancet Infect Dis* 2006;6:589-601.

138. Nation RL, Li J. Colistin in the 21st century. *Curr Opin Infect Dis* 2009;22:535-543.

139. Gregoire N, Mimoz O, Megarbane B, et al. New colistin population pharmacokinetic data in critically ill patients suggesting an alternative loading dose rationale. *Antimicrob Agents Chemother* 2014;58:7324-7330.

140. Li J, Milne RW, Nation RL, et al. Stability of colistin and colistin methanesulfonate in aqueous media and plasma as determined by high-performance liquid chromatography. *Antimicrob Agents Chemother* 2003;47:1364-1370.

141. Bergen PJ, Li J, Rayner CR, et al. Colistin methanesulfonate is an inactive prodrug of colistin against *Pseudomonas aeruginosa*. *Antimicrob Agents Chemother* 2006;50:1953-1958.

142. Bergen PJ, Li J, Nation RL. Dosing of colistin-back to basic PK/PD. *Curr Opin Pharmacol* 2011;11:464-469.

143. Li J, Milne RW, Nation RL, et al. Simple method for assaying colistin methanesulfonate in plasma and urine using high-performance liquid chromatography. *Antimicrob Agents Chemother* 2002;46:3304-3307.

144. Gobin P, Lemaitre F, Marchand S, et al. Assay of colistin and colistin methanesulfonate in plasma and urine by liquid chromatography-tandem mass spectrometry. *Antimicrob Agents Chemother* 2010;54:1941-1948.

145. Jansson B, Karvanen M, Cars O, et al. Quantitative analysis of colistin A and colistin B in plasma and culture medium using a simple precipitation step followed by LC/MS/MS. *J Pharm Biomed Anal* 2009;49:760-767.

146. Li J, Nation RL, Turnidge JD. Defining the dosage units for colistin methanesulfonate: urgent need for international harmonization. *Antimicrob Agents Chemother* 2006;50:4231; author reply 4231-4232.

147. Nation RL, Li J, Cars O, et al. Consistent global approach on reporting of colistin doses to promote safe and effective use. *Clin Infect Dis* 2014;58:139-141.

148. Li J, Milne RW, Nation RL, et al. Use of high-performance liquid chromatography to study the pharmacokinetics of colistin sulfate in rats following intravenous administration. *Antimicrob Agents Chemother* 2003;47:1766-1770.

149. Li J, Milne RW, Nation RL, et al. Pharmacokinetics of colistin methanesulphonate and colistin in rats following an intravenous dose of colistin methanesulphonate. *J Antimicrob Chemother* 2004;53:837-840.

150. Marchand S, Lamarche I, Gobin P, et al. Dose-ranging pharmacokinetics of colistin methanesulphonate (CMS) and colistin in rats following single intravenous CMS doses. *J Antimicrob Chemother* 2010;65:1753-1758.

151. Marchand S, Gobin P, Brillault J, et al. Aerosol therapy with colistin methanesulfonate: a biopharmaceutical issue illustrated in rats. *Antimicrob Agents Chemother* 2010;54:3702-3707.

152. Li J, Coulthard K, Milne R, et al. Steady-state pharmacokinetics of intravenous colistin methanesulphonate in patients with cystic fibrosis. *J Antimicrob Chemother* 2003;52:987-992.

153. Markou N, Markantonis SL, Dimitrakis E, et al. Colistin serum concentrations after intravenous administration in critically ill patients with serious multidrug-resistant, Gram-negative bacilli infections: a prospective, open-label, uncontrolled study. *Clin Ther* 2008;30:143-151.

154. Plachouras D, Karvanen M, Friberg LE, et al. Population pharmacokinetic analysis of colistin methanesulfonate and colistin after intravenous administration in critically ill patients with infections caused by Gram-negative bacteria. *Antimicrob Agents Chemother* 2009;53:3430-3436.

155. Garonzik SM, Li J, Thamlikitkul V, et al. Population pharmacokinetics of colistin methanesulfonate and formed colistin in critically ill patients from a multicenter study provide dosing suggestions for various categories of patients. *Antimicrob Agents Chemother* 2011;55:3284-3294.

156. Couet W, Gregoire N, Gobin P, et al. Pharmacokinetics of colistin and colistimethate sodium after a single 80-mg intravenous dose of CMS in young healthy volunteers. *Clin Pharmacol Ther* 2011;89:875-879.

157. Rao GG, Ly NS, Haas CE, et al. New Dosing Strategies for an 'Old' Antibiotic: Pharmacodynamics of Front-Loaded Regimens of Colistin at Simulated Pharmacokinetics of Patients with Kidney or Liver Disease. *Antimicrob Agents Chemother* 2013.

158. Hancock RE, Chapple DS. Peptide antibiotics. *Antimicrob Agents Chemother* 1999;43:1317-1323.

159. Moore RA, Bates NC, Hancock RE. Interaction of polycationic antibiotics with *Pseudomonas aeruginosa* lipopolysaccharide and lipid A studied by using dansyl-polymyxin. *Antimicrob Agents Chemother* 1986;29:496-500.

160. Hancock RE. Peptide antibiotics. *Lancet* 1997;349:418-422.

161. Rastogi N, Henrotte JG, David HL. Colistin (polymyxin E)--induced cell leakage in Mycobacterium aurum. *Zentralbl Bakteriol Mikrobiol Hyg A* 1987;263:548-551.

162. Biswas S, Brunel JM, Dubus JC, et al. Colistin: an update on the antibiotic of the 21st century. *Expert Rev Anti Infect Ther* 2012;10:917-934.

163. testing ECoas. MIC distributions and ECOFFs.

164. Dudhani RV, Turnidge JD, Coulthard K, et al. Elucidation of the pharmacokinetic/pharmacodynamic determinant of colistin activity against *Pseudomonas aeruginosa* in murine thigh and lung infection models. *Antimicrob Agents Chemother* 2010;54:1117-1124.

165. Gilleland HE, Murray RG. Ultrastructural study of polymyxin-resistant isolates of *Pseudomonas aeruginosa*. *J Bacteriol* 1976;125:267-281.

166. Miller AK, Brannon MK, Stevens L, et al. PhoQ mutations promote lipid A modification and polymyxin resistance of *Pseudomonas aeruginosa* found in colistin-treated cystic fibrosis patients. *Antimicrob Agents Chemother* 2011;55:5761-5769.

167. Chen HD, Groisman EA. The biology of the PmrA/PmrB two-component system: the major regulator of lipopolysaccharide modifications. *Annu Rev Microbiol* 2013;67:83-112.

168. Beceiro A, Llobet E, Aranda J, et al. Phosphoethanolamine modification of lipid A in colistin-resistant variants of Acinetobacter baumannii mediated by the pmrAB two-component regulatory system. *Antimicrob Agents Chemother* 2011;55:3370-3379.

169. Adams MD, Nickel GC, Bajaksouzian S, et al. Resistance to colistin in Acinetobacter baumannii associated with mutations in the PmrAB two-component system. *Antimicrob Agents Chemother* 2009;53:3628-3634.

170. Moskowitz SM, Ernst RK, Miller SI. PmrAB, a two-component regulatory system of *Pseudomonas aeruginosa* that modulates resistance to cationic antimicrobial peptides and addition of aminoarabinose to lipid A. *J Bacteriol* 2004;186:575-579.

171. Breazeale SD, Ribeiro AA, McClerren AL, et al. A formyltransferase required for polymyxin resistance in Escherichia coli and the modification of lipid A with 4-Amino-4-deoxy-L-arabinose. Identification and function oF UDP-4-deoxy-4-formamido-L-arabinose. *J Biol Chem* 2005;280:14154-14167.

172. Lacour S, Bechet E, Cozzone AJ, et al. Tyrosine phosphorylation of the UDP-glucose dehydrogenase of Escherichia coli is at the crossroads of colanic acid synthesis and polymyxin resistance. *PLoS One* 2008;3:e3053.

173. Helander IM, Kilpelainen I, Vaara M. Increased substitution of phosphate groups in lipopolysaccharides and lipid A of the polymyxin-resistant pmrA mutants of Salmonella typhimurium: a 31P-NMR study. *Mol Microbiol* 1994;11:481-487.

174. Barthe C, Nandakumar S, Derlich L, et al. Exploring the expression of *Pseudomonas aeruginosa* genes directly from sputa of cystic fibrosis patients. *Lett Appl Microbiol* 2015.

175. Boisson M, Jacobs M, Gregoire N, et al. Comparison of intrapulmonary and systemic pharmacokinetics of colistin methanesulfonate (CMS) and colistin after aerosol delivery and intravenous administration of CMS in critically ill patients. *Antimicrob Agents Chemother* 2014;58:7331-7339.

176. Drobnic ME, Sune P, Montoro JB, et al. Inhaled tobramycin in non-cystic fibrosis patients with bronchiectasis and chronic bronchial infection with *Pseudomonas aeruginosa*. *Ann Pharmacother* 2005;39:39-44.

177. Ramsey BW, Pepe MS, Quan JM, et al. Intermittent administration of inhaled tobramycin in patients with cystic fibrosis. Cystic Fibrosis Inhaled Tobramycin Study Group. *N Engl J Med* 1999;340:23-30.

178. McCoy KS, Quittner AL, Oermann CM, et al. Inhaled aztreonam lysine for chronic airway *Pseudomonas aeruginosa* in cystic fibrosis. *Am J Respir Crit Care Med* 2008;178:921-928.

179. Conole D, Keating GM. Colistimethate Sodium Dry Powder for Inhalation: A Review of Its Use in the Treatment of Chronic *Pseudomonas aeruginosa* Infection in Patients with Cystic Fibrosis. *Drugs* 2014;74:377-387.

180. Yapa SWS, Li J, Porter CJ, et al. Population pharmacokinetics of colistin methanesulfonate in rats: achieving sustained lung concentrations of colistin for targeting respiratory infections. *Antimicrob Agents Chemother* 2013;57:5087-5095.

181. Gontijo AV, Gregoire N, Lamarche I, et al. Biopharmaceutical Characterization of Nebulized Antimicrobial Agents in Rats. 2. Colistin. *Antimicrob Agents Chemother* 2014.

182. Oldham MJ, Robinson RJ. Predicted tracheobronchial and pulmonary deposition in a murine asthma model. *Anat Rec (Hoboken)* 2007;290:1309-1314.

183. Madl P, Hofmann W, Oldham MJ, et al. Stochastic morphometric model of the BALB/c mouse lung. *Anat Rec (Hoboken)* 2010;293:1766-1775.

184. Phalen RF, Mendez LB, Oldham MJ. New developments in aerosol dosimetry. *Inhal Toxicol* 2010;22 Suppl 2:6-14.

185. Londahl J, Moller W, Pagels JH, et al. Measurement techniques for respiratory tract deposition of airborne nanoparticles: a critical review. *J Aerosol Med Pulm Drug Deliv* 2014;27:229-254.

186. Petrosyan F, Culver DA, Reddy AJ. Role of bronchoalveolar lavage in the diagnosis of acute exacerbations of idiopathic pulmonary fibrosis: a retrospective study. *BMC Pulm Med* 2015;15:70.

187. Lee W, Chung WS, Hong KS, et al. Clinical usefulness of bronchoalveolar lavage cellular analysis and lymphocyte subsets in diffuse interstitial lung diseases. *Ann Lab Med* 2015;35:220-225.

188. Chellapandian D, Lehrnbecher T, Phillips B, et al. Bronchoalveolar lavage and lung biopsy in patients with cancer and hematopoietic stem-cell transplantation recipients: a systematic review and meta-analysis. *J Clin Oncol* 2015;33:501-509.

189. Kiem S, Schentag JJ. Interpretation of antibiotic concentration ratios measured in epithelial lining fluid. *Antimicrob Agents Chemother* 2008;52:24-36.

190. Kiem S, Schentag JJ. Interpretation of Epithelial Lining Fluid Concentrations of Antibiotics against Methicillin Resistant *Staphylococcus aureus*. *Infect Chemother* 2014;46:219-225.

191. Garcia I, Pascual A, Salvador J, et al. Effect of paclitaxel alone or in combination on the intracellular penetration and activity of quinolones in human neutrophils. *J Antimicrob Chemother* 1996;38:859-863.

192. Gontijo AV, Brillault J, Gregoire N, et al. Biopharmaceutical Characterization of Nebulized Antimicrobial Agents in Rats. 1. Ciprofloxacin, Moxifloxacin and Grepafloxacin. *Antimicrob Agents Chemother* 2014.

193. Bayat S, Louchahi K, Verdiere B, et al. Comparison of 99mTc-DTPA and urea for measuring cefepime concentrations in epithelial lining fluid. *Eur Respir J* 2004;24:150-156.

194. Marcy TW, Merrill WW, Rankin JA, et al. Limitations of using urea to quantify epithelial lining fluid recovered by bronchoalveolar lavage. *Am Rev Respir Dis* 1987;135:1276-1280.

195. Effros RM, Murphy C, Ozker K, et al. Kinetics of urea exchange in air-filled and fluid-filled rat lungs. *Am J Physiol* 1992;263:L619-626.

196. Yamazaki K, Ogura S, Ishizaka A, et al. Bronchoscopic microsampling method for measuring drug concentration in epithelial lining fluid. *Am J Respir Crit Care Med* 2003;168:1304-1307.

197. Hutschala D, Skhirtladze K, Zuckermann A, et al. In-vivo measurement of levofloxacin penetration into lung tissue after cardiac surgery. *Antimicrob Agents Chemother* 2005;49:5107-5111.

198. Marchand S, Dahyot C, Lamarche I, et al. Microdialysis study of imipenem distribution in skeletal muscle and lung extracellular fluids of noninfected rats. *Antimicrob Agents Chemother* 2005;49:2356-2361.

199. Medinsky MA, Bond JA. The importance of anatomical realism for validation of physiological models of disposition in inhaled toxicants. *Toxicol Appl Pharmacol* 1998;153:139-140.

200. Mercer RR, Russell ML, Roggli VL, et al. Cell number and distribution in human and rat airways. *Am J Respir Cell Mol Biol* 1994;10:613-624.

201. Price PS, Conolly RB, Chaisson CF, et al. Modeling interindividual variation in physiological factors used in PBPK models of humans. *Crit Rev Toxicol* 2003;33:469-503.

202. Wagner C, Zhao P, Pan Y, et al. Application of Physiologically Based Pharmacokinetic (PBPK) Modeling to Support Dose Selection: Report of an FDA Public Workshop on PBPK. *CPT Pharmacometrics Syst Pharmacol* 2015;4:226-230.

203. Campbell J, Van Landingham C, Crowell S, et al. A preliminary regional PBPK model of lung metabolism for improving species dependent descriptions of 1,3-butadiene and its metabolites. *Chem Biol Interact* 2015;238:102-110.

204. Dudhani RV, Nation RL, Li J. Evaluating the stability of colistin and colistin methanesulphonate in human plasma under different conditions of storage. *J Antimicrob Chemother* 2010;65:1412-1415.

205. Wallace SJ, Li J, Rayner CR, et al. Stability of colistin methanesulfonate in pharmaceutical products and solutions for administration to patients. *Antimicrob Agents Chemother* 2008;52:3047-3051.

206. Nation RL, Li J, Cars O, et al. Framework for optimisation of the clinical use of colistin and polymyxin B: the Prato polymyxin consensus. *Lancet Infect Dis* 2014.

207. Mohamed AF, Karaiskos I, Plachouras D, et al. Application of a loading dose of colistin methanesulfonate in critically ill patients: population pharmacokinetics, protein binding, and prediction of bacterial kill. *Antimicrob Agents Chemother* 2012;56:4241-4249.

208. He H, Li JC, Nation RL, et al. Pharmacokinetics of four different brands of colistimethate and formed colistin in rats. *J Antimicrob Chemother* 2013.

209. Wesson DE, Simoni J. Acid retention during kidney failure induces endothelin and aldosterone production which lead to progressive GFR decline, a situation ameliorated by alkali diet. *Kidney Int* 2010;78:1128-1135.

210. Wesson DE, Simoni J, Broglio K, et al. Acid retention accompanies reduced GFR in humans and increases plasma levels of endothelin and aldosterone. *Am J Physiol Renal Physiol* 2011;300:F830-837.

211. Jitmuang A, Nation RL, Koomanachai P, et al. Extracorporeal clearance of colistin methanesulphonate and formed colistin in end-stage renal disease patients receiving intermittent haemodialysis: implications for dosing. *J Antimicrob Chemother* 2015;70:1804-1811.

212. Nielsen EI, Friberg LE. Pharmacokinetic-pharmacodynamic modeling of antibacterial drugs. *Pharmacol Rev* 2013;65:1053-1090.

213. Lee HJ, Bergen PJ, Bulitta JB, et al. Synergistic activity of colistin and rifampin combination against multidrug-resistant Acinetobacter baumannii in an *in-vitro* pharmacokinetic/pharmacodynamic model. *Antimicrob Agents Chemother* 2013;57:3738-3745.

214. Mohamed AF, Nielsen EI, Cars O, et al. Pharmacokinetic-pharmacodynamic model for gentamicin and its adaptive resistance with predictions of dosing schedules in newborn infants. *Antimicrob Agents Chemother* 2012;56:179-188.

215. Rowland M, Toser T. Clinical Pharmacokinetics and Pharmacodynamics: Concepts and Applications. *Lippincott Williams & Wilkins, Baltimore, MD* 2011.

216. Craig WA, Andes DR. In-vivo pharmacodynamics of ceftobiprole against multiple bacterial pathogens in murine thigh and lung infection models. *Antimicrob Agents Chemother* 2008;52:3492-3496.

217. Smith GM, Abbott KH. Development of experimental respiratory infections in neutropenic rats with either penicillin-resistant *Streptococcus pneumoniae* or beta-lactamase-producing Haemophilus influenzae. *Antimicrob Agents Chemother* 1994;38:608-610.

218. Gerber AU, Brugger HP, Feller C, et al. Antibiotic therapy of infections due to *Pseudomonas aeruginosa* in normal and granulocytopenic mice: comparison of murine and human pharmacokinetics. *J Infect Dis* 1986;153:90-97.

219. Ahmed A, Jafri H, Lutsar I, et al. Pharmacodynamics of vancomycin for the treatment of experimental penicillin- and cephalosporin-resistant pneumococcal meningitis. *Antimicrob Agents Chemother* 1999;43:876-881.

220. Kugelberg E, Norstrom T, Petersen TK, et al. Establishment of a superficial skin infection model in mice by using *Staphylococcus aureus* and Streptococcus pyogenes. *Antimicrob Agents Chemother* 2005;49:3435-3441.

221. Drusano GL, Fregeau C, Liu W, et al. Impact of burden on granulocyte clearance of bacteria in a mouse thigh infection model. *Antimicrob Agents Chemother* 2010;54:4368-4372.

222. de Araujo BV, Diniz A, Palma EC, et al. PK-PD modeling of beta-lactam antibiotics: *in-vitro* or in-vivo models? *J Antibiot (Tokyo)* 2011;64:439-446.

223. Liu X, Yin H, Xu X, et al. Real-time monitoring of catheter-related biofilm infection in mice. *J Microbiol Biotechnol* 2015.

224. Zhou J, Bi Y, Xu X, et al. Bioluminescent tracking of colonization and clearance dynamics of plasmid-deficient Yersinia pestis strains in a mouse model of septicemic plague. *Microbes Infect* 2014;16:214-224.

225. Gonzalez RJ, Weening EH, Frothingham R, et al. Bioluminescence imaging to track bacterial dissemination of Yersinia pestis using different routes of infection in mice. *BMC Microbiol* 2012;12:147.

226. Mizgerd JP, Skerrett SJ. Animal models of human pneumonia. *Am J Physiol Lung Cell Mol Physiol* 2008;294:L387-398.

227. Bakker-Woudenberg IA. Experimental models of pulmonary infection. *J Microbiol Methods* 2003;54:295-313.

228. Lopez Hernandez Y, Yero D, Pinos-Rodriguez JM, et al. Animals devoid of pulmonary system as infection models in the study of lung bacterial pathogens. *Front Microbiol* 2015;6:38.

229. Lipscomb MF, Lyons CR, Izzo AA, et al. Experimental pulmonary cryptococcal infection in mice. *O Zak, MA Sande (Eds), Handbook of Animal Models of Infection, Academic Press, London (1999), pp 681–686*.

230. Debarbieux L, Leduc D, Maura D, et al. Bacteriophages can treat and prevent *Pseudomonas aeruginosa* lung infections. *J Infect Dis* 2010;201:1096-1104.

231. Carles M, Wagener BM, Lafargue M, et al. Heat-shock Response Increases Lung Injury Caused by *Pseudomonas aeruginosa* via an Interleukin-10-dependent Mechanism in Mice. *Anesthesiology* 2014.

232. Migiyama Y, Kaneko Y, Yanagihara K, et al. Efficacy of AiiM, an N-Acylhomoserine Lactonase, against *Pseudomonas aeruginosa* in a Mouse Model of Acute Pneumonia. *Antimicrob Agents Chemother* 2013;57:3653-3658.

233. Majhi A, Kundu K, Adhikary R, et al. Combination therapy with ampicillin and azithromycin in an experimental pneumococcal pneumonia is bactericidal and effective in down regulating inflammation in mice. *J Inflamm (Lond)* 2014;11:5.

234. Kishta OA, Iskandar M, Dauletbaev N, et al. Pressurized whey protein can limit bacterial burden and protein oxidation in *Pseudomonas aeruginosa* lung infection. *Nutrition* 2013;29:918-924.

Abstract

Antibiotics are among the most commonly prescribed drugs, however optimal dosages are not yet well defined. The aim of this thesis was to develop pharmacokinetic (PK) and pharmacokinetic-pharmacodynamics (PK/PD) models that characterize the course of antimicrobial drug concentrations and effects over time, with an emphasis on the development of resistance. These models were applied to optimize dosing regimens of antimicrobial therapies.

A population PK model for colistin and its prodrug, colistin methanesulfonate (CMS) was developed in critically ill patients receiving colistin by nebulization and/or undergoing an intermittent hemodialysis (HD). Results predicted clear benefits of using aerosol delivery of 2MIU CMS dose for the treatment of pulmonary infections. For patients with HD session dosing regimen of CMS should be 1.5 MIU twice daily with an additional dose of 1.5 MIU after each HD session.

An assessment of the performances of different PK-PD models by using a simulation approach have shown the importance of longer study designs and of complementary microbiological data to predict accurately bacterial resistance development.

A semi-mechanistic PK/PD model that incorporates mutation rate and adaptive resistance development of a bioluminescent strain of *Pseudomonas aeruginosa* against colistin was developed based on *in-vitro* data. A high, quick and partially reversible resistance was described. These results confirm that the first 24 h of treatment are critical in the management of infections, that colistin alone cannot eradicate completely the mutants of *Pseudomonas aeruginosa* that were selected during the experiments and that combination therapies seem necessary.

Résumé

Les antibiotiques sont actuellement parmi les médicaments les plus utilisés, mais les schémas thérapeutiques optimaux ne sont pas toujours bien définis. Le but de cette thèse était de développer des modèles pharmacocinétiques (PK) et pharmacodynamiques (PK/PD) décrivant les profils de concentrations des antibiotiques ainsi que leurs effets et le développement de résistances bactériennes afin d'optimiser les schémas thérapeutiques.

Un modèle PK de population sur la colistine et sa prodrogue, le colistine methanesulfonate (CMS), a été développé chez les patients recevant la colistine par voie aérosol et/ou sous hémodialyse (HD). Les résultats ont montré un net avantage de la voie aérosol pour le traitement des infections pulmonaires avec une dose de 2 MUI de CMS. Pour les patients sous HD une dose de 1.5 MUI de CMS 2 fois par jour est recommandée avec une dose supplémentaire de 1.5 MUI de CMS après chaque séance de HD.

L'évaluation des performances de différents modèles PK/PD via à une approche par simulation a montré l'importance d'effectuer des études suffisamment longues ainsi que d'obtenir des données microbiologiques complémentaires afin de décrire le développement de la résistance bactérienne.

Un modèle PK/PD incluant taux de mutation et résistance adaptative à la colistine d'une souche bioluminescente de *Pseudomonas aeruginosa* a été développé à partir de données *in-vitro*. Une résistance rapide, importante et partiellement réversible a été décrite. Ces résultats confirment l'importance des 24 premières heures dans le traitement des infections, que la colistine seule ne peut pas complétement éliminer les mutants de *Pseudomonas aeruginosa* et que des associations semblent nécessaires.